A COMPUTER-AIDED INVESTIGATION OF DESTROYER STERN ACCELERATION -- With a Demonstration of a Statistically Oriented System Analysis

Thesis

LT. CLINTON W. KREITNER May, 1965

A COMPUTER-AIDED INVESTIGATION OF DESTROYER STERN ACCELERATION - With a Demonstration of a Statistically Oriented System Analysis

- - - - - -

A THESIS PRESENTED TO THE
FACULTY OF
WEBB INSTITUTE OF NAVAL ARCHITECTURE

- - - - - -

IN PARTIAL FULFILLMENT OF
THE REQUIREMENTS FOR THE
DEGREE OF MASTER OF SCIENCE
IN NAVAL ARCHITECTURE

- - - - - -

Submitted By
LIEUTENANT CLINTON W. KREITNER, U.S.NAVY
24 May 1965

ACKNOWLEDGEMENTS

I would like to express my sincere appreciation particularly to the following individuals:

Captain Robert A. Hinners, USN (Ret), Head of the Luckenbach Graduate School, Webb Institute of Naval Architecture (thesis advisor) whose unfailing wisdom, experienced judgement and willingness to provide guidance I am most thankful for;

Professor Edward V. Lewis, Webb Institute of Naval Architecture (thesis advisor) who gave freely of his time for encouragement and technical advice;

Dr. Michel K. Ochi, David Taylor Model Basin, who graciously assisted me in improving my knowledge of probability and statistical theory and its application to seakeeping;

Dr. Otto J. Karst, Professor E.G.U. Band and Mr. Roger H. Compton, Webb Institute of Naval Architecture, whose advice on various phases of work on this thesis has been of considerable value;

Mrs. Margaret D. Ochi, Mr. Alvin Gersten, Mr. Sigmund S. Hagara, Mr. Raymond Wermter, Mr. Ernest E. Zarnick, and Mr. Z. George Wachnik, David Taylor Model Basin, whose kindness and advice greatly enhanced the thesis work I was able to do while on temporary duty at the Model Basin;

Mr. Raymond Mejia, Mr. James H. Kasab and LTJG Robert P. Schulhof, USN, David Taylor Model Basin, who gave considerable assistance while I was programming for the computations done on the UNIVAC LARC at the Model Basin;

Mr. Seymour Gross, Mr. Donald A. Nichols, Mr. Glendon E. Christensen and Mr. Stanley Rupinski of the U.S. Navy Underwater Sound Laboratory, for their help in making available the full-scale data used for correlation with predicted stern accelerations as well as for their general interest in my work.

Finally, to my wife and children, I express my deepest appreciation for their patience in waiting for the day when this thesis was completed so that Dad could spend more time with them.

TABLE OF CONTENTS

APPENDICES

ABSTRACT

Vertical stern accelerations for five geometrically similar destroyer hull forms of different lengths in the 250-550 foot range are predicted on the basis of model tests for a ship speed of 17 knots at various headings in representative short-crested irregular seas of varying severity.

Using the concept of statistical inference, the model test predictions are treated as a statistical sample and used to predict what would occur in the total population of possible stern accelerations.

Then, with strong emphasis on the systems approach, it is shown how these predictions can be used as input to a probability analysis that leads to a prediction of long range system behavior/effectiveness, the system under consideration being the Destroyer/Variable Depth Sonar System.

NOMENCLATURE

DD	- Destroyer type ship.
VDS	- Variable Depth Sonar.
RAO	- Response Amplitude Operator.
λ	- Actual wave length of regular waves in feet measured perpendicular to lines of crests.
Effective λ	- Wave length apparent to a ship proceeding obliquely through regular waves.
L	- Ship length in feet measured along designer's waterline
Amplitude	- For a regular or irregular function, peak to peak value divided by two. Sometimes referred to as single amplitude.
Height	- For a regular or irregular function, peak to peak value. Sometimes referred to as double amplitude.
$\bar{\Psi}_o$	- Amplitude of ship pitch angle in radians; vertex of angle is defined as being at ship's center of gravity.
Ψ_o	- Instantaneous value of pitch.
$\bar{z}_o$	- Amplitude of heave (vertical translation) of ship in feet at center of gravity.
z_o	- Instantaneous value of heave.
⊠	- Amidships
z_x	- Vertical translation at a point x feet from ⊠.
$\bar{h}$	- Wave amplitude in feet.

h	- Instantaneous value of distance in feet between wave surface and calm water zero datum.
ϑ_{max}	- Maximum wave slope. See Page 9.
ε_{ψ}	- Phase angle between pitch and wave. See Pages 8 and 9.
ε_{z}	- Phase angle between heave and wave. See Pages 8 and 9.
$\varepsilon_{z\psi}$	- Phase angle between heave and pitch. See Page 9.
μ, μ_0, μ_ω	- See Figure 3 on page 11 for angular nomenclature.
v_s	- Ship speed in feet per second.
ω	- Circular frequency of wave in radians per second.
ω_e	- Encounter frequency in radians per second.
t	- Time in seconds.
g	- Acceleration due to gravity; 32.2 ft. per $(\text{second})^2$
x	- Distance along ship's length from ⊠ to some point, (+) forward, (-) aft. In Appendix A, ordinate of irregular stern acceleration record.
$\bar{A}_x$	- Amplitude of vertical acceleration at a point x along ship's length. In this thesis x = -181 feet for the 370 foot ship length. (x changes with geometric similarity for other ship lengths)
ln	- Logarithm to the natural base e.
δ	- Increment of.
corr.ft^2	- Pierson-Moskowitz sea spectrum ordinate. "Corr" implies corrected. See Page 16
H	- Lag number; sea spectrum abscissa frequency coordinate. See Pages 16 and 17.

$\bar{H}_{1/3}$	- Significant wave height in feet; defined as the average of the 1/3 highest wave heights extant in any given seaway.
RSC	- Response Spectrum Component. See Figure 9.
IRS	- Integrated Response Spectrum. See Figure 9.
$\sqrt{E}$	- Ship response parameter. See Appendix A.
Sample	- A relatively small portion of the set of values in the universe of a random variable.
$\bar{x}$	- Mean of sample probability distribution of stern vertical $\sqrt{E}$ acceleration.
s^2	- Variance of sample probability distribution of stern vertical $\sqrt{E}$ acceleration.
s	- Deviation of sample probability distribution of stern vertical $\sqrt{E}$ acceleration.
$N(\bar{x},s^2)$	- A normal (Gaussian) probability distribution function whose mean is $\bar{x}$ and whose variance is S^2.
Population	- The set of all possible values in the universe of a random variable.
μ	- Mean of population probability distribution of stern vertical $\sqrt{E}$ acceleration.
σ^2	- Variance of population probability distribution of stern vertical $\sqrt{E}$ acceleration; when used in a general sense, the variance of any normal probability distribution function.
σ	- Deviation of population probability distribution of stern vertical $\sqrt{E}$ acceleration.
μ_o, σ_o	- True population parameters.
Pr [ ]	- Probability of [ ].
μ_u, σ_u	- Estimate of μ_o, σ_o. See Figure 17 on Page 56.
P	- Location of $\bar{x}$ and s in σ/μ parameter space.
n	- Size of a statistical sample.

N	- Number of cycles of a certain ship motion.
R	- Parameter of the Rayleigh probability distribution function.
RMS	- Root mean square of some variable. See Appendix A.
$\sqrt{E}$	- See Appendix A.

Superscripts

$\bar{}$	- Denotes amplitude of a sinusoidal function as distinguished from instantaneous value. In the case of an irregular function, denotes peak to peak divided by two. This superscript does not imply the above when used in $\bar{x}$; in that case it indicates an arithmetic mean.
$\tilde{}$	- Average of.

Subscripts

o	- Measured at ship's center of gravity.
max	- Maximum value.
$\mathcal{Z}$	- heave relative to wave.
Ψ	- pitch relative to wave.
$\mathcal{Z}\Psi$	- pitch relative to heave.
x	- at location x feet along ships length from $\mathbb{D}$.
e	- Encounter.
i	- the ith value of a variable.
u	- upper.
L	- lower.
PTP	- peak-to-peak value (double amplitude or height)

1/3	- the highest 1/3 of a group of values of a variable.
1	- original value, before being changed.
2	- value after having been changed from original value.

LIST OF FIGURES

INTRODUCTION

The basic method used in this thesis to predict the various modes of response of a particular ship to a given seaway was introduced over ten years ago (1)* and has been extensively employed in the intervening time. The challenge of the present day is how to most effectively utilize such response data in order that the systems designer might be provided with reliable long-range estimates of system behavior and as well, that the system user might have reliable estimates of system effectiveness.

The approach developed in this thesis is a broad and general one that is applied to one particular aspect of behavior of one system. It is suggested that the reader keep in mind the generality of the method, while considering the specific case which is developed herein for illustration as well as for its current naval interest.

The system considered in this thesis is the DD/VDS system. The particular aspect of system behavior considered is the vertical acceleration of the VDS tow-point at the destroyer's stern.

---

*Numbers in parentheses refer to references listed on Page 91.

The development undertaken herein can be divided into three principal areas, namely:

(1) prediction of vertical stern acceleration (in terms of the $\sqrt{E}$ parameter which is discussed in detail in Appendix A), for various ship lengths, headings and sea states;

(2) utilization of the concept of statistical inference to predict the population distribution of vertical stern acceleration* (in terms of the $\sqrt{E}$ parameter), treating the predicted values in (1) above as a statistical sample;

(3) a demonstration of how these predicted stern accelerations can be used in a probability-based system analysis leading to long-range prediction of DD/VDS system behavior over the lifetime of such a system.

---

*The term "population" is used here to signify all the possible values of vertical stern acceleration (in terms of the $\sqrt{E}$ parameter) that a destroyer of the particular type considered might experience in its lifetime. In theoretical probability and statistics, "population" and "universe" are used interchangeably to describe the set of all the possible values of a given random variable.

PREDICTION OF STERN ACCELERATION RESPONSE

General Procedure for Prediction of Ship Response

In 1953, St. Denis and Pierson (1) introduced a method utilizing the principle of superposition whereby a ship's response in irregular waves may be predicted provided the response in regular waves is known, as it is, for example, from model tests in regular waves.

The method basically consists of (a) representing the sea as an energy spectrum, (b) transforming model response data taken in regular waves into a response amplitude operator (RAO) (referred to by some as a transfer function) and (c) multiplying the RAO by the sea spectrum to arrive at a response spectrum having certain probability properties regarding the response being considered.

One section each will be devoted to the description of developing RAO's from model data, to the selection of sea spectra, and to the computational procedure used to combine sea spectrum and RAO to arrive at a response spectrum.

Development of RAO's from Model Data

The most comprehensive source of destroyer model motions data available at the present time is the Dutch

data that can be found in (2). It is particularly unique in that model response at various headings to the waves was measured and this is, of course, a necessary prerequisite if one desires to make predictions in short-crested seas and to investigate the general effect of heading on ship response. This Dutch data is also unique in that phase angles were measured and presented. The primary limitation of this data is that the above variations were done at only one speed, namely 17 knots full scale.

The vertical acceleration at the stern of a ship is caused primarily by pitching and somewhat less by heaving. Roll is the only other possible contributor to vertical acceleration, but its effect was ignored because the stern VTS towpoint is on the ship's centerline. The vertical acceleration also is a function of the phase angle between heaving and pitching. Consequently, the data from (2) used in this investigation consisted of heave, pitch and the heave-to-wave and pitch-to-wave phase angles. Samples of the model data are shown in Figures 1 and 2.

The model used was 1700Z. It is a model of Her Netherlands Majesty's Ship Friesland. Its hull parameters are as shown in Table I.

$\mu = 45°$

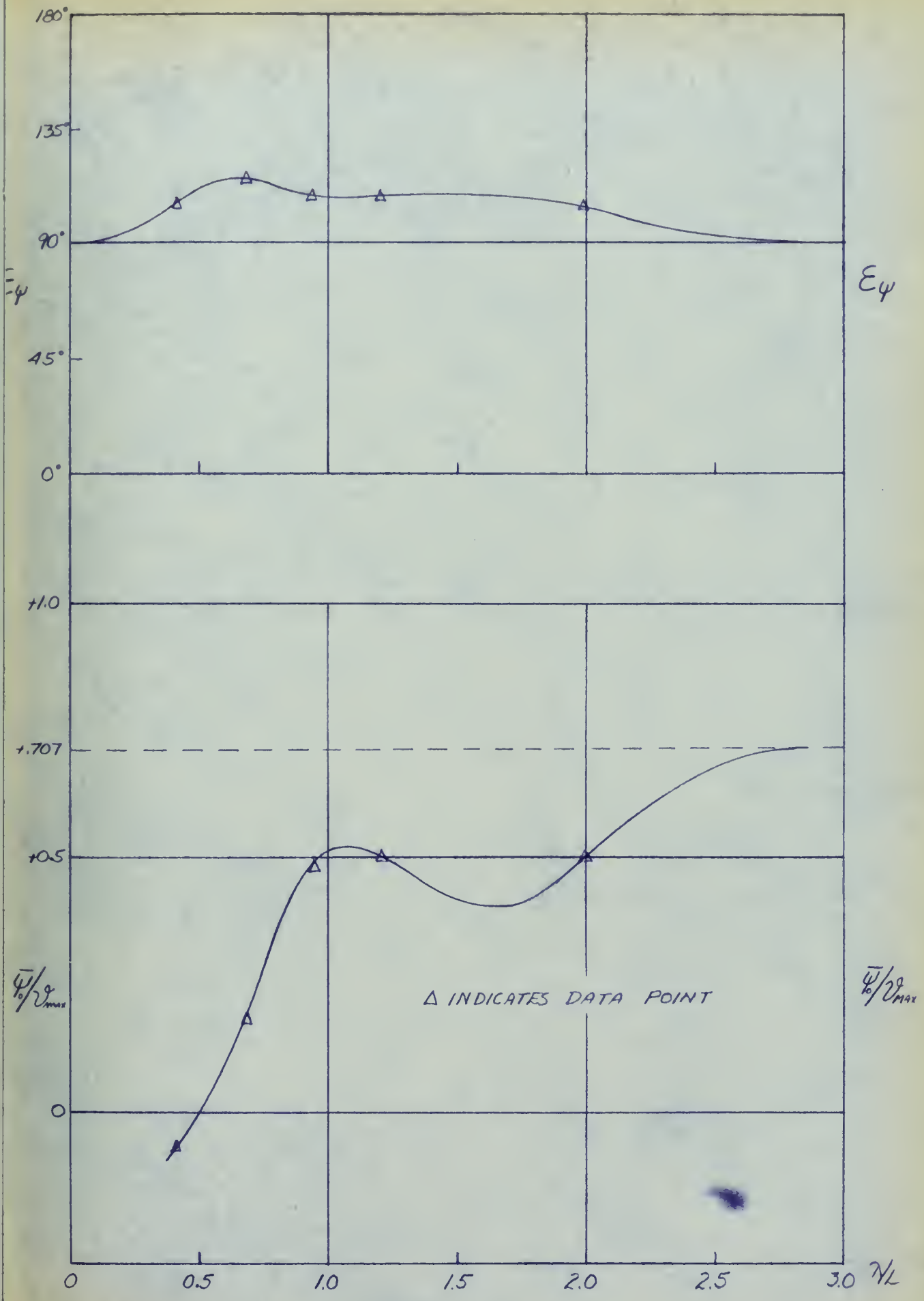

SAMPLE OF MODEL DATA - PITCH

FIGURE 1

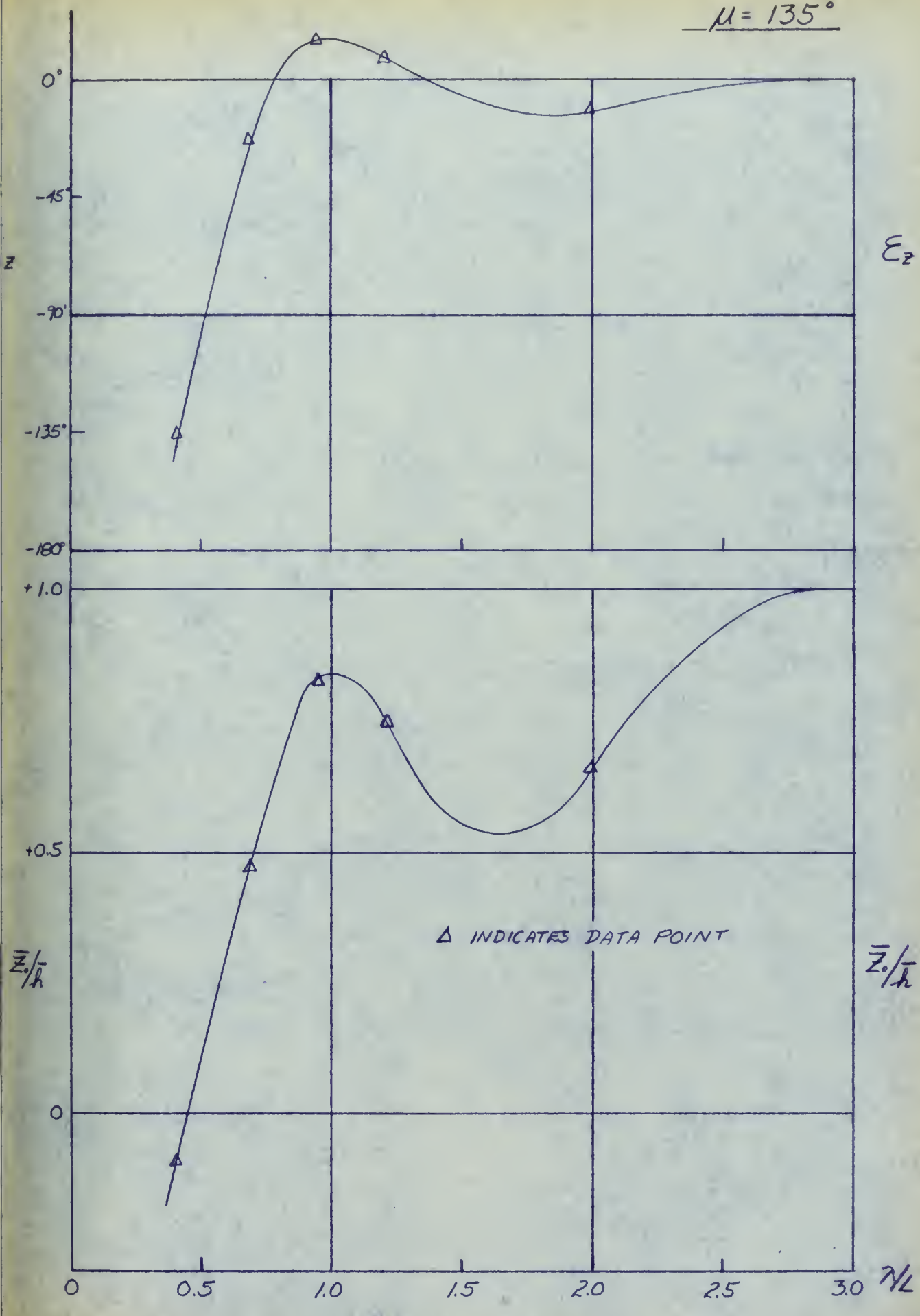

SAMPLE OF MODEL DATA - HEAVE

FIGURE 2

TABLE I

L	370 ft.	Waterplane Coefficient	0.805
Beam	38.6 ft.	Prismatic Coefficient	0.688
Draft	13.2 ft.	Displacement	3010 tons
Block Coefficient	0.566	Number of Rudders	2

It can be seen from Figures 1 and 2 that a certain amount of extrapolation of the model data was necessary. On the high end of the λ/L scale, $\bar{Z}_o \to \bar{h}$ and $\bar{\Psi}_o \to 2\pi \bar{h}/\lambda = \bar{\vartheta}_{max}$, but the question immediately arose as to just <u>where</u> on the λ/L scale it would be reasonable to assume that this occurs. Extensive examination of other destroyer model data (3), (4) showed that a λ/L of 3.75 to 4.00 is reasonable for heave and pitch having attained their limiting values. Since the angle between ship's course and wave direction had to be taken into account, $\bar{\Psi}_o$ was faired to effective wave slope (based on effective λ, where effective λ is the λ apparent to a ship proceeding obliquely through the waves) and $\bar{Z}_o$ was faired to h at whatever actual λ resulted (about 3.00 in the cases shown in Figures 2 and 3) when effective $\lambda/L \to 3.75$ to 4.00.

As for phase angle extrapolation, the statements in (2) are generally supported by vibration theory for a single degree of freedom system. The limiting values to which ε_ψ and ε_z were extrapolated (using the same effective λ limits as described above) were taken from

the following:

ζ_z ranges from (-180° to 0°) in head, bow and beam seas as effective λ/L increases from zero to about 4.00.

ζ_x ranges from (0° to 0°) in quartering seas over the effective λ/L range of zero to 4.00.

ζ_z was zero throughout the λ/L range for following seas because of very small encounter frequency.

ζ_ψ ranges from (+90° to - 90°) in head and bow seas as effective λ/L increases from zero to about 4.00.

ζ_ψ was 90° throughout the λ/L range in beam and following seas. In the beam seas, $\lambda >>$ ship beam and thus there is effectively zero pitch phase lag and in the following seas case ω_e is very small.

ζ_ψ ranges from (90° to 90°) in quartering seas.

Before proceeding further, it is in order to present the basic conventions and relationships used so as to prevent confusion. There are many different systems in use so the best policy obviously was to set up a system and adhere to it. I have followed that policy based on these conventions and relationships:*

(a) If the wave motion amidships is described by

$$h = \bar{h} \cos(\omega_e t)$$

the resulting pitch motion is described by

$$\psi_o = \bar{\psi}_o \cos(\omega_e t + \zeta_\psi)$$

*In the notation used here a bar ($\bar{\ }$) above a symbol implies an amplitude as distinguished from an instantaneous value.

and the heave motion by

$$Z_o = \bar{Z}_o \cos(\omega_e t + \varepsilon_z)$$

(b) heave is taken as positive upwards and positive pitch angle is taken as bow downwards.

(c) it can be seen from the equations in (a) that negative phase angles imply motion lagging wave and positive phase angles imply motion leading wave

(d) The phase angle between heave and pitch is defined by the equation

$$\varepsilon_{z\psi} = \varepsilon_z - \varepsilon_\psi$$

Negative values of $\varepsilon_{z\psi}$ imply heave lagging pitch and positive values of $\varepsilon_{z\psi}$ imply heave leading pitch.

(e) From basic wave theory we know that maximum wave slope

$$\overline{\vartheta}_{max} = \frac{2\pi \bar{h}}{\lambda}$$

(f) It can be shown that encounter frequency

$$\omega_e = \omega - \frac{\omega^2 v_s}{g} \cos\mu_o \quad *$$

where $\omega = \sqrt{2\pi g/\lambda}$ according to basic wave theory.

(g) The Dutch models were tested in waves of proportions:

$$\frac{2\bar{h}}{\lambda} = \frac{1}{40}$$

Equipped with (a) through (g) above, it is possible to determine the amplitude of vertical displacement at any

*See Figure 3 for angular nomenclature.

point x along the ship's length, $\bar{Z}_x$, from

$$\bar{Z}_x^2 = \bar{Z}_o^2 + x^2 \bar{\Psi}_o^2 - 2\bar{Z}_o x \bar{\Psi}_o \cos \varepsilon_{z\Psi} \qquad (5)$$

where x = distance along ship's length from amidships to the point under consideration, (+) forward (-) aft. In this thesis x = -181 feet for the 370 foot ship length and x changes in a geometrically similar manner for the other ship lengths investigated. The x distance was chosen to be a reasonable location of the VDS towpoint.

The amplitude of vertical acceleration at any point x along the ship's length, $\bar{Ax}$, can be computed from

$$\bar{Ax} = \omega_e^2 \bar{Z}x$$

The ordinate of the RAO is

$$\left[\frac{\bar{Ax}/g}{2\pi h/\lambda}\right]^2$$

and the abscissa is ln ω.

RAO's for μ = 180°, 135°, 90°, 45° and 0° were computed directly from the model data curves, extrapolated as necessary to cover a ln ω range of +0.2 to -1.6. The reason for the limits of this range will become evident later.

Then, in order to have RAO's at 22.5° increments, the original RAO's were first plotted on an ω_e base to align the peaks and then crossplotted at constant values of ω_e. The resulting RAO's for μ = 157 1/2°, 112 1/2°, 67 1/2° and 22 1/2° were then converted to a ln ω base and plotted with the original ones, resulting in a

Angular Nomenclature

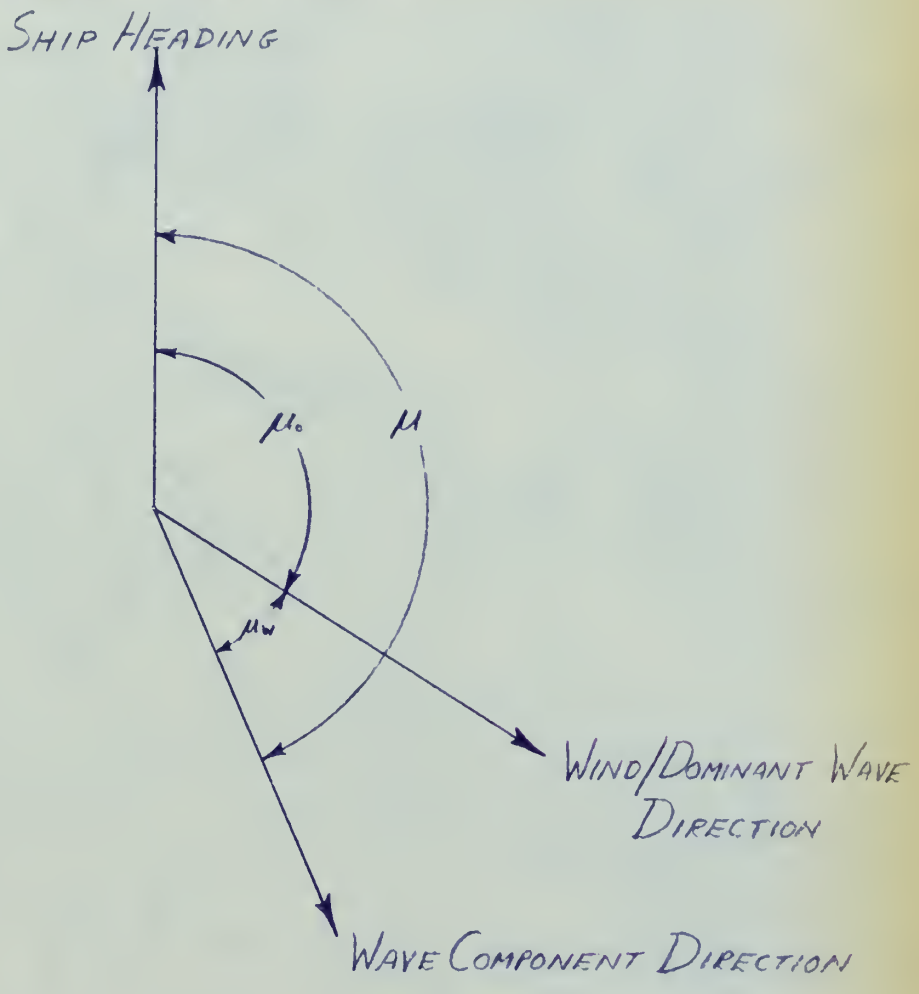

μ =	180°	Head Seas
	135°	Bow Seas
	90°	Beam Seas
	45°	Quartering Seas
	0°	Following Seas

Figure 3

complete selection of RAO's at 22 1/2° increments as shown in Figure 4.

The RAO's thus derived are for the full scale length of the destroyer hull considered, namely 370 feet (this was the L used in the λ/L scale of the original model data).

To arrive at RAO's for geometrically similar hulls of other lengths is a simple matter when they are plotted on a ln ω base (5). As stated previously,

$$\omega = \sqrt{2\pi g/\lambda}$$

At λ/L = a constant value,

$\omega_1 = k\sqrt{1/L_1}$ Subscript 1 indicates original value

$\omega_2 = k\sqrt{1/L_2}$ Subscript 2 indicates changed value

and

$$\frac{\omega_1}{\omega_2} = \sqrt{L_2/L_1}$$

Taking the natural base logarithm of both sides of this equation, $\ln \omega_1 - \ln \omega_2 = 1/2(\ln L_2 - \ln L_1)$ and therefore, $\ln \omega_2 - \ln \omega_1 = \delta \ln \omega = -1/2(\ln L_2 - \ln L_1)$. It follows that: $\delta \ln \omega = -1/2 \ln\left(\frac{L_2}{L_1}\right)$

This last equation shows that RAO's for other ship lengths can be obtained by translating the original RAO's along the abscissa.

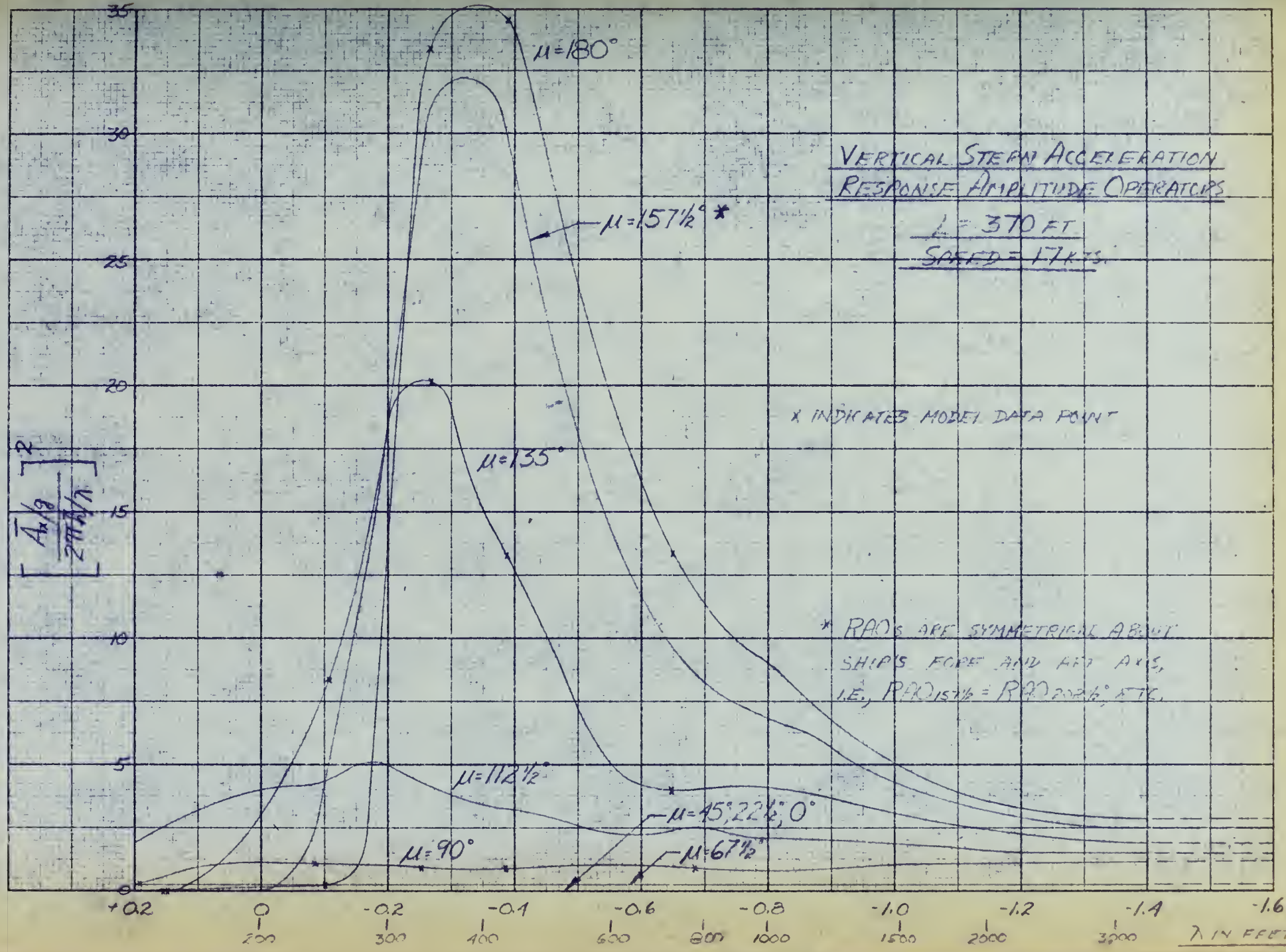
VERTICAL STEEM ACCELERATION
RESPONSE AMPLITUDE OPERATORS
L = 370 FT
SPEED = 17 KTS.
X INDICATES MODEL DATA POINT
* RAO'S ARE SYMMETRICAL ABOUT SHIP'S FORE AND AFT AXIS, I.E., RAO157½ = RAO202½°
μ=180°
μ=157½°
μ=135°
μ=112½°
μ=90°
μ=67½°
μ=45°,22½°,0°
35
30
25
20
15
10
5
0
+0.2
0
-0.2
-0.1
-0.6
-0.8
-1.0
-1.2
-1.4
-1.6 ln(λ)
200
300
400
600
800
1000
1500
2000
3000
λ IN FEET

13

FIGURE 4

For example, let $\delta \ln \omega = 0.1$

$$0.1 = -1/2 \ln \frac{L_2}{L_1}$$

$$\frac{L_2}{L_1} = .819$$

and $L_2 = .819\ (370) = 302'$

Similarly, if $\delta \ln \omega = -0.1$, $\frac{L_2}{L_1} = 1.222$ and $L_2 = 452'$

Thus, if the RAO's are shifted to the right, keeping the ln ω scale fixed in space, ship length increases and conversely a leftward shift causes a decrease in ship length. Shifting increments of 0.2, 0.1, -0.1, and -0.2 were chosen, resulting in RAO's for snip lengths of 248 ft., 302 ft., 452 ft. and 552 ft.

Figure 5 shows the 157 1/2° RAO shifted as described by the above procedure. All the others were shifted in exactly the same manner.

Selection of Sea Spectra

Through the principle of superposition, the large number of component waves comprising an irregular long-crested seaway may be represented in a spectral form having an ordinate representing energy and an abscissa representing wavelength or frequency. This is a well-established concept and is described rather well in (6). (The term long-crested is used by oceanographers

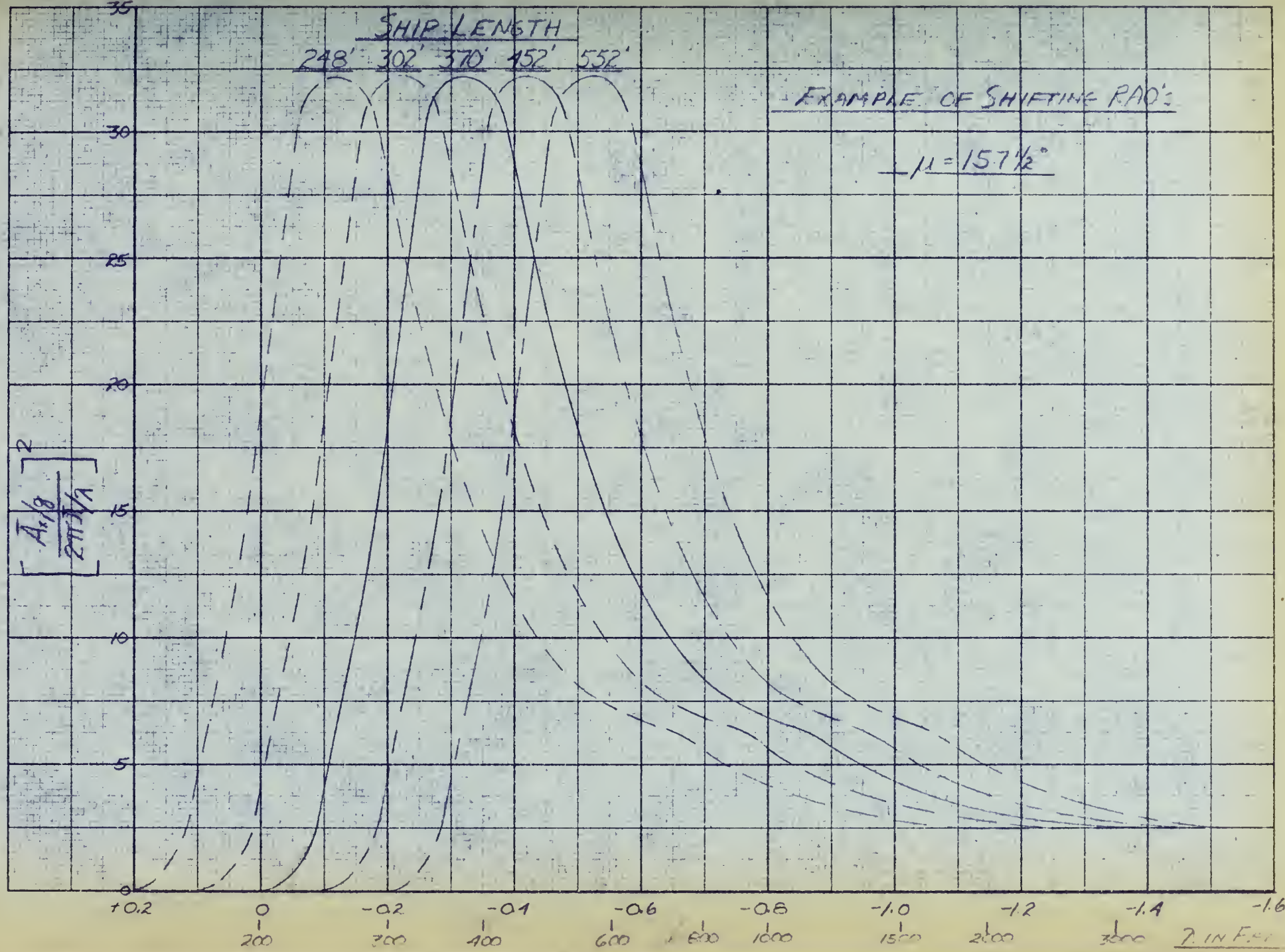
SHIP LENGTH
248' 302' 370' 452' 552'
EXAMPLE OF SHIFTING RAO:
μ = 157½°
$\left[\frac{A_{1/3}}{2\pi A/\lambda}\right]^2$
35
30
25
20
15
10
5
0
+0.2
0
-0.2
-0.4
-0.6
-0.8
-1.0
-1.2
-1.4
-1.6
Log
200
300
400
600
800
1000
1500
2000
3000
λ IN FEET

FIGURE 5

to describe the situation where all the waves in a system are coming toward the observer from the same direction such that he sees a well-defined pattern of long, parallel crests).

The log-slope form of sea spectrum representation developed by Lewis (5) was used in this present work. For my purpose it has one large advantage over other representations which have, for example, (wave amplitude)^2 as ordinate and encounter frequency or lag number as abscissa, namely:

> RAO's for geometrically similar hulls of different lengths can be easily developed by the simple expedient of translating them along the $\ln\omega$ axis.

The ordinate of the log-slope sea spectrum is $\left[\frac{r\ (\ln\omega)}{\lambda/2\pi}\right]^2$ and the abscissa is $\ln\omega$.

Since a statistical sampling approach was desired for this analysis, the Pierson-Moskowitz collection of sea spectra (7), (8) was chosen because it is the largest, most recent collection of actually measured sea spectra. Pierson and Moskowitz use "corr.ft^2"* as their spectral ordinate and lag number, H, for their abscissa. See Figure 5A for an illustration of a typical Pierson-Moskowitz sea spectrum. The pertinent conversion

---

*Corr.ft^2 means "corrected" ft^2-Pierson and Moskowitz corrected some spectral ordinates to smooth out occasional unreasonable values due mainly to vagaries in the measured waveheight data.

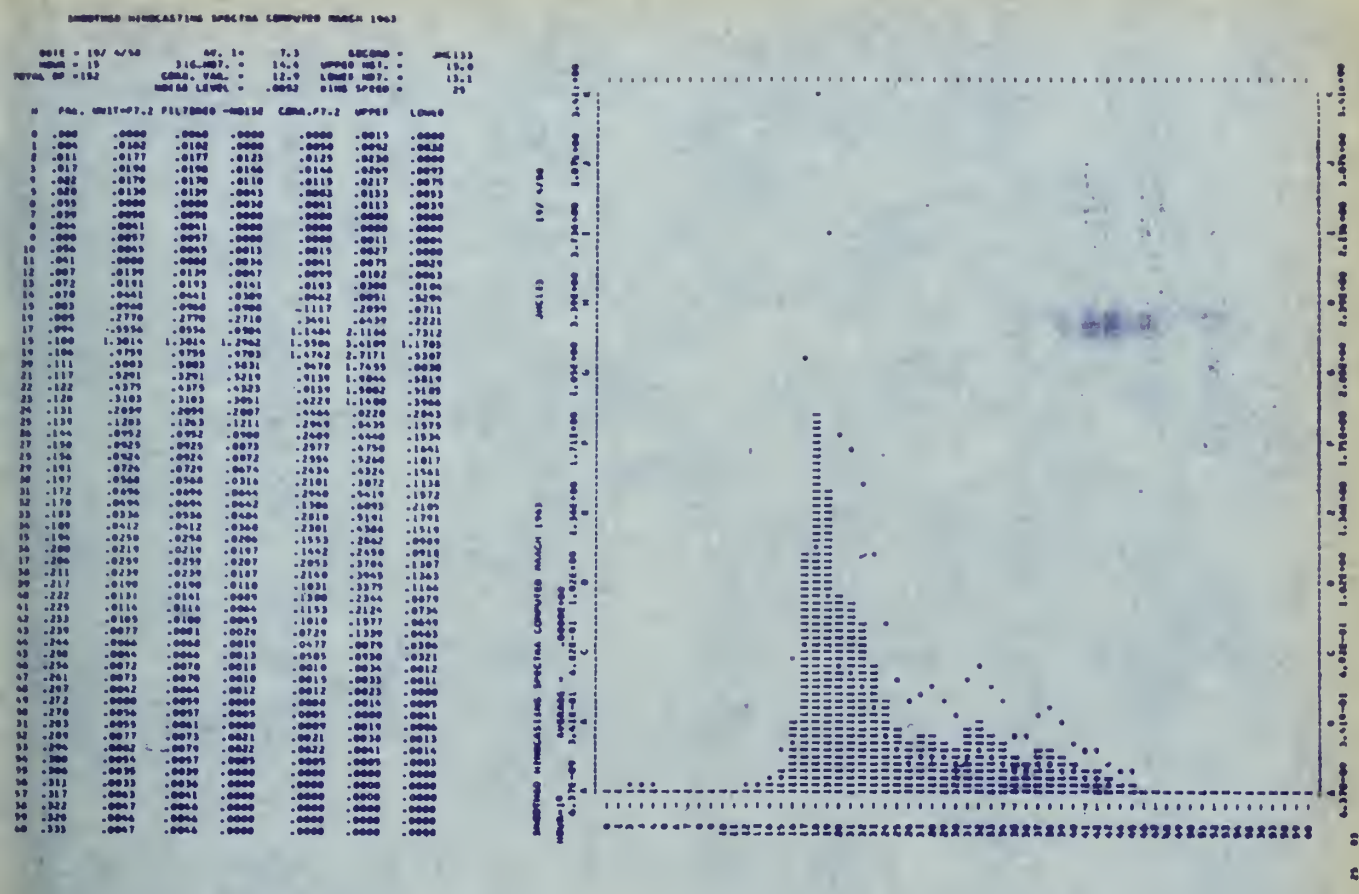

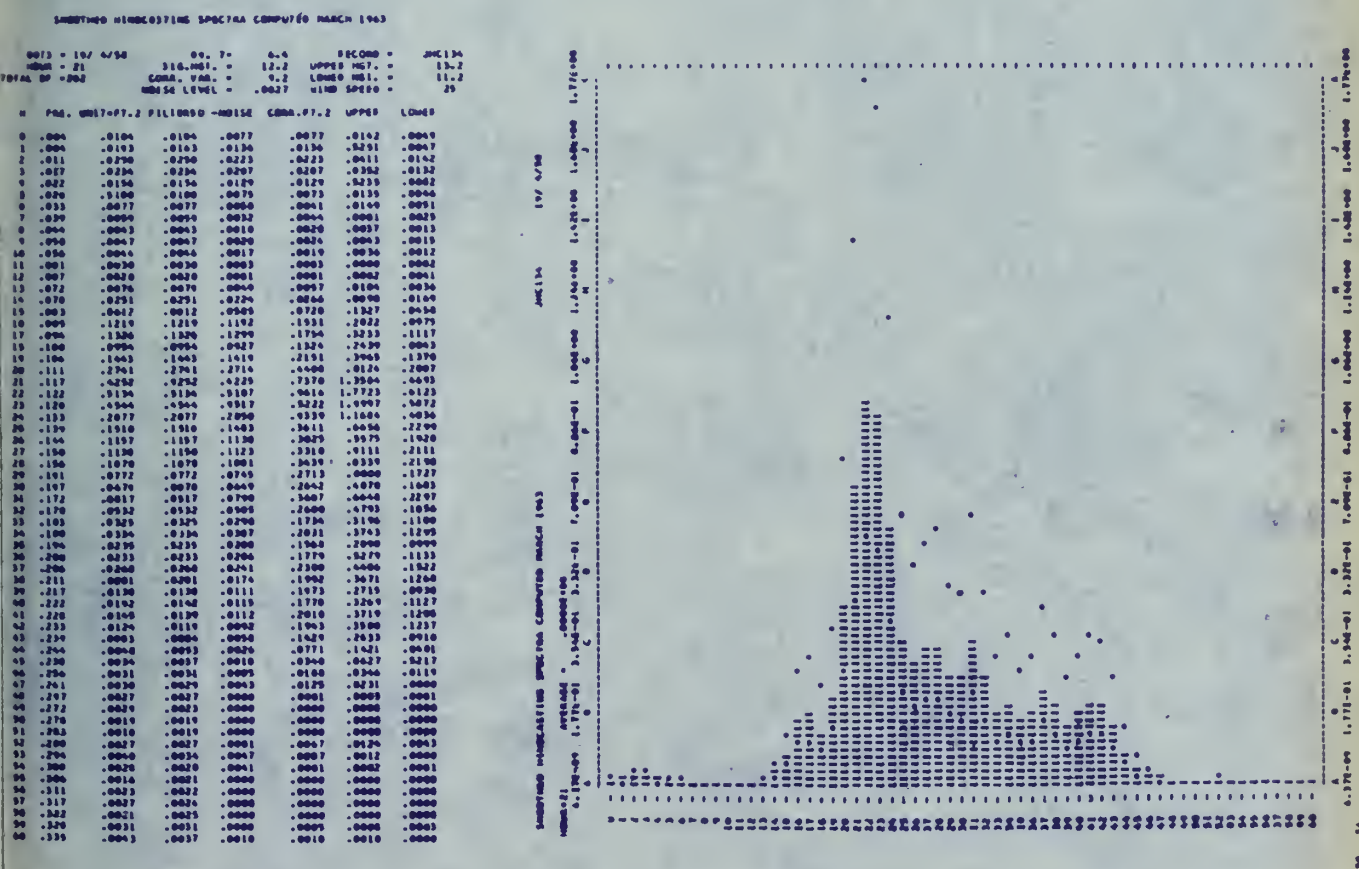

FIGURE 5A - SAMPLE PRESENTATION OF SEA SPECTRA FROM REF. (7), (8)

relationships are as follows:

$$H = 180 \times \text{frequency} = \frac{180\,\omega}{2\pi}$$

$$\left[\frac{r(\ln \omega)}{\lambda/2\pi}\right]^2 = \frac{\omega^5}{g^2}\left[r(\omega)\right]^2 = \frac{\omega^5}{g^2} \times \frac{180}{\pi} \times (\text{corr.ft}^2)$$

A short computer program, written in Fortran II source language, and shown in Figure 6, was used to convert the Pierson-Moskowitz Spectra to the log-slope form used in this thesis. A sample of the print-out is shown in Figure 7.

The next matter of interest is that of short-crestedness. This is not an easy matter to dispose of, simply because a short-crested sea may arise from different causes. As its name implies, a short-crested sea is one where the waves are coming toward the observer from various directions, thus producing a short-crested, choppy effect. The difficulty arises from the fact that a short-crested sea can be caused by one storm system, two storm systems or <u>any</u> number of storm systems. If we place ourselves on a ship lying to in the ocean, maintaining a steady true compass heading, it is perfectly possible to conceive of a storm system a few miles off the bow sending wind waves toward us and another storm system a long distance off the starboard quarter sending swell waves toward us. But there could just as well have been just one storm system or more than two and they could have been off in many com-

```
LAMFL
C
C     PROGRAM TO CONVERT CORA FT SEA SPECTRA TO LOG SLOPE FORM AND BA
      1 FORMAT (I5)
      2 FORMAT (12A6,A2)
      3 FORMAT (1H1,12A6,A2,/,1H0,'FREQUENCY IN OMEGA/2PI,CPS',/,' CORA FT
     1 ,'LOG LOG SLOPE FORM',/,1H0,'FREQ',7X,'DB')
      4 FORMAT (/,1X,F10.5,F11.4,3X,I5)
        DIMENSION CH(12),A(80),VAR(80)
        I = .0444
        N = 80
        READ 1, NBASES
        DO 22 K=1,NBASES
        DO 21 II = 1,80,10
        JJ = II+9
        READ 2,(CH(J), J=II,JJ)
        WRITE 2,(VAR(K), K=II,JJ)
        PRINT 3
        DO 22 J = 1,30
        C = J*I
        AC=C
        SL=0.*(10.**(-1.*A(J)))
        DEV=ABS(ABS(SL)-ABS(VAR(J)))
        DM=B*C
        DML=LOG10(DM)
        PRINT 4, AC,DM,DML,A(J),SL,DEV
     22 CONTINUE
     23 CALL SYSTEM
        END
```

FORTRAN II SOURCE PROGRAM TO CONVERT SEA SPECTRA FROM PIERSON-MOSKOWITZ FORM TO LOG-SLOPE FORM

FIGURE 6

LAG NO	OMEGA	LN OMEGA	CORR FT SQ	LOG SLOPE
6	.20940000E 00	-.15635090E 01	.55000000E-02	.12267494E-06
7	.24430000E 00	-.14093583E 01	.27000000E-02	.13016399E-06
8	.27920000E 00	-.12758269E 01	.70000000E-03	.65793785E-07
9	.31410000E 00	-.11580439E 01	.60000000E-03	.10162503E-06
10	.34900000E 00	-.10526834E 01	.47000000E-02	.13481393E-05
11	.38390000E 00	-.95737318E 00	.16700000E-01	.77146601E-05
12	.41880000E 00	-.87036180E 00	.24800000E-01	.17700878E-04
13	.45370000E 00	-.79031909E 00	.56900000E-01	.60599066E-04
14	.48860000E 00	-.71621112E 00	.16150000E 00	.24914353E-03
15	.52350000E 00	-.64721825E 00	.24090000E 00	.52472287E-03
16	.55840000E 00	-.58267972E 00	.20030000E 00	.60244550E-03
17	.59330000E 00	-.52205510E 00	.28600000E 00	.11647898E-02
18	.62820000E 00	-.46489669E 00	.44610000E 00	.24178628E-02
19	.66310000E 00	-.41082947E 00	.37000000E 00	.26278867E-02
20	.69800000E 00	-.35953618E 00	.25020000E 00	.22965409E-02
21	.73290000E 00	-.31074601E 00	.19010000E 00	.22269758E-02
22	.76780000E 00	-.26422600E 00	.16510000E 00	.24406043E-02
23	.80270000E 00	-.21977423E 00	.21000000E 00	.38769962E-02
24	.83760000E 00	-.17721462E 00	.26980000E 00	.61621896E-02
25	.87250000E 00	-.13639262E 00	.27310000E 00	.76499508E-02
26	.90740000E 00	-.97171911E-01	.14240000E 00	.48530373E-02
27	.94230000E 00	-.50431583E-01	.50600000E-01	.20826018E-02
28	.97720000E 00	-.23063939E-01	.72200000E-01	.35642180E-02
29	.10121000E 01	.12027381E-01	.99100000E-01	.58304295E-02
30	.10470000E 01	.45928933E-01	.73500000E-01	.51230726E-02
31	.10819000E 01	.78718755E-01	.30700000E-01	.25210633E-02
32	.11168000E 01	.11046745E 00	.25800000E-01	.24831703E-02
33	.11517000E 01	.14123911E 00	.34500000E-01	.38728055E-02
34	.11866000E 01	.17109208E 00	.27900000E-01	.36360989E-02
35	.12215000E 01	.20007961E 00	.13600000E-01	.20488777E-02

PIERSON-MOSKOWITZ
SEA SPECTRUM DL-88

SAMPLE OF PRINTOUT FROM SEA SPECTRUM CONVERSION PROGRAM

FIGURE 7

binations of distance and direction, so it is only possible to express what is happening at a certain place in the ocean at a certain time by a forecasting or hindcasting technique. Probably the most typical situation is a combination of wind waves caused by a local storm and swell coming from a distant storm or storms. This is a matter of great current interest to oceanographers and it is my hope that in another five to ten years they will have accumulated a large enough body of directional sea spectra so as to make a reasonably sized statistical sample possible.

However, for the moment, we must content ourselves with something less in our prediction methods, namely, either the use of long-crested seas or "unistorm" short-crested seas. It is the latter that I have chosen. This is a situation where one storm disturbance, because of its movement and irregular winds causes some spread in the wind direction and thus leads to a certain type of short-crestedness in the seas. These seas are characterized by a large amount of energy coming from a certain direction and progressively lesser amounts of energy as we look away from that direction until there is essentially zero energy coming from about 70 degrees on either side of the original direction.

This directional distribution of seaway energy may be characterized by multiplying a long-crested spectrum by a "spreading function." The one I have chosen is based on the work of Pierson, Neumann and James in (6) and is

$$\frac{2}{\pi} \cos^2 \mu w$$

The result of this directional spreading of seaway energy can be seen at the top of Figure 9. I have chosen this technique because it is computationally practical and is at the very least, one step closer to reality than assuming long-crested seas. It is pertinent to note that my experience while working at the David Taylor Model Basin showed that short-crested predictions by this method are consistently 8-9% lower than long-crested predictions of ship motion; at least for the head seas case.

With the foregoing background in mind it is in order now to proceed with a discussion of considerations that led to a final choice of sea spectra to represent the sea severity range of interest in these predictions.

It seems reasonable to state that as far as ship response is concerned, there are two characteristics of a seaway that are particularly important, namely the total energy, which is proportional to the area under the spectrum representing that seaway, and the

distribution of energy among the various component waves, an indication of which is given by the shape of the sea spectrum. One need only leaf through (7) to see that nature provides us with sea spectra of many different sizes and shapes.

Now, if we wish to investigate the effect of sea severity on ship response, it is necessary to establish a primary weather severity parameter. But in doing so, caution must be exercised in order that other parameters affecting ship-response are not ignored.

I have chosen significant wave height ($\breve{H}_{1/3}$) as the primary sea severity parameter because it is proportional to sea spectrum area and thus total seaway energy. ($\breve{H}_{1/3}$ is, by definition, the average height of the one-third highest waves in a seaway record. (6)). But, in order not to neglect the effect of sea spectrum shape on ship response, a family of sea spectra was needed where at each increment of the primary sea severity parameter, $\breve{H}_{1/3}$, there would be several spectra of close to the same $\breve{H}_{1/3}$, but having typical variations in shape among them.

The Moskowitz family of mean synoptic sea spectra found in (8) is the best family presently available most closely satisfying the above requirements.

The family consists of five mean sea spectra, each spectrum being the mean of 8 to 14 component spectra as shown in Table II. See Figure 8 for a plot of these five mean sea spectra.

TABLE II

Moskowitz Synoptic* Mean Spectrum Name	Number of Component Spectra	Average of Component Spectra $\hat{H}_{1/3}$ in.ft.
20KT	12	7.4
25	8	13.1
30	12	20.4
35	8	23.8
40	14	32.2

In each subset, the $\tilde{H}_{1/3}$ of the component spectra vary in most cases by no more than a few percent, thus assuring that the primary differences are those of spectral shape.

By comparing the ship response caused by the $\hat{H}_{1/3}$ = 7.4 ft. mean spectrum with the response caused by, say the $\breve{H}_{1/3}$ = 20.4 ft. mean spectrum, one can determine the effect of total seaway energy on response. On the other hand, by comparing the ship responses due to each of the 12 component spectra in the $\tilde{H}_{1/3}$ = 7.4 ft. subset, for example, one is able to evaluate the effect of spectral shape on ship response i.e., determine the

*Moskowitz classifies his spectra on the basis of wind speed in knots.

variance in response for a particular $\check{H}_{1/3}$. To my knowledge, it has not been attempted in previous work to separate these two effects and it is my hope that such an analysis will shed some light in our quest to learn more about the nature of ship response to a seaway.

The Moskowitz Synoptic Family of Mean Sea Spectra converted to the log-slope form is shown in Figure 8. It is noted that Moskowitz required that the sea records chosen for his family satisfy certain synoptic criteria as regards non-transient wind conditions, duration, fetch, etc, all of which tend to insure that the seas represented are fully developed or close to it. He has also eliminated swell from all records used. So one must keep in mind that the ship response predictions correspond to the nearly fully developed wind sea with no swell situation which, of course, is not a precise duplication of nature.

When there is available a larger source of sea spectrum data, I believe the soundest approach would be to pick out all those records having very close to the same $\check{H}_{1/3}$ without requiring that any synoptic criteria be satisfied. Thus, if the sample were large enough, one would be reasonably assured that a representative variation in degree of sea development would be

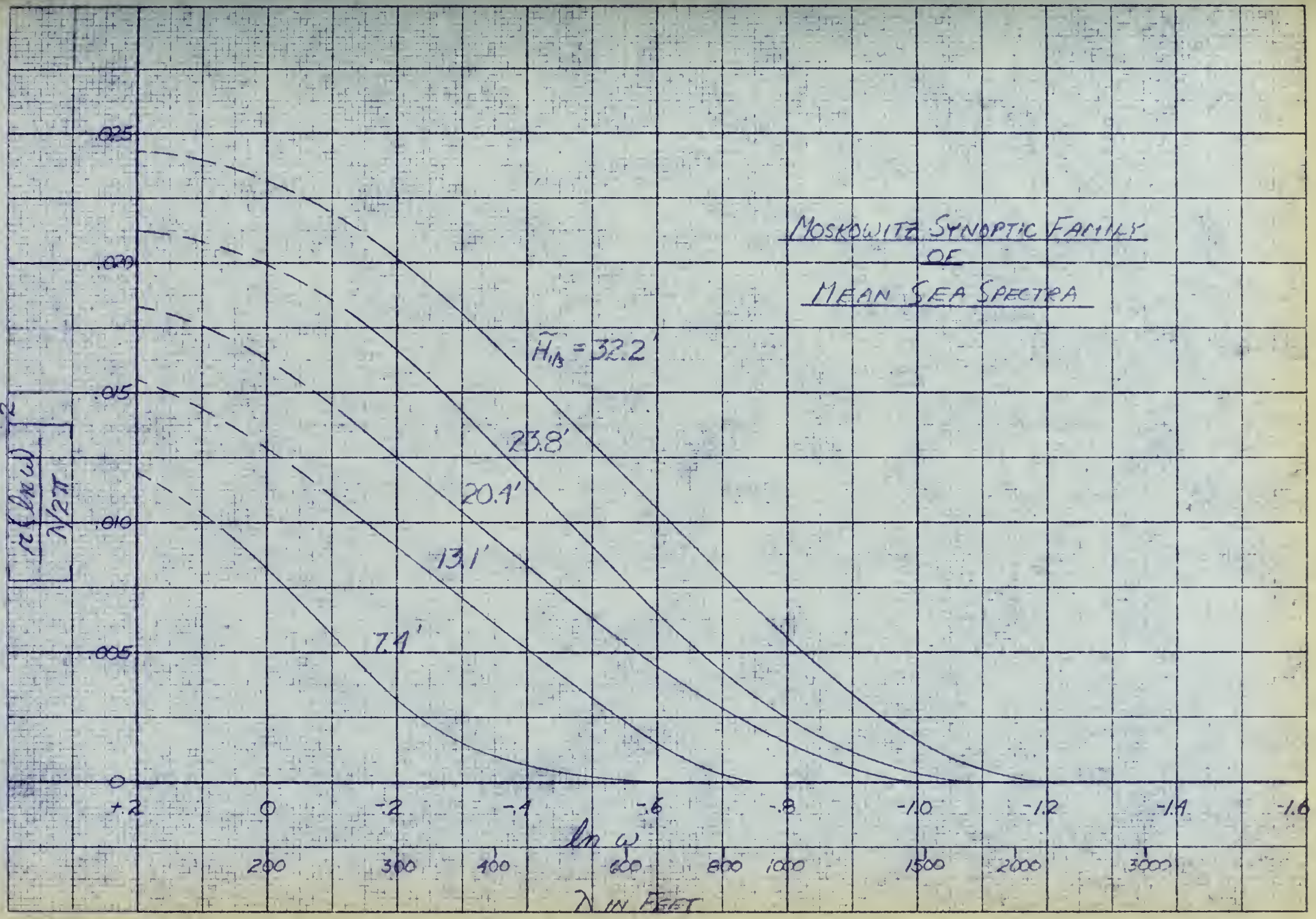
MOSKOWITZ SYNOPTIC FAMILY
OF
MEAN SEA SPECTRA
$\bar{H}_{1/3} = 32.2'$
23.8'
20.1'
13.1'
7.1'
$\frac{\pi^2 H^2_{1/3}}{\lambda/2\pi} \frac{2}{\ln \omega}$
.025
.020
.015
.010
.005
0
+.2
0
-.2
-.4
-.6
-.8
-1.0
-1.2
-1.4
-1.6
ln ω
200
300
400
600
800
1000
1500
2000
3000
λ IN FEET

FIGURE 8

included. Each sample of records having the same $\bar{H}_{1/3}$, then, would have the variation in spectral shape previously referred to, and then one could proceed as in this analysis.

Computation of Response Data

Once the prerequisite information, namely sea spectra and RAO's are in hand, one may proceed to calculate ship response.

A verbal description of the computations will be given to accompany the graphic illustration given in Figure 9. First, the long-crested sea spectrum is "spread" or directionalized using the $\frac{2}{\pi}\cos^2\mu_w$ spreading function previously described. This operation results in the short-crested sea spectra shown by dotted lines.

Next, the directional RAO's are plotted on the same $\ln\omega$ abscissa and a decision is made as to which RAO's are going to be multiplied by which sea spectrum component at each increment of $\ln\omega$. Figures 10 and 10a will aid in this "matching" process. Say, for example, we want to compute acceleration response for the head seas case ($\mu = 180^\circ$) as is shown in Figure 9. We align the heavy wind arrow on Figure 10 with the Head Seas marker on Figure 10a and see that the 180° RAO must be multiplied by the 0° sea spectrum component, the 157 1/2°/202 1/2°

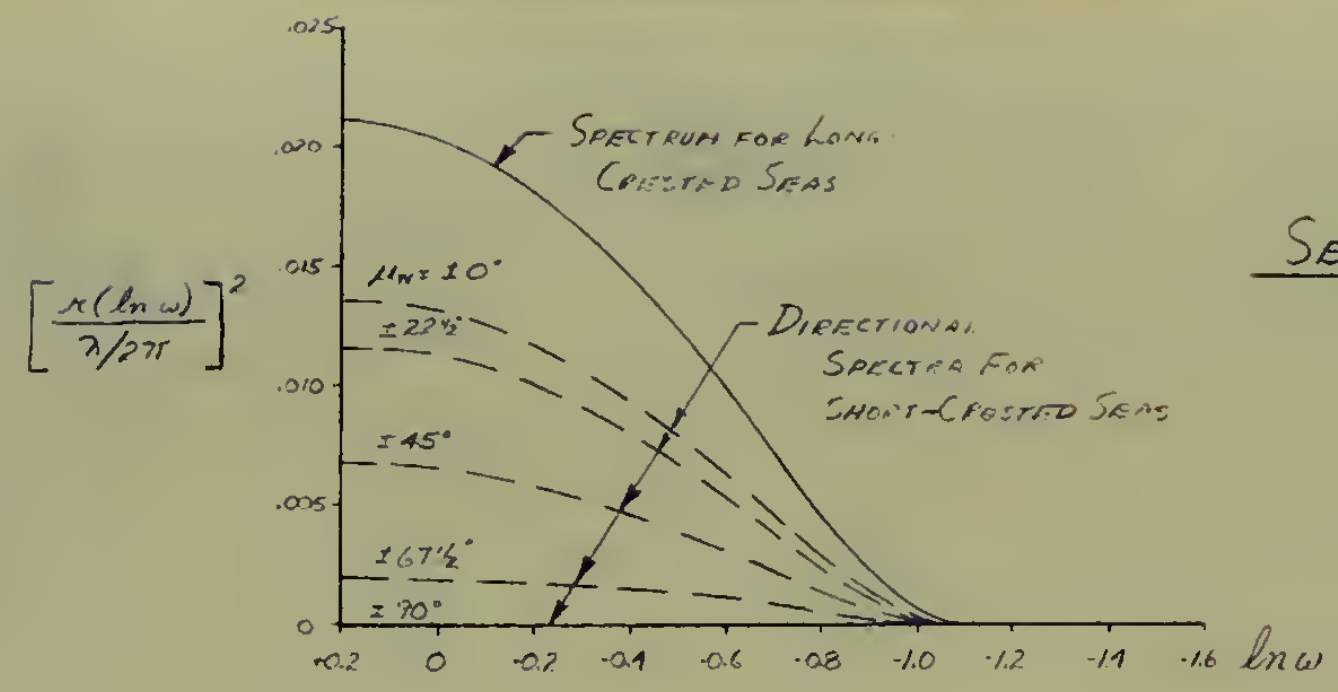

SEA SPECTRUM

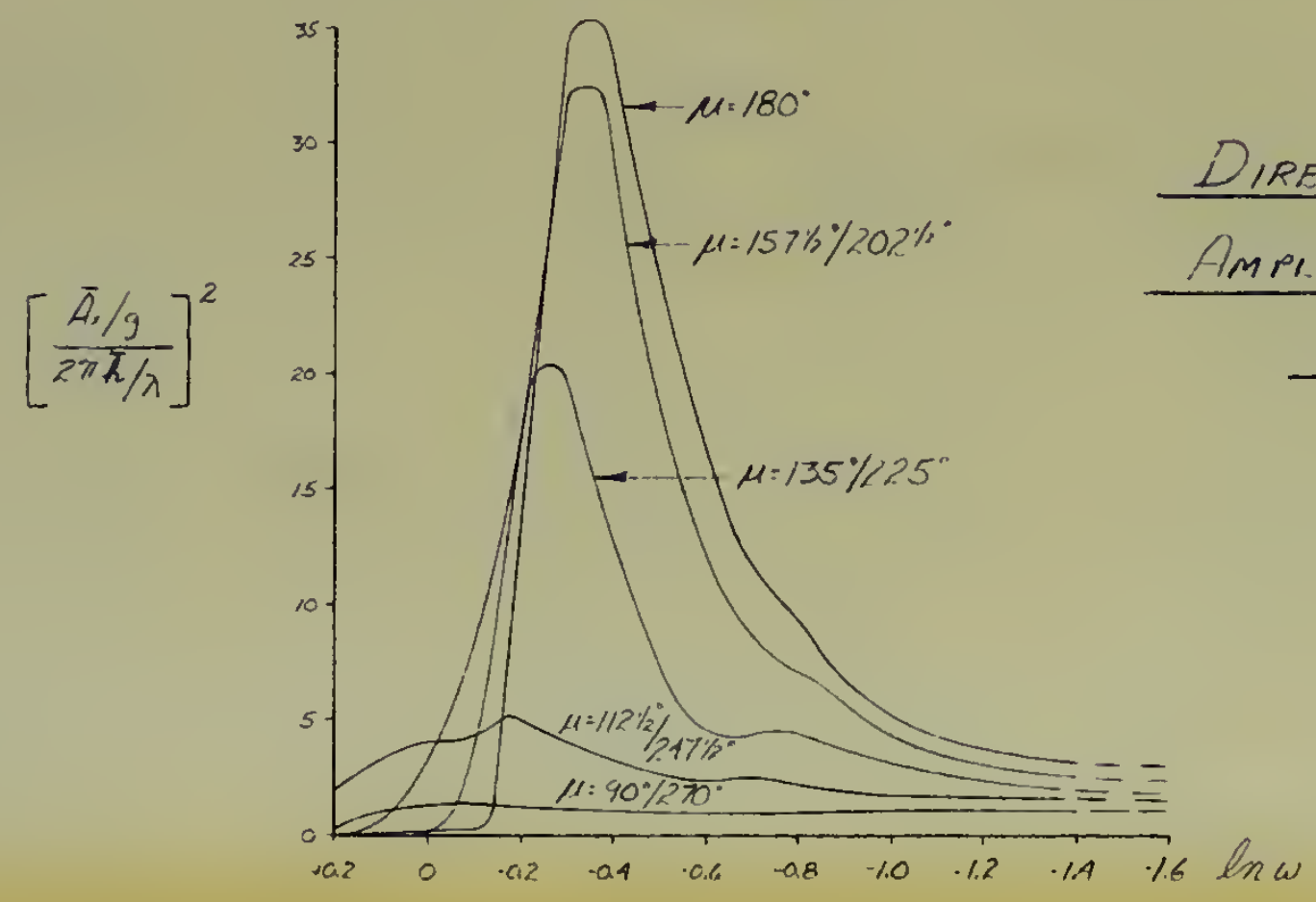

DIRECTIONAL RESPONSE AMPLITUDE OPERATORS

$L = 370'$

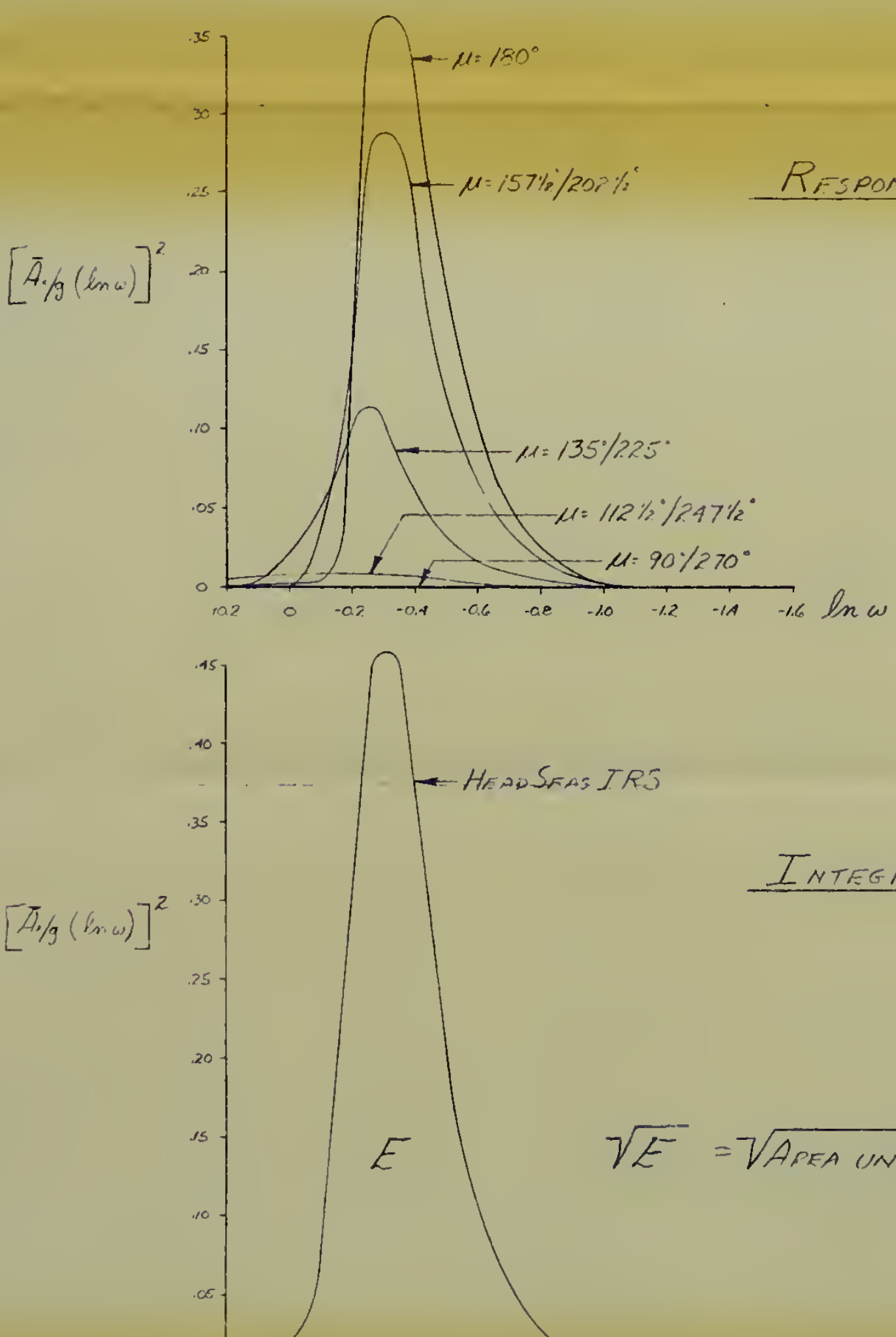

RESPONSE SPECTRUM COMPONENTS

INTEGRATED RESPONSE SPECTRUM

$\mu = 180°$

$$E \qquad \sqrt{E} = \sqrt{\text{AREA UNDER IRS}}$$

FIGURE 2

Directional Sea Spectrum

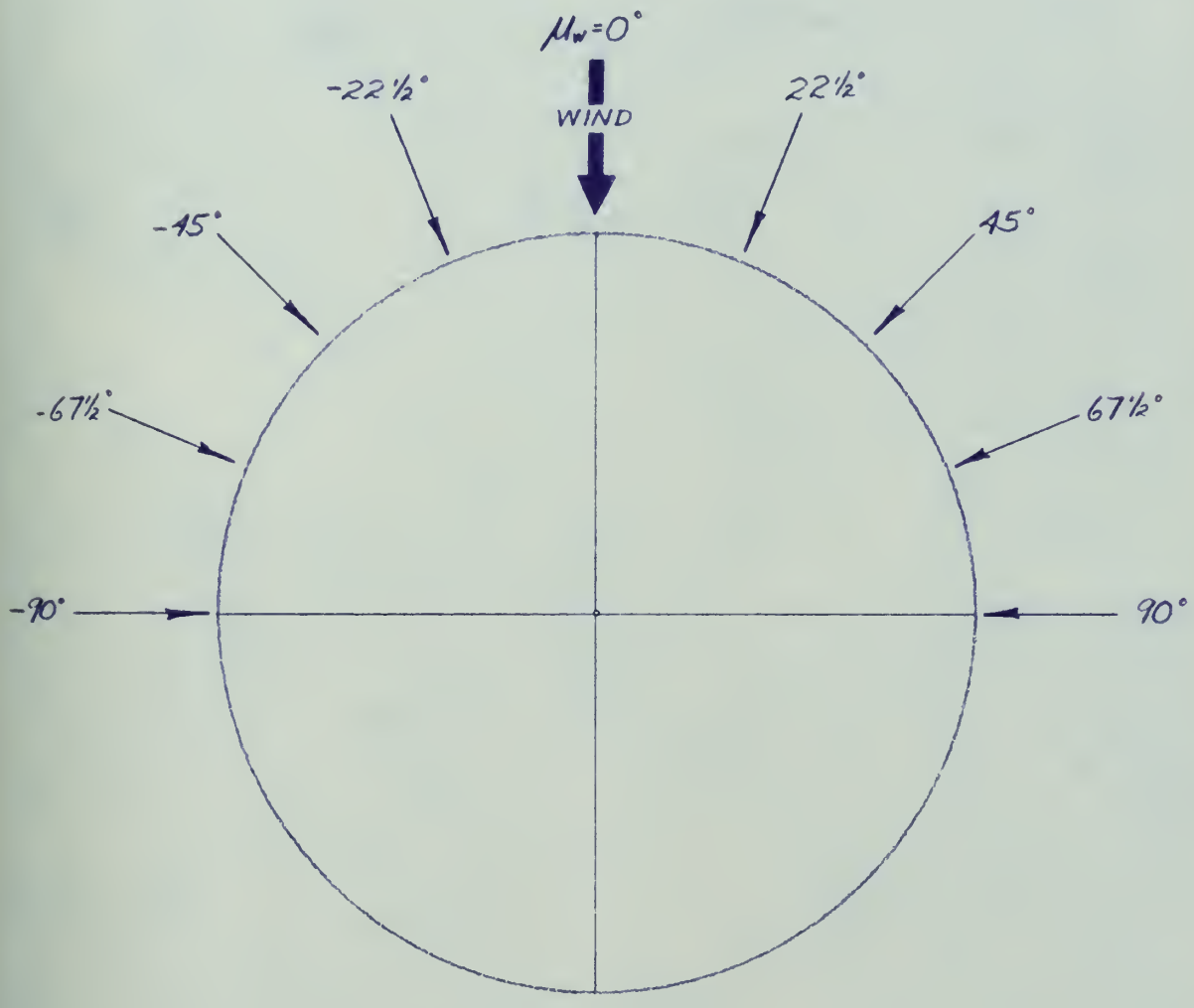

Sea Spectrum/RAO Alignment Aid

Part 1

Figure 10

RESPONSE AMPLITUDE OPERATORS

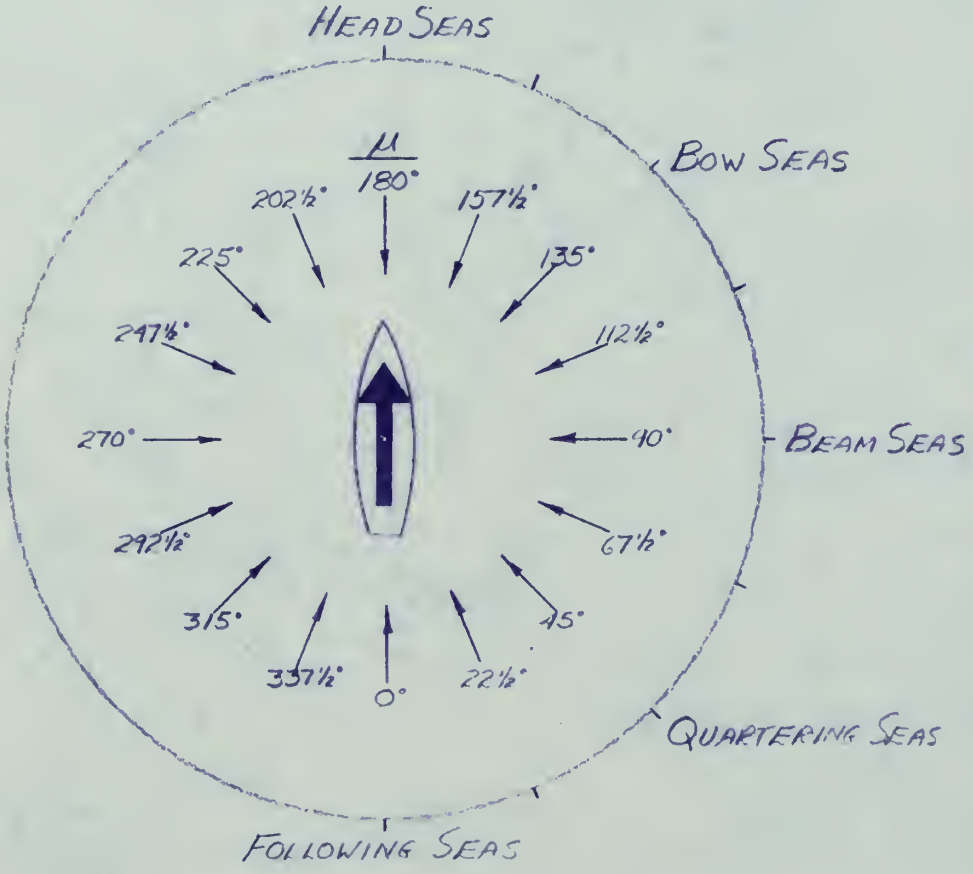

SEA SPECTRUM/RAO ALIGNMENT AID

PART 2

FIGURE 10a

RAO's (which are the same, of course, by symmetry) must be multiplied by the 22 1/2° sea spectrum component and so on for as many of the RAO components as are affected by the various sea spectrum components.

This is done at each increment of $\ln\omega$ and results in the nine response spectrum components (only five curves show because of symmetry).

Now if one imagines a third dimension to the Response Spectrum Component curves whose axis is normal to the plane of the paper and whose coordinate is μ, it is possible to visualize the integration with respect to μ of the points from the Response Spectrum Component curves on the crossplot for each $\ln\omega$ increment to arrive at a point on the Integrated Response Spectrum for that value of $\ln\omega$. After the Integrated Response Spectrum is thus computed, one may integrate over $\ln\omega$ to arrive at the area under it which is the value of $(\sqrt{E})^2$ for the case considered, namely head seas, ship length = 370 ft. ($\sqrt{E}$ is a ship response parameter that is discussed in detail in Appendix A. Briefly, the $\sqrt{E}$ parameter reflects certain statistical properties of a short-term sample record of response during invariant conditions of weather, speed and heading.) The angular integration and then the $\ln\omega$ integration were done using Simpson's Rule in the computational scheme employed. Nineteen $\ln\omega$ increments

of 0.1 each were used along with the 22 1/2° angular increments as shown. The right and left hand extremities of the $\ln\omega$ scale, namely, -1.6 and +0.2, respectively, were determined by the termination of most typical sea spectra on the right hand end and the termination of the RAO's on the left hand end.

The process described above can then be done for the eight other headings between head and following seas so that each sea spectrum and each set of RAO's for a given ship length results in nine $\sqrt{E}$ values, one for each heading from head to following seas at 22 1/2° increments.

This was done for the five Moskowitz Synoptic Mean Spectra for each of the five ship lengths and at nine headings, resulting in the 225 $\sqrt{E}$ values found in Figure 11.

Since each one of these $\sqrt{E}$ values is the result of the process of computation just described, where sea spectrum components are multiplied by RAO components to arrive at the Response Spectrum Components which are integrated to arrive at the Integrated Response Spectrum which in turn is integrated to arrive at the $\sqrt{E}$ value, it can readily be seen that a very large number of numerical calculations are involved. However, since

FIGURE 11

SAMPLE MEAN $\sqrt{3}$ ACCELERATION VALUES ($\bar{x}$) in g's

$\hat{H}_{1/3}$ = 7.4' (Moskowitz 20KT Synoptic Mean Spectrum)

Ship Length → / ↓	248'	302'	370'	452'	552'
180°	.2108	.1676	.1238	.0885	.0594
157 1/2	.2021	.1631	.1212	.0882	.0594
135	.1783	.1476	.1148	.0874	.0625
112 1/2	.1467	.1261	.0999	.0776	.0559
90	.1037	.0946	.0812	.0676	.0516
67 1/2	.0660	.0621	.0544	.0453	.0348
45	.0352	.0354	.0335	.0296	.0233
22 1/2	.0157	.0158	.0151	.0130	.0101
0	.0090	.0090	.0090	.0085	.0063

$\hat{H}_{1/3}$ = 13.1' (Moskowitz 25KT Synoptic Mean Spectrum)

180°	.3181	.2843	.2467	.2062	.1623
157 1/2	.3033	.2727	.2369	.1993	.1574
135	.2644	.2408	.2122	.1815	.1462
112 1/2	.2117	.1967	.1747	.1521	.1242
90	.1470	.1412	.1298	.1168	.0985
67 1/2	.0921	.0901	.0838	.0758	.0646
45	.0489	.0497	.0484	.0452	.0393
22 1/2	.0222	.0224	.0218	.0199	.0173
0	.0128	.0128	.0128	.0124	.0105

$\hat{H}_{1/3}$ = 20.4' (Moskowitz 30KT Synoptic Mean Spectrum)

180°	.3753	.3447	.3106	.2742	.2356
157 1/2	.3576	.3300	.2975	.2634	.2264
135	.3112	.2901	.2641	.2363	.2047
112 1/2	.2481	.2349	.2147	.1942	.1689
90	.1722	.1675	.1572	.1483	.1283
67 1/2	.1079	.1066	.1008	.0934	.0828
45	.0578	.0588	.0576	.0547	.0489
22 1/2	.0265	.0267	.0262	.0244	.0217
0	.0154	.0154	.0154	.0150	.0131

FIGURE 11 (Cont'd)

SAMPLE MEAN $\sqrt{E}$ ACCELERATION VALUES ($\bar{x}$) in g's

$\tilde{H}_{1/3}$ = 23.8' (Moskowitz 35KT Synoptic Mean Spectrum)

Ship Length → / μ ↓	248'	302'	370'	452'	552'
180°	.4287	.3994	.3646	.3252	.2823
157 1/2	.4082	.3819	.3488	.3121	.2711
135	.3548	.3348	.3085	.2787	.2439
112 1/2	.2817	.2698	.2496	.2282	.2006
90	.1951	.1914	.1812	.1691	.1509
67 1/2	.1222	.1214	.1158	.1084	.0972
45	.0655	.0667	.0657	.0628	.0569
22 1/2	.0302	.0304	.0299	.0280	.0254
0	.0176	.0176	.0176	.0171	.0152

$\hat{H}_{1/3}$ = 32.2' (Moskowitz 40 KT Synoptic Mean Spectrum)

180°	.4782	.4524	.4220	.3871	.3485
157 1/2	.4554	.4323	.4032	.3707	.3337
135	.3957	.3784	.3554	.3289	.2973
112 1/2	.3139	.3038	.2858	.2668	.2416
90	.2179	.2153	.2064	.1955	.1786
67 1/2	.1369	.1366	.1315	.1248	.1142
45	.0741	.0754	.0745	.0718	.0660
22 1/2	.0345	.0347	.0341	.0323	.0296
0	.0201	.0201	.0201	.0196	.0177

these calculations are of a repetitive nature, including several cyclic permutations, they are especially amenable to calculation by electronic computer, and this is how they were carried out.

The program shown in Figure 12, based on a similar one in use at Webb Institute, was written by the author in the Fortran II source language while on temporary duty at the David Taylor Model Basin and the calculations were carried out on the UNIVAC LARC facility there. A sample of the print-out can be seen in Figure 13. It might interest the reader to know that the computer took less than three minutes to compute the 225 $\sqrt{E}$ values and having done similar calculations with a desk computer, I estimate it would take about a month of 8-hour days to calculate the same number of $\sqrt{E}$ values manually. Thus it is seen how the electronic computer can greatly enhance the scope of an investigation like this one.

The tabulation of $\sqrt{E}$ values in Figure 11 shows the effect of seaway total energy on acceleration response, but it does not show the effect of sea spectrum shape.

As previously described, the effect of sea spectrum shape on ship response was to be evaluated by computing $\sqrt{E}$ values for each of the component sea spectra in the

```
LABEL     CKSRD
C     FORTRAN TWO PROGRAM TO COMPUTE SMIH RESPONSE SPECTRA FROM RSI
C     RSC IS RESPONSE SPECTRUM COMPONENT, S IS SEA SPECTRUM
C     RSI IS INTEGRATED RESPONSE SPECTRUM, SM IS SIMPSONS MULTIPLIER
C     RAO IS RESPONSE OPERATOR, SPECTRUM IS QUOTIENT OF OMEGA
C     AREA UNDER RSI EQUALS 0.09999999SUM1, 9 IS NUMBER OF SINGLE AMPLITUDES
    1 FORMAT (8F7.4)
    2 FORMAT (10E12.7)
    3 FORMAT (I5)
    5 FORMAT (5F10.4          SHIP LENGTH )
    6 FORMAT (30H SMS RESPONSE FOR MU EQUAL 0 OF HEADING IS ,E12.4)
    4 FORMAT (1H1, 47X, 18H SEA SPECTRUM)
      DIMENSION SM(29), RSI(19, 9, 9), X(17,19,9), RC(17), PR(17), S(19)
      A = 0.624
      B = 0.262
      SM (1) = 1.
      SM (2) = 4.
      SM (3) =2.
      SM (4) = 4.
      SM (5) = 2.
      SM (6) =4.
      SM (7) = 2.
      SM (8) = 4.
      SM (9) = 2.
      SM(10) = 4.
      SM(11) = 2.
      SM(12) = 4.
      SM(13) = 2.
      SM(14) = 4.
      SM(15) = 2.
      SM(16) = 4.
      SM(17) = 2.
      SM(18) = 4.
      SM(19) = 1.
      DO 39 L = 1,5
      DO 99 I = 1,19
      READ 1,X(1,I,L),X(2,I,L),X(3,I,L),X(4,I,L),X(5,I,L),X(6,I,L)
      READ 1,X(7,I,L),X(8,I,L),X(9,I,L),X(10,I,L),X(11,I,L),X(12,I,L)
      READ 1,X(13,I,L),X(14,I,L),X(15,I,L),X(16,I,L),X(17,I,L)
  99  CONTINUE
      READ 3, KASES
      DO 69 I = 1,KASES
  32  READ 2,S(1),S(2),S(3),S(4),S(5),S(6),S(7),S(8),S(9),S(10)
      READ 2,S(11),S(12),S(13),S(14),S(15),S(16),S(17),S(18),S(19)
      PRINT 9
      DO 69 L = 1,5
      PRINT 7
      DMUW = 0.9927
      DO 69 MUZ = 1,9
      SUM = 0.0
      PMUZ = MUZ-1
      PMUZ = 22.5*PMUZ
      DO 66 LO = 1,19,1
      RSI (LO) = 0.0
      LLO = LO- 3
      JMU = MUZ
      AMUW = -1.5708
      DO 63 N=1,5,1
      RC(JMU) = X(JMU,LO,L)*S(LO)*0.637*(COSF(AMUW))**2
      PR(JMU)=RC(JMU)*B
```

FORTRAN II SOURCE PROGRAM TO COMPUTE ACCELERATION RESPONSE

FIGURE 12

```
      PJMU=JM(I-1)
      P JMU = 2PI * P JMU - 8D+11
      S(I)=SIN(P(I)+P(JMU))
      JM(I)=JMU
      GO TO 1000
      DBJM=DMAX1(DBJM,DB)
      P(JMU) = JM(I)
      P JMU = P JMU + P(JMU) - 8D+11
      S(I)=S(I)+S(I-1)+P(JMU)
      JM(I)=JMU+1
  961 CONTINUE
      S(NM)=S(I)+S(NM-1)+P(JMU)
  964 CONTINUE
      Q=SQRT(S(NM)/(NM-1))
      APIAI 6.+PMU8+9
   DA+ CONTINUE
      CALL EXIT
      END
END OF TAPE
```


FIGURE 12 CONT'D

SEA SPECTRUM SHC 063 ACCELERATION RESPONSE

SHIP LENGTH 1 248'

RMS RESPONSE FOR MJ SJB 0 OF 0.0 IS 0.9350E-02
RMS RESPONSE FOR MJ SJB 0 OF 22.5 IS 0.1539E-01
RMS RESPONSE FOR MJ SJB 0 OF 45.0 IS 0.3707E-01
RMS RESPONSE FOR MJ SJB 0 OF 67.5 IS 0.6931E-01
RMS RESPONSE FOR MJ SJB 0 OF 90.0 IS 0.1089E 00
RMS RESPONSE FOR MJ SJB 0 OF 112.5 IS 0.1521E 00
RMS RESPONSE FOR MJ SJB 0 OF 135.0 IS 0.1827E 00
RMS RESPONSE FOR MJ SJB 0 OF 157.5 IS 0.2059E 00
RMS RESPONSE FOR MJ SJB 0 OF 180.0 IS 0.2141E 00

SHIP LENGTH 2 302'

RMS RESPONSE FOR MJ SJB 0 OF 0.0 IS 0.9350E-02
RMS RESPONSE FOR MJ SJB 0 OF 22.5 IS 0.1546E-01
RMS RESPONSE FOR MJ SJB 0 OF 45.0 IS 0.3681E-01
RMS RESPONSE FOR MJ SJB 0 OF 67.5 IS 0.6371E-01
RMS RESPONSE FOR MJ SJB 0 OF 90.0 IS 0.9629E-01
RMS RESPONSE FOR MJ SJB 0 OF 112.5 IS 0.1256E 00
RMS RESPONSE FOR MJ SJB 0 OF 135.0 IS 0.1461E 00
RMS RESPONSE FOR MJ SJB 0 OF 157.5 IS 0.1501E 00
RMS RESPONSE FOR MJ SJB 0 OF 180.0 IS 0.1642E 00

SHIP LENGTH 3 370'

RMS RESPONSE FOR MJ SJB 0 OF 0.0 IS 0.9350E-02
RMS RESPONSE FOR MJ SJB 0 OF 22.5 IS 0.1570E-01
RMS RESPONSE FOR MJ SJB 0 OF 45.0 IS 0.3487E-01
RMS RESPONSE FOR MJ SJB 0 OF 67.5 IS 0.5593E-01
RMS RESPONSE FOR MJ SJB 0 OF 90.0 IS 0.8302E-01
RMS RESPONSE FOR MJ SJB 0 OF 112.5 IS 0.1005E 00
RMS RESPONSE FOR MJ SJB 0 OF 135.0 IS 0.1146E 00
RMS RESPONSE FOR MJ SJB 0 OF 157.5 IS 0.1209E 00
RMS RESPONSE FOR MJ SJB 0 OF 180.0 IS 0.1217E 00

SHIP LENGTH 4 452'

RMS RESPONSE FOR MJ SJB 0 OF 0.0 IS 0.8743E-02
RMS RESPONSE FOR MJ SJB 0 OF 22.5 IS 0.1347E-01
RMS RESPONSE FOR MJ SJB 0 OF 45.0 IS 0.3054E-01
RMS RESPONSE FOR MJ SJB 0 OF 67.5 IS 0.4604E-01
RMS RESPONSE FOR MJ SJB 0 OF 90.0 IS 0.5829E-01
RMS RESPONSE FOR MJ SJB 0 OF 112.5 IS 0.7635E-01
RMS RESPONSE FOR MJ SJB 0 OF 135.0 IS 0.8521E-01
RMS RESPONSE FOR MJ SJB 0 OF 157.5 IS 0.8356E-01
RMS RESPONSE FOR MJ SJB 0 OF 180.0 IS 0.8360E-01

SHIP LENGTH 5 552'

RMS RESPONSE FOR MJ SJB 0 OF 0.0 IS 0.5527E-02
RMS RESPONSE FOR MJ SJB 0 OF 22.5 IS 0.1011E-01
RMS RESPONSE FOR MJ SJB 0 OF 45.0 IS 0.2347E-01
RMS RESPONSE FOR MJ SJB 0 OF 67.5 IS 0.3413E-01
RMS RESPONSE FOR MJ SJB 0 OF 90.0 IS 0.5057E-01
RMS RESPONSE FOR MJ SJB 0 OF 112.5 IS 0.5224E-01
RMS RESPONSE FOR MJ SJB 0 OF 135.0 IS 0.4720E-01
RMS RESPONSE FOR MJ SJB 0 OF 157.5 IS 0.3089E-01
RMS RESPONSE FOR MJ SJB 0 OF 180.0 IS 0.4985E-01

SAMPLE PRINTOUT FROM ACCELERATION RESPONSE COMPUTER PROGRAM

FIGURE 13

five Moskowitz subsets. Since there are a total of 54 component spectra in the Moskowitz Synoptic Family of five mean spectra, converting each of these to the log-slope form, plotting them, tabulating and card-punching them as input to the ship response computer program would have been too formidable a task to undertake in this thesis. Instead, the above was done only for the 12 component spectra of the $\hat{H}_{1/3}$ = 7.4 ft. mean spectrum and the 14 component spectra of the $\tilde{H}_{1/3}$ = 32.2 ft. mean spectrum so as to bracket the range of the primary sea severity parameter $\hat{H}_{1/3}$. The response characteristics for intermediate values of $\tilde{H}_{1/3}$ were obtained using straight line interpolation which turned out to be a quite reasonable procedure as will be discussed later.

The $\sqrt{E}$ values for all nine headings and five ship lengths in the 12 component sea spectra of the $\hat{H}_{1/3}$ = 7.4 ft. subset and in the 14 component sea spectra of the $\tilde{H}_{1/3}$ = 32.2 ft. subset were computed using the same computational scheme as was previously described and then for each combination of ship length and heading, the following important characteristics of the $\sqrt{E}$ distribution were determined:

(a) the sample mean of $\sqrt{E}$ was computed using

$$\bar{x} = \frac{1}{n} \sum_{i=1}^{n} x_i$$

where n = 12 or 14 depending on which subset was under consideration and $\bar{x}$ = sample mean $\sqrt{E}$ and $x_i = (\sqrt{E})_i$

(b) the variance of $\sqrt{E}$ was computed using:

$$s^2 = \frac{1}{n-1}\left(\sum_{i=1}^{n} (x_i)^2 - n\,\bar{x}^2\right)$$

again where n = 12 or 14 and s^2 = sample variance and s = sample deviation

These computations also were done on the DTMB UNIVAC LARC using the Fortran II source program written for this purpose which is shown in Figure 14. This program is similar to the one in Figure 12 except that a section for computation of sample means and deviations was added onto the section that computed the $\sqrt{E}$ values. The print-out of results from this program may be seen in Figures 15 and 15a.

At this point, one small issue was disposed of. For each ship length and heading, the mean $\sqrt{E}$ values in Figure 15, for example, should agree with the $\sqrt{E}$ values given in Figure 11 for the $\hat{H}_{1/3}$ = 7.4 ft. mean sea spectrum, that is to say that the mean value of $\sqrt{E}$ obtained using the subset component spectra should be equal to the $\sqrt{E}$ obtained using the mean sea spectrum. This is mainly a crosscheck on the computational scheme used. A comparison of the data shows a maximum difference in the order of 4 percent, so the procedure of using a mean sea spectrum to obtain mean $\sqrt{E}$ response seems justified. This conclusion engenders confidence in the $\sqrt{E}$ values shown in Figure 11, because the ones for the

```
LABEL      CKSRL
C      FORTRAN TWO PROGRAM TO COMPUTE SHIP RESPONSE DATA PLUS SAMPLE
C      MEANS AND DEVIATIONS  FEB 65
C      RSI IS INTEGRATED RESPONSE SPECTRUM, SM IS SIMPSONS MULTIPLIER
C      SEA AND RESPONSE SPECTRA ARE AGAINST LN OMEGA
C      RC IS RESPONSE SPECTRUM COMPONENT, S IS SEA SPECTRUM
C      AREA UNDER RSI EQUALS 0.03333(SUM), G IS RMS OF SINGLE AMPLITUDES
C      DEV IS SAMPLE DEVIATION, XBAR IS SAMPLE MEAN
    1 FORMAT (6F7.4)
    2 FORMAT (10E7.2)
    3 FORMAT (I5)
    7 FORMAT (/17H      SHIP LENGTH ,I3)
    8 FORMAT (30H RMS RESPONSE FOR MU SUB 0 OF ,F6.1,4H IS ,E12.4)
    9 FORMAT (1H1, 37X, 13H SEA SPECTRUM, 20X,22H ACCELERATION RESPONSE)
   10 FORMAT (1H1, 37X, 13H SEA SPECTRUM, 20X, 18H VELOCITY RESPONSE)
   11 FORMAT (1H1, 37X, 13H SEA SPECTRUM, 20X,22H DISPLACEMENT RESPONSE)
    3 FORMAT (1H1, 42X, 24H ACCELERATION DEVIATIONS)
   31 FORMAT (1H1, 44X, 20H VELOCITY DEVIATIONS)
   36 FORMAT (34H SAMPLE DEVIATION FOR MU SUB 0 OF ,F6.1,4H IS ,E14.8,13
     1H AND XBAR IS ,E14.8)
   38 FORMAT (1H1, 42X, 24H DISPLACEMENT DEVIATIONS)
      DIMENSION SM(19), RSI(19), X(17,19,5), RC(17), PR(17), S(19), W(26
     1,5,9), QS(20,5,9)
      A = 0.524
      B = 0.262
      SM (1) = 1.
      SM (2) = 4.
      SM (3) =2.
      SM (4) = 4.
      SM (5) = 2.
      SM (6) =4.
      SM (7) = 2.
      SM (8) = 4.
      SM (9) = 2.
      SM(10) = 4.
      SM(11) = 2.
      SM(12) = 4.
      SM(13) = 2.
      SM(14) = 4.
      SM(15) = 2.
      SM(16) = 4.
      SM(17) = 2.
      SM(18) = 4.
      SM(19) = 1.
      DO 19 LI = 1,3
      DO 39 L = 1,5
      DO 39 I = 1,19
      READ 1,X(1,I,L),X(2,I,L),X(3,I,L),X(4,I,L),X(5,I,L),X(6,I,L)
      READ 1,X(7,I,L),X(8,I,L),X(9,I,L),X(10,I,L),X(11,I,L),X(12,I,L)
      READ 1,X(13,I,L),X(14,I,L),X(15,I,L),X(16,I,L),X(17,I,L)
  039 CONTINUE
      READ 3, KASES
      DO 69 I = 1,KASES
   32 READ 2,S(1),S(2),S(3),S(4),S(5),S(6),S(7),S(8),S(9),S(10)
      READ 2,S(11),S(12),S(13),S(14),S(15),S(16),S(17),S(18),S(19)
      GO TO (33,34,35), LI
   33 PRINT 9
      GO TO 37
   34 PRINT 10
      GO TO 37
```

FORTRAN II SOURCE PROGRAM TO COMPUTE SAMPLE MEANS & DEVIATIONS

FIGURE 13

```
 35 PRINT 11
 37 DO 69 L = 1,5
    PRINT 7, L
    DMUW = 0.3927
    DO 69 MUZ = 1,9
    SUM = 0.0
    PMUZ = MUZ-1
    PMUZ = 22.5*PMUZ
    DO 66 LO = 1,19,1
    RSI(LO) = 0.0
    LLO = LO- 2
    JMU = MUZ
    AMUW = -1.5708
    DO 63 N=1,5,1
    RC(JMU) = X(JMU,LO,L)*S(L  )*0.637*(COSF(AMUW))**2
    PR(JMU)=RC(JMU)*8
    PJMU=JMU-1
    PJMU = 22.5 * PJMU - 90.0
    RSI(LO)=RSI(LO)+PR(JMU)
    AMUW=AMUW+DMUW
    JMU=JMU+1
    GO TO (57,57,57,57,63),N
 57 RC(JMU) = X(JMU,LO,L)*S(LO)*0.637*(COSF(AMUW))**2
    PR(JMU)=RC(JMU)*A
    PJMU = JMU-1
    PJMU = 22.5 * PJMU - 90.0
    RSI(LO)=RSI(LO)+PR(JMU)
    AMUW=AMUW+DMUW
    JMU=JMU+1
063 CONTINUE
    SUM=RSI(LO)*SM(LO)+SUM
066 CONTINUE
    Q(I,L,MUZ) = SQRTF (SUM*0.03333)
    PRINT 8, PMUZ, Q(I,L,MUZ)
069 CONTINUE
    READ 3, K
    XK = K
    GO TO (55,56,58), L
 55 PRINT 30
    GO TO 12
 56 PRINT 31
    GO TO 12
 58 PRINT 38
 12 DO 16 L = 1,5
    PRINT 7, L
    DO 16 MUZ = 1,9
    SUM = 0.0
    TSUM = 0.0
 13 DO 15 I = 1,12
    QS(I,L,MUZ) = Q(I,L,MUZ)**2
    SUM = SUM + Q(I,L,MUZ)
    TSUM = TSUM + QS(I,L,MUZ)
 15 CONTINUE
    XB = SUM/XK
    R = XK*((XB)**2)
    VAR = (1.0/(XK-1.0))*(TSUM - R)
    DEV = SQRTF(VAR)
    N1 = MUZ - 1
    N1 = 22.5*N1
    PRINT 36, N1, DEV, XB
```


FIGURE 14 CONT'D

```
   16 CONTINUE
      READ 3, K
      XK = K
      GO TO (155,156,158), L1
  155 PRINT 30
      GO TO 88
  156 PRINT 31
      GO TO 88
  158 PRINT 38
   88 DO 19 L = 1,5
      PRINT 7, L
      DO 19 MUZ = 1,9
      SUM = .0
      TSUM = 0.0
   14 DO 17 I = 16,26
      GS(I,L,MUZ) = Q(I,L,MUZ)**2
      SUM = SUM + G(I,L,MUZ)
      TSUM = TSUM + GS(I,L,MUZ)
   17 CONTINUE
      XB = SUM/XK
      R = XK*((XB)**2)
      VAR = (1.0/(XK-1.0 ))*(TSUM - R)
      DEV = SQRT(VAR)
      N1 = MUZ - 1
      N1 = 22.5*N1
      PRINT 36, N1, DEV, XB
   19 CONTINUE
      CALL SYSTEM
      END
END OF TAPE
```


Errata 19 Cont'd

ACCELERATION DEVIATIONS — Fig. Moskowitz $H_{1/3}$ = 7.4' Synoptic Subset

SHIP LENGTH 1 248

SAMPLE DEVIATION FOR MU SUB 0 OF 0.0 IS .8956741SE-03 AND XBAR IS .8869703IE-02
SAMPLE DEVIATION FOR MU SUB 0 OF 22.0 IS .1427737+E-02 AND XBAR IS .1546817+E-01
SAMPLE DEVIATION FOR MU SUB 0 OF 45.0 IS .3018013+E-02 AND XBAR IS .3478301+E-01
SAMPLE DEVIATION FOR MU SUB 0 OF 67.0 IS .7+251520E-02 AND XBAR IS .655609+5E-01
SAMPLE DEVIATION FOR MU SUB 0 OF 90.0 IS .1154777+E-01 AND XBAR IS .1032349+E 00
SAMPLE DEVIATION FOR MU SUB 0 OF 112.0 IS .1453810+E-01 AND XBAR IS .1465539+E 00
SAMPLE DEVIATION FOR MU SUB 0 OF 135.0 IS .1079325+E-01 AND XBAR IS .1780574+E 00
SAMPLE DEVIATION FOR MU SUB 0 OF 157.0 IS .2+649937E-01 AND XBAR IS .2020011+E 00
SAMPLE DEVIATION FOR MU SUB 0 OF 180.0 IS .2+771056E-01 AND XBAR IS .2107458+E 00

SHIP LENGTH 2 302'

SAMPLE DEVIATION FOR MU SUB 0 OF 0.0 IS .8956741SE-03 AND XBAR IS .8869703IE-02
SAMPLE DEVIATION FOR MU SUB 0 OF 22.0 IS .1426783+E-02 AND XBAR IS .1559505+E-01
SAMPLE DEVIATION FOR MU SUB 0 OF 45.0 IS .3052469IE-02 AND XBAR IS .3497654+E-01
SAMPLE DEVIATION FOR MU SUB 0 OF 67.0 IS .6+235813E-02 AND XBAR IS .6159501+E-01
SAMPLE DEVIATION FOR MU SUB 0 OF 90.0 IS .9+104343E-02 AND XBAR IS .9379540+E-01
SAMPLE DEVIATION FOR MU SUB 0 OF 112.0 IS .1252430+E-01 AND XBAR IS .1250900+E 00
SAMPLE DEVIATION FOR MU SUB 0 OF 135.0 IS .1447588+E-01 AND XBAR IS .1461452+E 00
SAMPLE DEVIATION FOR MU SUB 0 OF 157.0 IS .1+532129E-01 AND XBAR IS .1614034+E 00
SAMPLE DEVIATION FOR MU SUB 0 OF 180.0 IS .1759595+E-01 AND XBAR IS .1556739+E 00

SHIP LENGTH 3 370'

SAMPLE DEVIATION FOR MU SUB 0 OF 0.0 IS .8956741SE-03 AND XBAR IS .8869703IE-02
SAMPLE DEVIATION FOR MU SUB 0 OF 22.0 IS .1172967+E-02 AND XBAR IS .1501430+E-01
SAMPLE DEVIATION FOR MU SUB 0 OF 45.0 IS .3+513551E-02 AND XBAR IS .3330424+E-01
SAMPLE DEVIATION FOR MU SUB 0 OF 67.0 IS .4+256371E-02 AND XBAR IS .5411109+E-01
SAMPLE DEVIATION FOR MU SUB 0 OF 90.0 IS .6+099237E-02 AND XBAR IS .8056814+E-01
SAMPLE DEVIATION FOR MU SUB 0 OF 112.0 IS .7+819737E-02 AND XBAR IS .9885564+E-01
SAMPLE DEVIATION FOR MU SUB 0 OF 135.0 IS .1+109139E-01 AND XBAR IS .1190854+E 00
SAMPLE DEVIATION FOR MU SUB 0 OF 157.0 IS .1+883859E-01 AND XBAR IS .1189794+E 00
SAMPLE DEVIATION FOR MU SUB 0 OF 180.0 IS .1+570918E-01 AND XBAR IS .1210434+E 00

SHIP LENGTH 4 452'

SAMPLE DEVIATION FOR MU SUB 0 OF 0.0 IS .7974503+E-03 AND XBAR IS .8441372+E-02
SAMPLE DEVIATION FOR MU SUB 0 OF 22.0 IS .1096225+E-02 AND XBAR IS .1306334+E-01
SAMPLE DEVIATION FOR MU SUB 0 OF 45.0 IS .2+322717E-02 AND XBAR IS .2958544+E-01
SAMPLE DEVIATION FOR MU SUB 0 OF 67.0 IS .3+387521E-02 AND XBAR IS .4517817+E-01
SAMPLE DEVIATION FOR MU SUB 0 OF 90.0 IS .4+274298E-02 AND XBAR IS .6726134+E-01
SAMPLE DEVIATION FOR MU SUB 0 OF 112.0 IS .5+380714E-02 AND XBAR IS .7662994+E-01
SAMPLE DEVIATION FOR MU SUB 0 OF 135.0 IS .1+928355E-01 AND XBAR IS .8606165+E-01
SAMPLE DEVIATION FOR MU SUB 0 OF 157.0 IS .1+791129E-01 AND XBAR IS .8566497+E-01
SAMPLE DEVIATION FOR MU SUB 0 OF 180.0 IS .2+078649E-01 AND XBAR IS .8552244+E-01

SHIP LENGTH 5 552'

SAMPLE DEVIATION FOR MU SUB 0 OF 0.0 IS .5624581SE-03 AND XBAR IS .6423609+E-02
SAMPLE DEVIATION FOR MU SUB 0 OF 22.0 IS .9+97745+E-03 AND XBAR IS .1015177+E-01
SAMPLE DEVIATION FOR MU SUB 0 OF 45.0 IS .1+552879E-02 AND XBAR IS .2333654+E-01
SAMPLE DEVIATION FOR MU SUB 0 OF 67.0 IS .3+469790E-02 AND XBAR IS .3469634+E-01
SAMPLE DEVIATION FOR MU SUB 0 OF 90.0 IS .5+510314E-02 AND XBAR IS .5165864+E-01
SAMPLE DEVIATION FOR MU SUB 0 OF 112.0 IS .1+135748E-01 AND XBAR IS .5516189+E-01
SAMPLE DEVIATION FOR MU SUB 0 OF 135.0 IS .1+423209E-01 AND XBAR IS .6169854+E-01
SAMPLE DEVIATION FOR MU SUB 0 OF 157.0 IS .2+280621E-01 AND XBAR IS .5684931+E-01
SAMPLE DEVIATION FOR MU SUB 0 OF 180.0 IS .2+462279E-01 AND XBAR IS .5631732+E-01

PRINTOUT OF SAMPLE MEANS AND DEVIATIONS FOR $H_{1/3}$ = 7.4' SYNOPTIC SUBSET

FIGURE 15

ACCELERATION DEVIATIONS FOR MOSKOWITZ $H_{1/3}$=32.2' SYNOPTIC SUBSET

SHIP LENGTH 1 748'

SAMPLE DEVIATION FOR MU SUB 0 OF 0.0 IS .18210253E-02 AND XBAR IS .19719455E-01
SAMPLE DEVIATION FOR MU SUB 0 OF 22.0 IS .30585523E-02 AND XBAR IS .33893582E-01
SAMPLE DEVIATION FOR MU SUB 0 OF 45.0 IS .56309659E-02 AND XBAR IS .72821981E-01
SAMPLE DEVIATION FOR MU SUB 0 OF 67.0 IS .10534282E-01 AND XBAR IS .13452745E 00
SAMPLE DEVIATION FOR MU SUB 0 OF 90.0 IS .20592370E-01 AND XBAR IS .21410284E 00
SAMPLE DEVIATION FOR MU SUB 0 OF 112.0 IS .30428807E-01 AND XBAR IS .30806578E 00
SAMPLE DEVIATION FOR MU SUB 0 OF 135.0 IS .39970107E-01 AND XBAR IS .38785513E 00
SAMPLE DEVIATION FOR MU SUB 0 OF 157.0 IS .44261301E-01 AND XBAR IS .44512499E 00
SAMPLE DEVIATION FOR MU SUB 0 OF 180.0 IS .47725914E-01 AND XBAR IS .46839793E 00

SHIP LENGTH 2 302'

SAMPLE DEVIATION FOR MU SUB 0 OF 0.0 IS .18210253E-02 AND XBAR IS .19719455E-01
SAMPLE DEVIATION FOR MU SUB 0 OF 22.0 IS .31557057E-02 AND XBAR IS .34045052E-01
SAMPLE DEVIATION FOR MU SUB 0 OF 45.0 IS .60240514E-02 AND XBAR IS .74111038E-01
SAMPLE DEVIATION FOR MU SUB 0 OF 67.0 IS .10699579E-01 AND XBAR IS .13410273E 00
SAMPLE DEVIATION FOR MU SUB 0 OF 90.0 IS .20297899E-01 AND XBAR IS .21113241E 00
SAMPLE DEVIATION FOR MU SUB 0 OF 112.0 IS .29209403E-01 AND XBAR IS .29737054E 00
SAMPLE DEVIATION FOR MU SUB 0 OF 135.0 IS .34748919E-01 AND XBAR IS .36989564E 00
SAMPLE DEVIATION FOR MU SUB 0 OF 157.0 IS .40332448E-01 AND XBAR IS .42221575E 00
SAMPLE DEVIATION FOR MU SUB 0 OF 180.0 IS .44405523E-01 AND XBAR IS .44168097E 00

SHIP LENGTH 3 370'

SAMPLE DEVIATION FOR MU SUB 0 OF 0.0 IS .18210253E-02 AND XBAR IS .19719455E-01
SAMPLE DEVIATION FOR MU SUB 0 OF 22.0 IS .31733990E-02 AND XBAR IS .33433915E-01
SAMPLE DEVIATION FOR MU SUB 0 OF 45.0 IS .60843038E-02 AND XBAR IS .73084765E-01
SAMPLE DEVIATION FOR MU SUB 0 OF 67.0 IS .10418051E-01 AND XBAR IS .12873092E 00
SAMPLE DEVIATION FOR MU SUB 0 OF 90.0 IS .19737459E-01 AND XBAR IS .20179018E 00
SAMPLE DEVIATION FOR MU SUB 0 OF 112.0 IS .28152183E-01 AND XBAR IS .27864985E 00
SAMPLE DEVIATION FOR MU SUB 0 OF 135.0 IS .37888556E-01 AND XBAR IS .34583465E 00
SAMPLE DEVIATION FOR MU SUB 0 OF 157.0 IS .41463079E-01 AND XBAR IS .39187165E 00
SAMPLE DEVIATION FOR MU SUB 0 OF 180.0 IS .43675946E-01 AND XBAR IS .40998654E 00

SHIP LENGTH 4 452'

SAMPLE DEVIATION FOR MU SUB 0 OF 0.0 IS .18187255E-02 AND XBAR IS .19235657E-01
SAMPLE DEVIATION FOR MU SUB 0 OF 22.0 IS .31070951E-02 AND XBAR IS .31556999E-01
SAMPLE DEVIATION FOR MU SUB 0 OF 45.0 IS .60311431E-02 AND XBAR IS .70192517E-01
SAMPLE DEVIATION FOR MU SUB 0 OF 67.0 IS .10450221E-01 AND XBAR IS .12157652E 00
SAMPLE DEVIATION FOR MU SUB 0 OF 90.0 IS .20317041E-01 AND XBAR IS .19022592E 00
SAMPLE DEVIATION FOR MU SUB 0 OF 112.0 IS .20883159E-01 AND XBAR IS .25852515E 00
SAMPLE DEVIATION FOR MU SUB 0 OF 135.0 IS .30446137E-01 AND XBAR IS .31798195E 00
SAMPLE DEVIATION FOR MU SUB 0 OF 157.0 IS .44318089E-01 AND XBAR IS .35766265E 00
SAMPLE DEVIATION FOR MU SUB 0 OF 180.0 IS .40320701E-01 AND XBAR IS .37320709E 00

SHIP LENGTH 5 552'

SAMPLE DEVIATION FOR MU SUB 0 OF 0.0 IS .18209858E-02 AND XBAR IS .17224280E-01
SAMPLE DEVIATION FOR MU SUB 0 OF 22.0 IS .20777315E-02 AND XBAR IS .28847819E-01
SAMPLE DEVIATION FOR MU SUB 0 OF 45.0 IS .57273180E-02 AND XBAR IS .64314153E-01
SAMPLE DEVIATION FOR MU SUB 0 OF 67.0 IS .10855642E-01 AND XBAR IS .11072549E 00
SAMPLE DEVIATION FOR MU SUB 0 OF 90.0 IS .21175843E-01 AND XBAR IS .17255785E 00
SAMPLE DEVIATION FOR MU SUB 0 OF 112.0 IS .30081925E-01 AND XBAR IS .23227647E 00
SAMPLE DEVIATION FOR MU SUB 0 OF 135.0 IS .41278025E-01 AND XBAR IS .28508579E 00
SAMPLE DEVIATION FOR MU SUB 0 OF 157.0 IS .48528453E-01 AND XBAR IS .31908544E 00
SAMPLE DEVIATION FOR MU SUB 0 OF 180.0 IS .51449496E-01 AND XBAR IS .33295110E 00

PRINTOUT OF SAMPLE MEANS AND DEVIATIONS FOR $H_{1/3}$=32.2' SYNOPTIC SUBSET

FIGURE 15a

three intermediate values of $\tilde{H}_{1/3}$ were computed using the mean sea spectra only.

The sample $\sqrt{E}$ deviations were linearly interpolated over the $\tilde{H}_{1/3}$ range and are shown in Figures 16 a-e for the various ship lengths and headings.

To summarize, it is seen that at this point, enough information is available so that the effect on acceleration response of both sea spectrum total energy and sea spectrum shape can be examined.

The effect of a variation in sea spectrum <u>total energy</u> manifests itself in the five groups of sample mean $\sqrt{E}$ values in Figure 11. The effect of a variation in sea spectrum <u>shape</u> manifests itself in the sample $\sqrt{E}$ deviations shown in Figures 16 a-e; these deviations from the mean exist <u>solely</u> because of this shape effect on ship response.

At this point, the $\sqrt{E}$ values in Figure 11 could be variously plotted to show the trends of $\sqrt{E}$ stern acceleration with heading, length and sea severity, but before this is done, it is desirable to treat these $\sqrt{E}$ values which are characteristic of short-term response, as a statistical sample and use them to achieve a reasonable estimate of what $\sqrt{E}$ values might be expected within the total universe or population of all possible destroyer stern acceleration $\sqrt{E}$ values during a destroyer's lifetime under similar conditions of heading, length and sea severity. The next section will be devoted to this estimation.

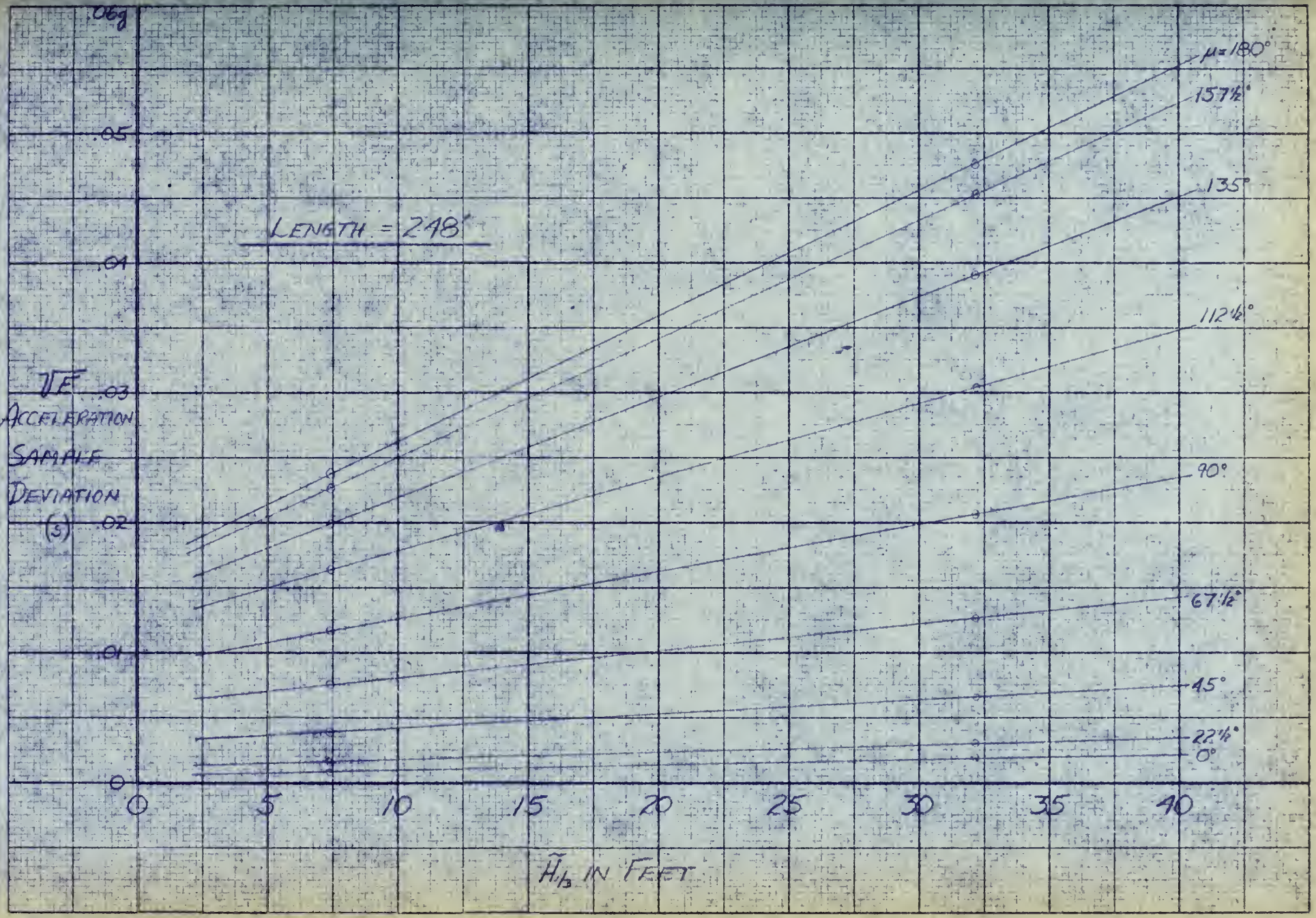

$\sqrt{E}$ Acceleration Sample Deviations

Figure 16a

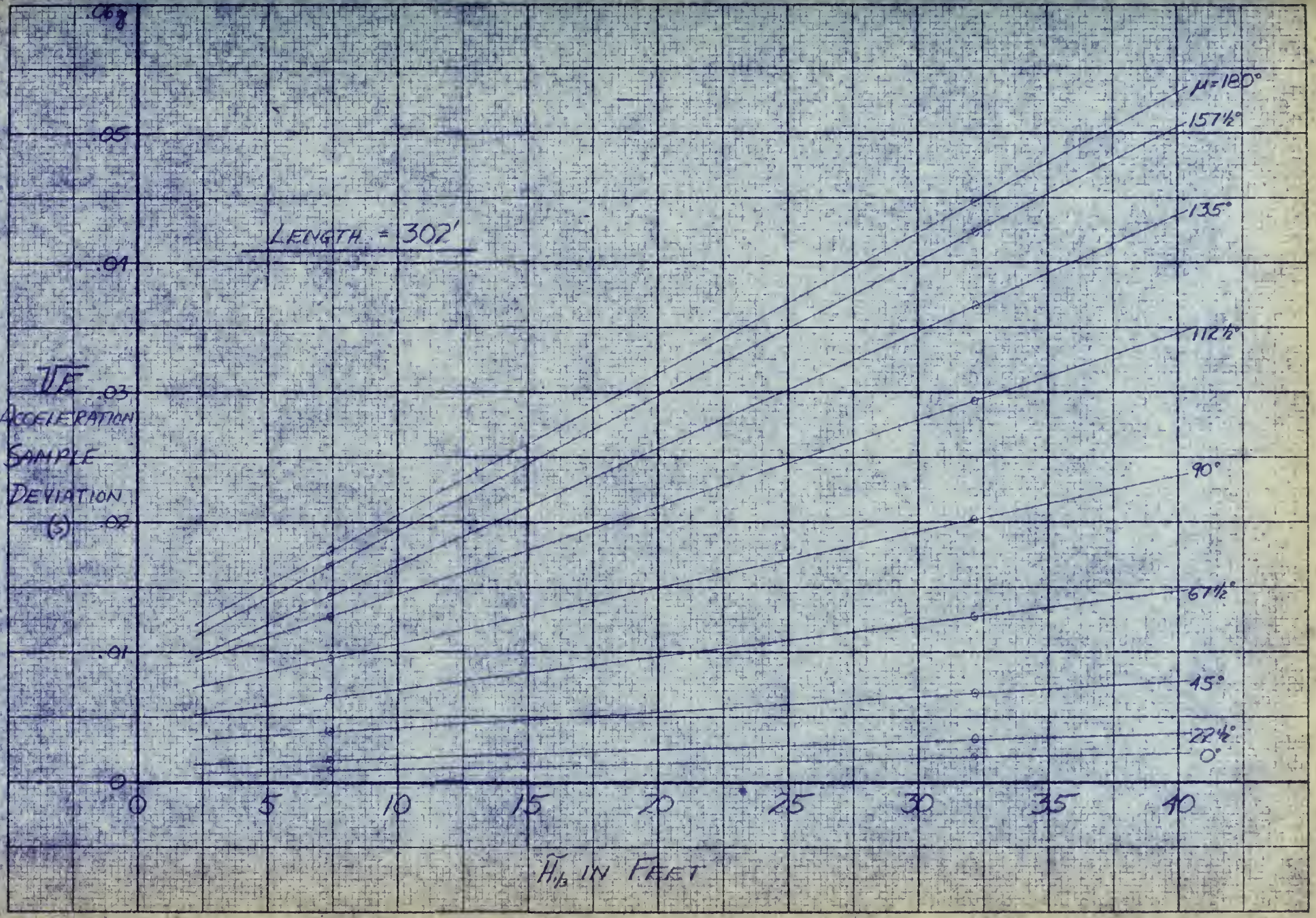

$\sqrt{E}$ Acceleration Sample Deviations

Figure 16.8

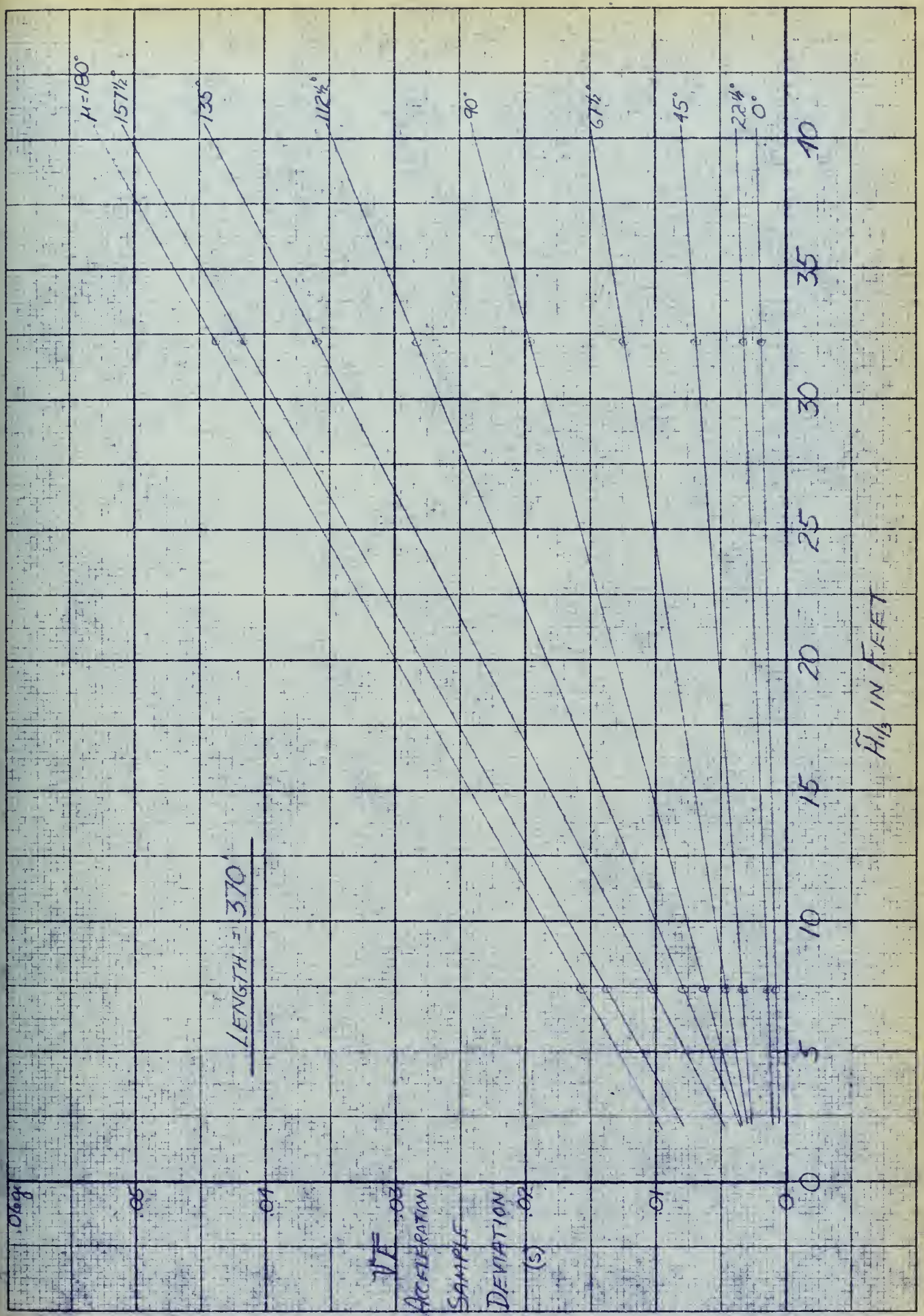

VE ACCELERATION SAMPLE DEVIATIONS

FIGURE 16c

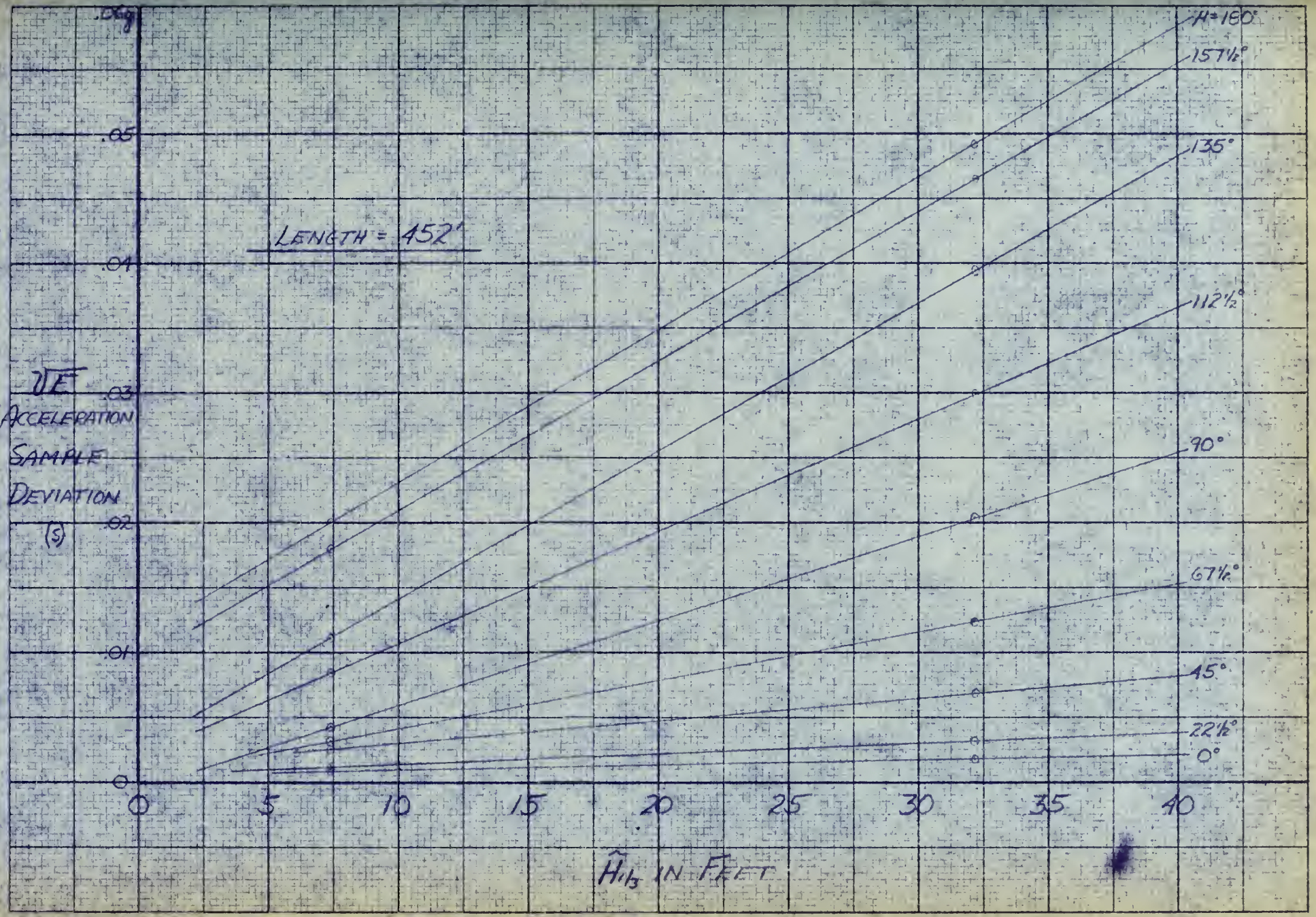

$\sqrt{E}$ Acceleration Sample Deviations

Figure 16a

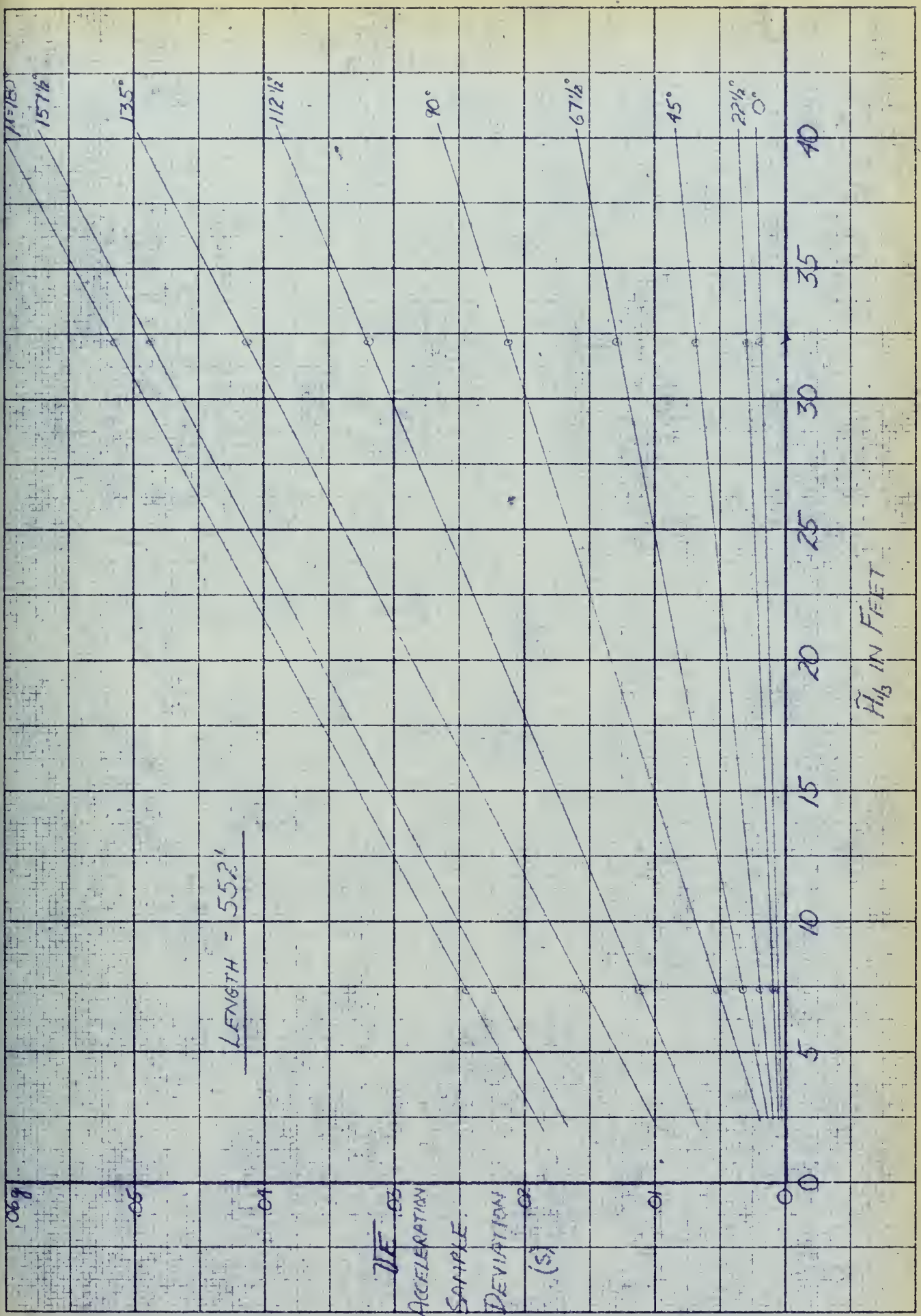

VE Acceleration Sample Deviations

Figure 16 a

STATISTICAL ESTIMATION OF POPULATION $\sqrt{E}$ VALUES

As discussed in the previous section, at each combination of heading, ship length and $\tilde{H}_{1/3}$, there is a mean value of $\sqrt{E}$ (Figure 11) and a distribution of $\sqrt{E}$ values above and below that mean, which distribution is characterized by the sample deviation found in Figures 16 a-e for the same combination of heading, length and $\tilde{H}_{1/3}$.

The assumption was made that this distribution is Gaussian or normal. The normal probability distribution is completely defined by a mean value and the deviation from that mean. The primary defense of this assumption of normality is that it does not seem unreasonable in the light of present knowledge. Perhaps when much more work in this area has been done, a slightly better distribution can be found. The size of the statistical sample used here is too small to permit construction of a valid histogram. This assumption of normality has also been used by other investigators (12).

The next and last hurdle is how to use a sample mean and deviation to predict the true total population

mean $\sqrt{E}$ and its deviation. This is where one may make good use of the concept of statistical inference, i.e., one may infer from the characteristics of a statistical sample the characteristics of the total population. In this case the assumption was made that in the sample, the $\sqrt{E}$ values are normally distributed with a mean, $\bar{x}$, and a deviation, s.

Sample: $N(\bar{x}, s^2)$

In the population, the $\sqrt{E}$ values are also assumed normally distributed, with a mean, μ, and a deviation, σ.

Population: $N(\mu, \sigma^2)$

The task now is to estimate μ and σ on the basis of $\bar{x}$ and s. Presently available theoretical statistics gives one two choices that are quite different in concept, namely the processes of point estimation and interval estimation.

I will first discuss point estimation. Maximum likelihood estimators may be derived which give a consistent, unbiased estimate of the population parameters. In the case under consideration, the unbiased maximum likelihood estimator for μ is:

$$\mu = \frac{1}{n} \sum x_i = \bar{x} \qquad (9)$$

and the unbiased maximum likelihood estimator for σ is:

$$\sigma = \sqrt{\frac{1}{n-1} \sum (x_i - \bar{x})^2} = s \qquad *$$

*It can be shown that this expression is equivalent to the one used on page 40.

This means that the best estimate one can make in this case, of μ and σ is to use $\bar{x}$ and s, respectively. However this somewhat vague approach is not very attractive unless the sample is of a respectable size, which in this investigation it is not. Perhaps the largest drawback to the use of point estimation is that when sample size is relatively small, one is provided with no specific expression of confidence that can be had in the estimation of the true parameters μ and σ.

It is due to the above that I decided to use the concept of interval estimation. With a specific level of confidence in mind, say 90%, one may predict a parameter interval or region which, with 90% confidence, will cover the true parameter value or values being sought.

It has been shown (9) that the statistic

$$\frac{\bar{x} - \mu_0}{\sigma_0/\sqrt{n}} \qquad *$$

is normally distributed with zero mean and unit variance, and that the statistic

$$\frac{ns^2}{\sigma_0^2} \qquad *$$

is chi-square distributed, where σ_0 and μ_0 are the true population parameter values.

Thus, using any convenient set of probability tables, the statement may be made that

---

* These two statistics are stochastically independent.

$$\Pr\left[-1.15 < \frac{\bar{x} - \mu_o}{\sigma_o/\sqrt{n}} < 1.15\right] = .875$$

from the standardized normal distribution and that

$$\Pr\left[4.57 < \frac{ns^2}{\sigma_o^2} < 19.7\right] = .900$$

from the χ^2 distribution with n-1 degrees of freedom where n = 12 in this case. (n = 12 was used for the sake of uniformity even though the $\hat{H}_{1/3} = 32.2$ subset had 14 component spectra-this will yield slightly conservative results)

The joint probability is (9)

$$P\left[-1.15 < \frac{\bar{x} - \mu_o}{\sigma_o/\sqrt{n}} < 1.15,\ 4.57 < \frac{ns^2}{\sigma_o^2} < 19.7\right] =$$

$$(.875)(900) = .788$$

These inequalities define a confidence region in the σ, μ parameter space as shown in Figure 17.

There is a 78.8% chance that the crosshatched parameter region covers the true parameter point (μ_o, σ_o), wherever it may be, that is to say that if 100 samples of 12 each were chosen and if the 100 resulting 78.8% confidence regions were plotted as above, about 79 of them would cover the true parameter point and the remaining 21 would fail to do so. This is the quintessence of the concept of interval estimation.

The approximately 80% confidence level was chosen as being reasonable and the following discussion is

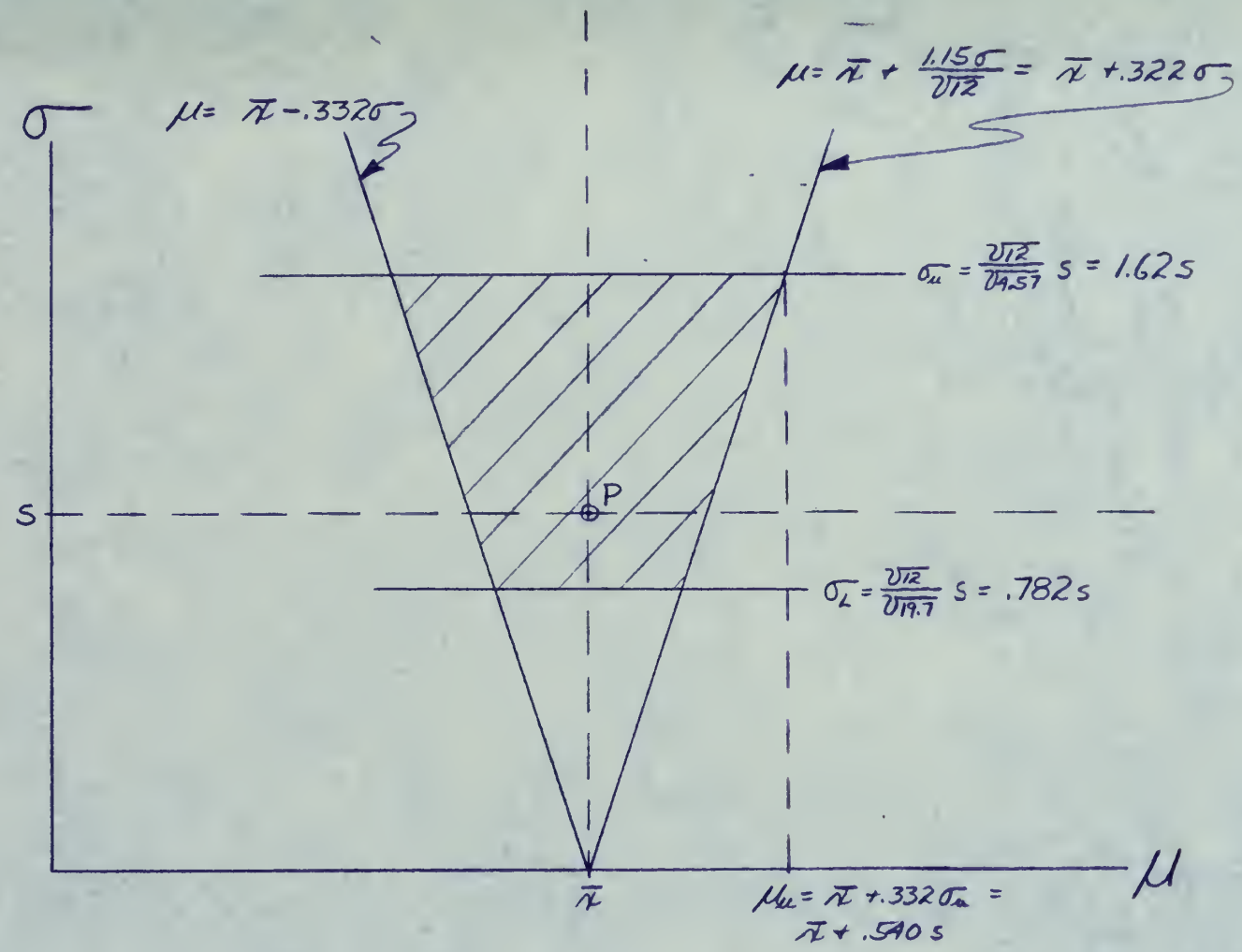

INTERVAL ESTIMATION OF (μ, σ)

FIGURE 17

intended to show that it is more than conservative enough for the purpose of these estimations.

The maximum likelihood estimators tell us that P is the most likely location of (μ_o, σ_o). With this and the approximately 80% confidence level in mind, I have chosen (μ_u, σ_u) which will give the "worst" normal distribution in terms of extreme values as the true parameter point. This is a fairly conservative choice, because of the likelihood that (σ_o, μ_o) is somewhere near P. I feel this is a situation where a little judicious conservatism is better than being inordinately bold in ignorance.

The parameters of $N(\mu_u, \sigma_u^2)$ may thus be evaluated from the following simple relationships:

$$\mu_u = \bar{x} + .540\ s$$

$$\sigma_u = 1.620\ s$$

These equations show the amount by which the sample parameters are increased so as to arrive at an estimate of the population parameters.

INVESTIGATION OF TRENDS IN $\sqrt{E}$ ACCELERATION

From this point, mean $\sqrt{E}$ acceleration will imply estimated population mean $\sqrt{E}$ acceleration (μu) and $\sqrt{E}$ acceleration deviation will imply estimated population deviation of $\sqrt{E}$ acceleration (σu).

From the data in Figure 11 ($\bar{x}$) and Figures 16 a-e (s), many combinations of ship heading, length and $\hat{H}_{1/3}$ can be used to investigate trends in $\sqrt{E}$ acceleration. For purposes of the present work, I have considered:

(a) one ship length (370 ft) - all headings - all $\hat{H}_{1/3}$

(b) one heading (head seas) - all lengths - all $\hat{H}_{1/3}$

These cases show the effect of ship length and heading as well as $\hat{H}_{1/3}$ on mean $\sqrt{E}$ acceleration response and its deviation. Other cases could, of course, be considered if desired, using other data from Figures 11 and 16 a-e.

Figures 18 and 18a deal with the 370-foot ship length case and show how mean $\sqrt{E}$ acceleration and its deviation vary with heading and $\hat{H}_{1/3}$. Figures 19 and 19a show trends with ship length and $\hat{H}_{1/3}$ for the head seas case.

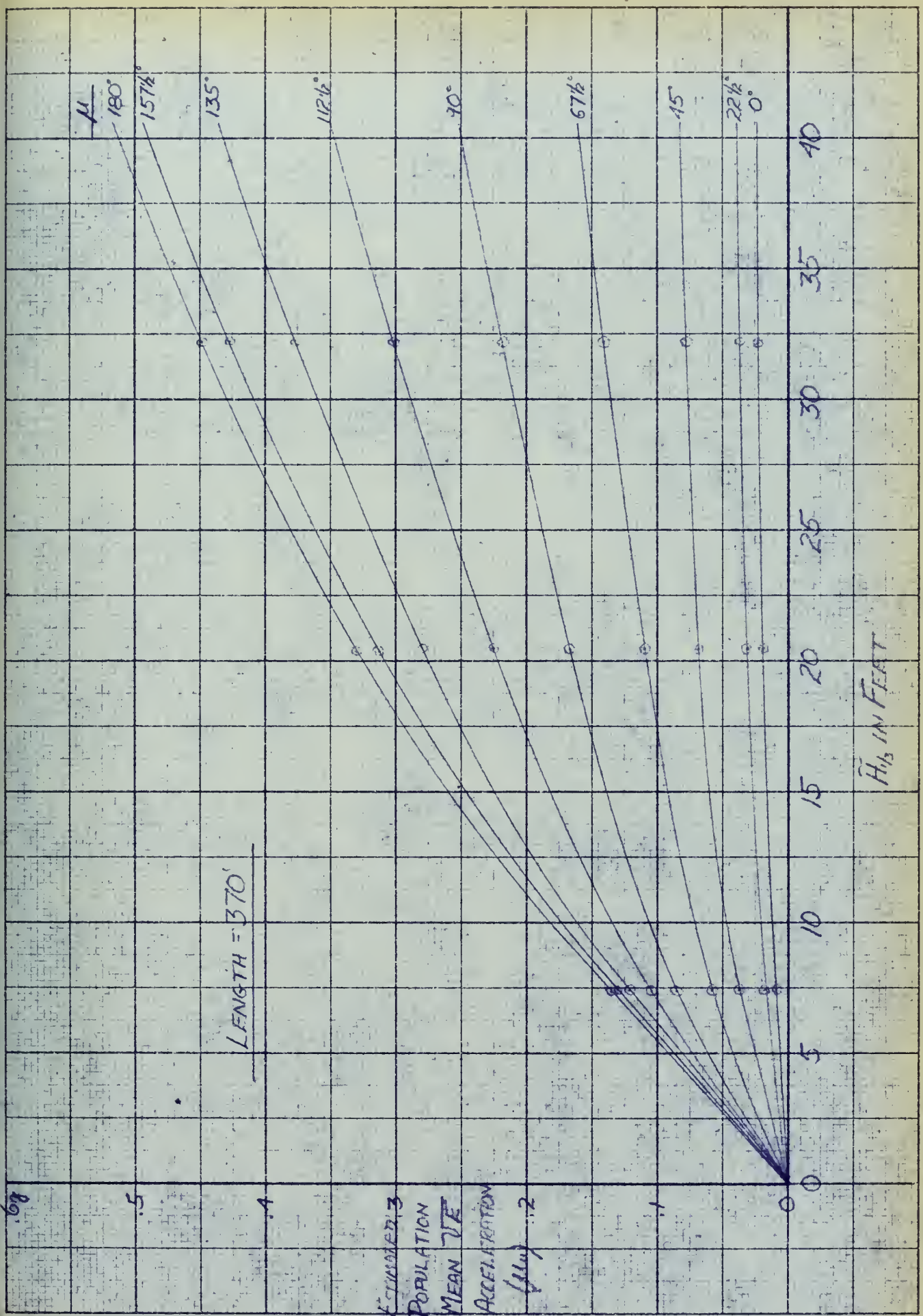

TRENDS OF μ_u WITH HEADING AND $H_{1/3}$ $L=370'$

FIGURE 18

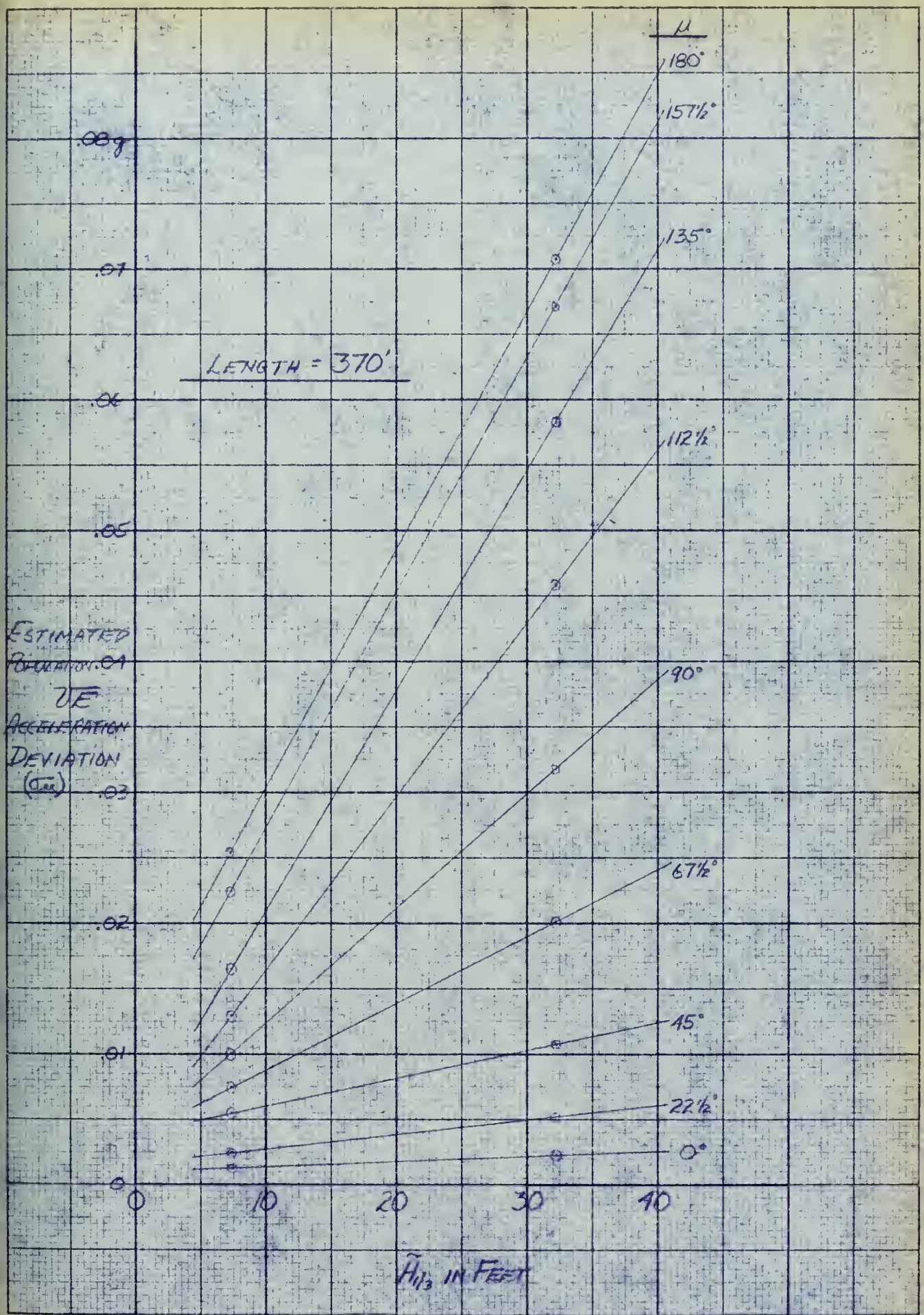

TRENDS OF $\sigma_{\ddot{z}}$ WITH HEADING AND $\bar{H}_{1/3}$ $L = 370'$ FIGURE 18a

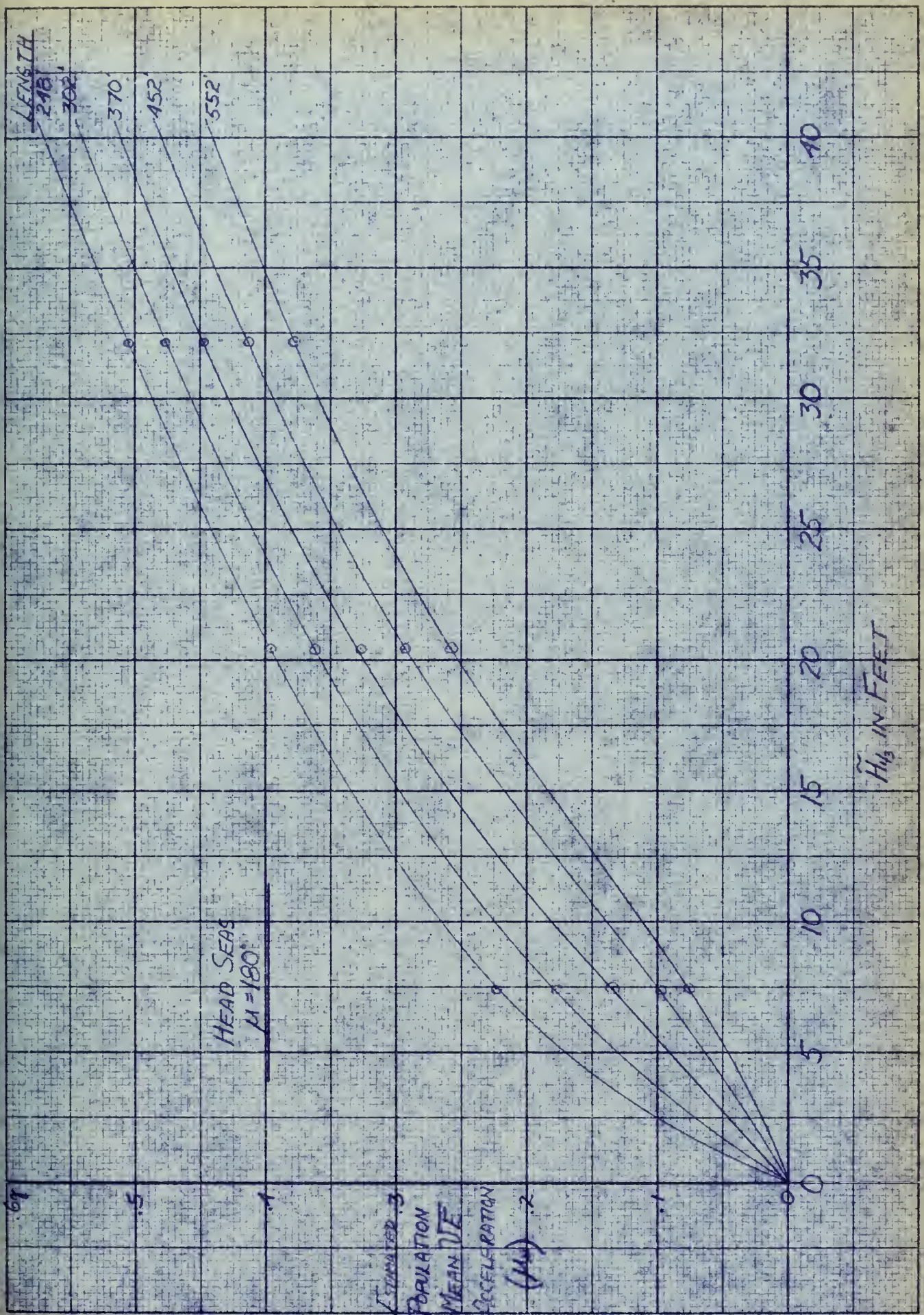

TRENDS OF $\mu_{\ddot{z}}$ WITH SHIP LENGTH AND $\hat{H}_{1/3}$ HEAD SEAS FIGURE 19

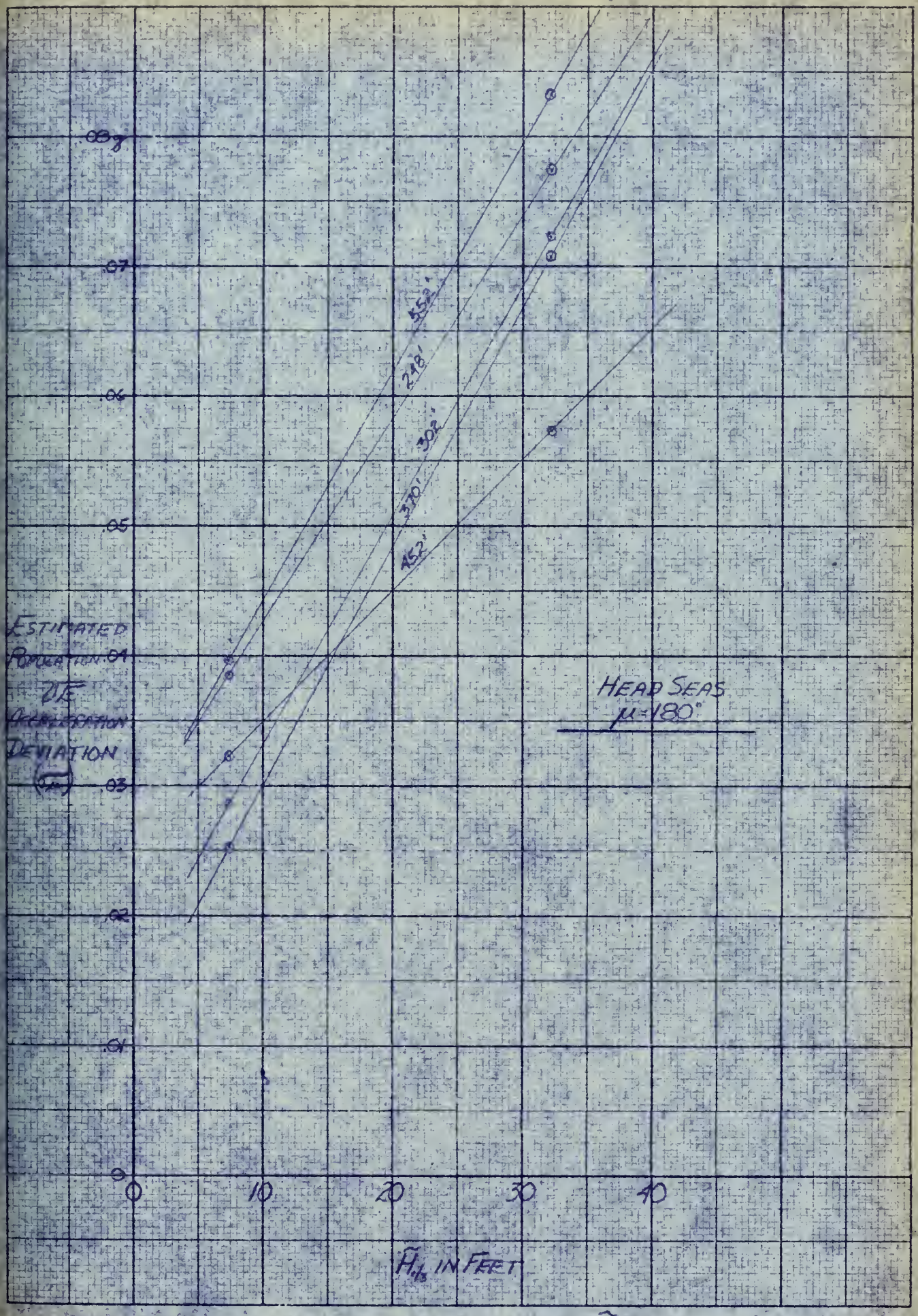

TRENDS OF σ_μ WITH SHIP LENGTH AND $H_{1/3}$ HEAD SEAS. FIGURE 19a

Finally, by crossplotting Figures 18 and 18a at discrete values of $\hat{H}_{1/3}$ (which can be thought of as different sea states - see Appendix B), Figure 20 was derived. Similarly crossplotting Figures 19 and 19a led to Figure 21. In the interest of clarity, only enough deviations are plotted on Figure 20 to demonstrate the fact that the deviations behave in much the same fashion as do the mean $\sqrt{E}$ values for any given ship length, i.e., a plot of deviations results in curves similar to the curves of mean $\sqrt{E}$ acceleration in Figure 20.

If one accepts this conclusion of similar behavior of means and deviations, the fairly mild curvature of the mean $\sqrt{E}$ curves between $\hat{H}_{1/3}$ = 7.4 and 32.2 feet in Figure 18 tends to justify the assumption of linearity used in interpolating the sample deviations in Figures 16 a-e in the same $\hat{H}_{1/3}$ range.

There are some important points to be learned from an examination of Figures 20 and 21.

Figure 20 illustrates a point of great operational significance. It is seen that if destroyers were designed so as to tolerate beam, quartering and following seas operation from a rolling and maneuverability standpoint, the stern accelerations could be greatly diminished and thus the effectiveness of the DD/VDS system is greatly enhanced in any given sea state. A step in the

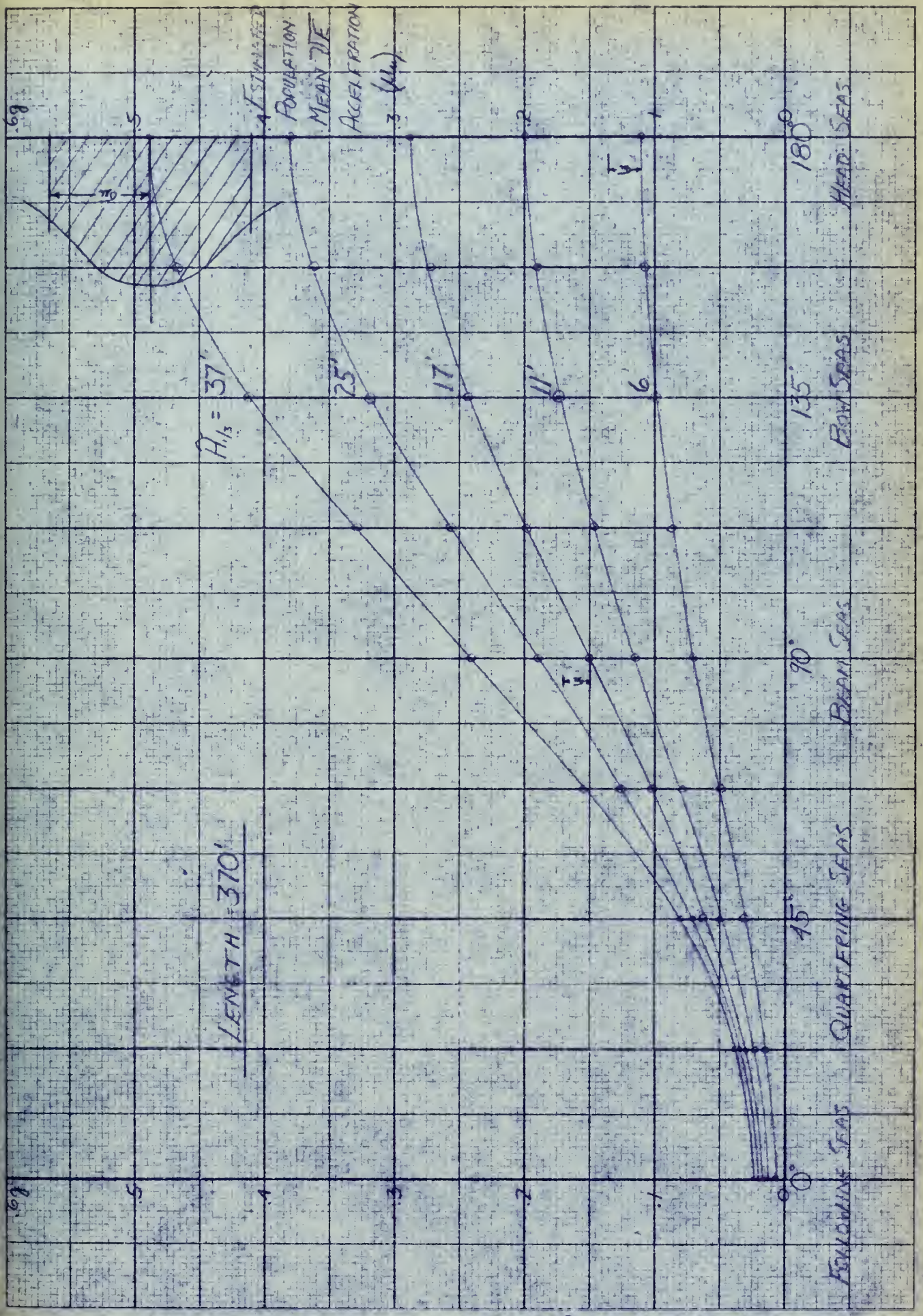

TRENDS OF μ_m WITH HEADING AT DISCRETE $H_{1/3}$ L=370' FIGURE 20

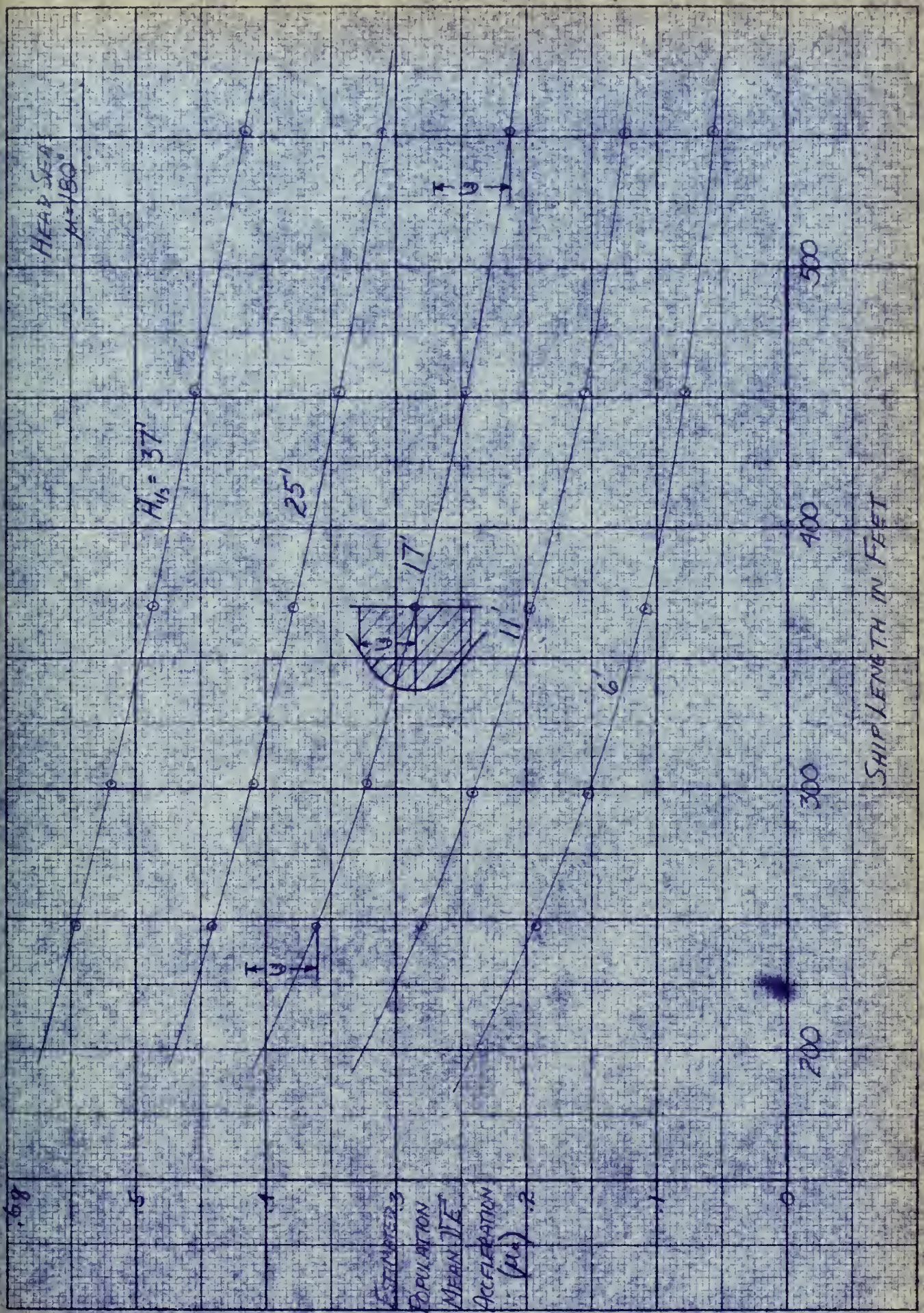

TRENDS OF μ_a WITH SHIPLENGTH AT DISCRETE $H_{1/3}$ HEAD SEAS FIGURE 21

right direction can be taken in the installation of anti-rolling fins on destroyer-type ships, because as a consequence of being able to tolerate beam seas operation, Figure 20 shows they could diminish stern accelerations to between 50 and 60 percent of the head seas accelerations.

As a slight digression, I see no reason why the same reasoning cannot be applied to problems associated with bow movement such as slamming, shipping of green water, degradation of bow sonar performance and general ability to maintain high speed in rough seas.

Figure 21 illustrates the fact that ship length has a greater percentage effect on stern acceleration in small waves than in large ones. Consequently, increased ship length pays significant dividends during the majority of the time because the small waves are much more prevalent than the large ones, but pays lesser dividends when considering relative performance in severe waves.

UTILIZATION OF $\sqrt{E}$ ACCELERATION DATA*

A crucial question is how to most effectively make use of data such as that plotted in Figures 20 and 21. By the means discussed in Appendix A, it is possible to predict from the $\sqrt{E}$ value the probability of occurrence of any particular value of stern acceleration.

However, it is highly desirable to simultaneously consider the normal distribution of $\sqrt{E}$ values (and thus the Rayleigh parameter R) and the Rayleigh distribution of acceleration single amplitudes. The theory for this has been developed by Nordenstrom in (12). He assumed that the parameter R in the short term Rayleigh distribution is normally distributed and proceeds to obtain overall distributions by numerical integration of the convolution of the Rayleigh and normal distributions. A sample of the results of this numerical integration can be found in Figure 22 with suitable nomenclature changes made to adapt it to the present work. One can enter this diagram with $\sigma u/\mu u$ and for different values of N (number

---

*A detailed discussion of the $\sqrt{E}$ parameter is given in Appendix A.

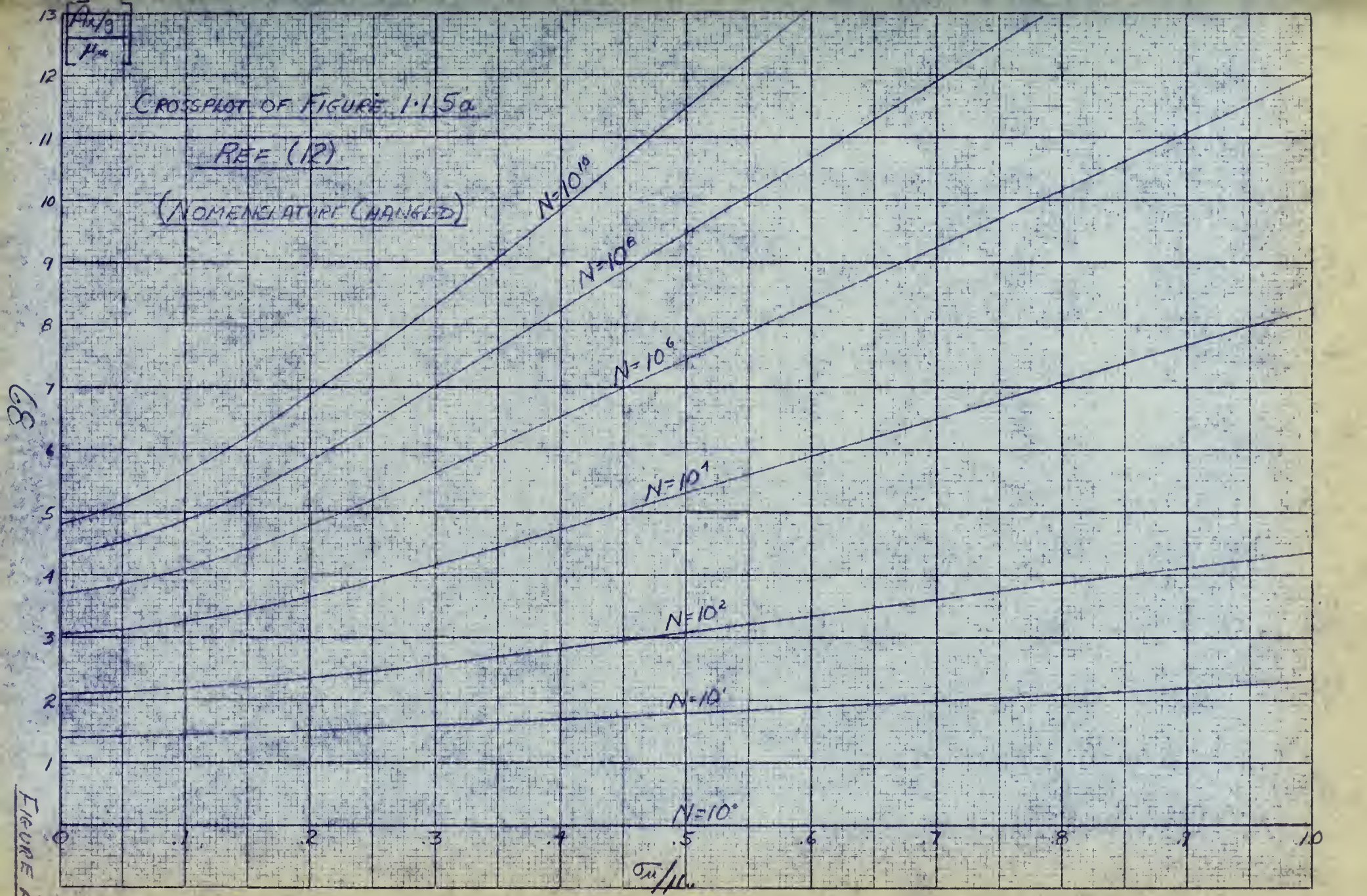
$\frac{\sigma_{xx}/g}{\mu_a}$
CROSSPLOT OF FIGURE 1.15a
REF (12)
(NOMENCLATURE CHANGED)
N=10^10
N=10^8
N=10^6
N=10^4
N=10^2
N=10^0
N=10^0
13
12
11
10
9
8
7
6
5
4
3
2
1
0
.1
.2
.3
.4
.5
.6
.7
.8
.9
1.0
σ_{xx}/μ_a

GS

FIGURE 22

of cycles) obtain a factor, which when multiplied by μ_u allows one to derive curves of Ax/g such as those shown in Figure 23 for the head seas and 370 ft ship length case.

It must be pointed out here that although these curves in Figure 23 could be termed short-term distribution curves in accordance with Jasper's definition (11), I will not do so, because it is absurd to consider that millions of cycles could take place during a short term of say, twenty minutes. However, I do not choose to call them long-term distribution curves, either, because this implies a natural variation of ship speed and heading, which is not the case here. These curves will be considered "long-term" only in the sense that each curve is the sum of many short-term distributions, keeping in mind the assumptions of invariant ship speed and heading that I have been forced to make, the former because of a paucity of model test data and the latter because of a lack of information available as to probability distribution of heading to the sea. This matter is discussed further in the next section.

A partial answer to this dilemma is to consider the probability of occurrence of the five sea states shown. It is then possible to weight these five curves

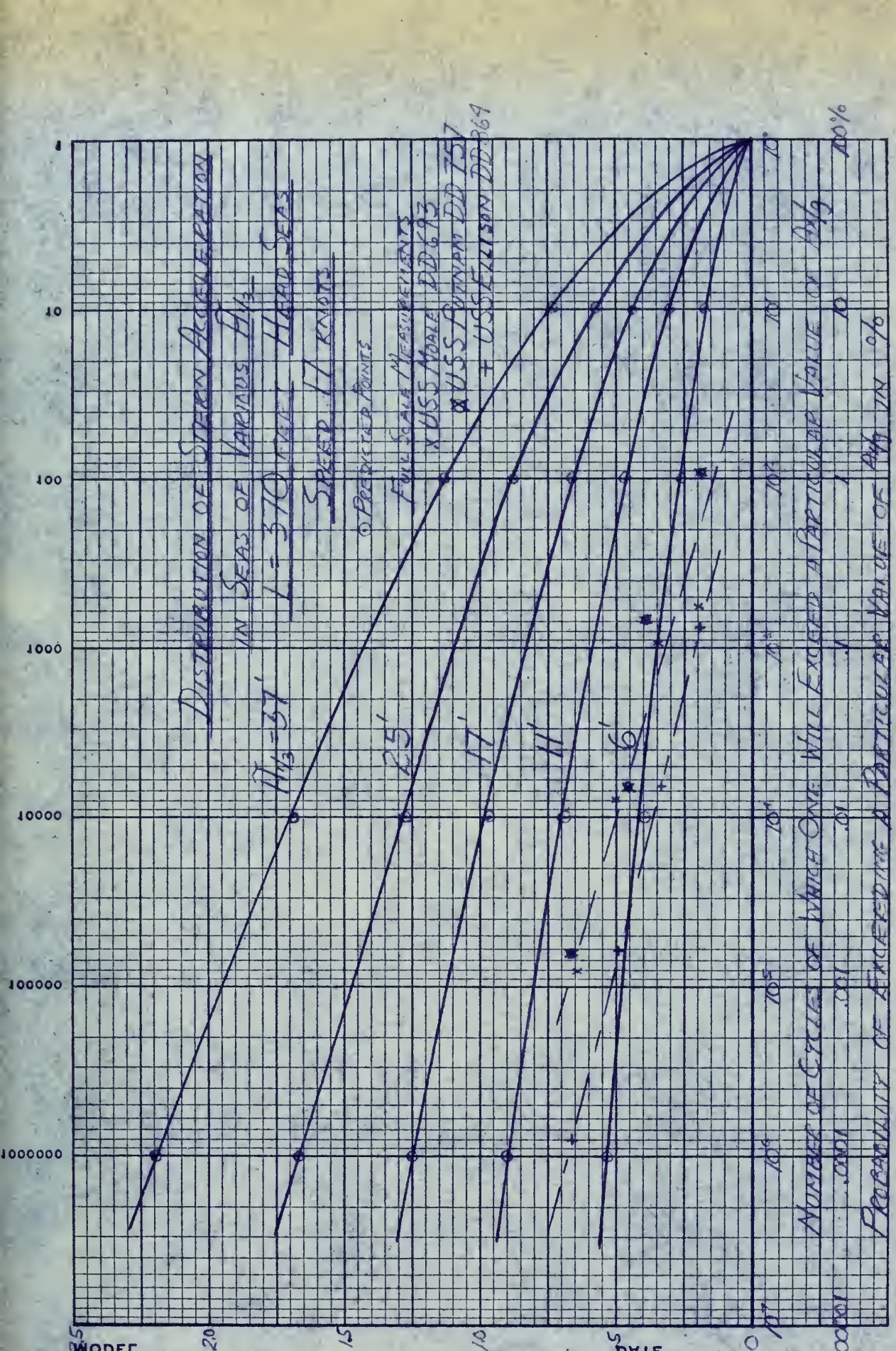
Distribution of Stern Acceleration
in Seas of Various $H_{1/3}$
$T = 370$ cycles Head Seas
Sheet 11 knots
$H_{1/3} = 37'$
25'
17'
11'
6'
Probability of Exceeding Ordinate Value of $\bar{A}_V/g$ in %
Number of Cycles of Which One Will Exceed a Particular Value of A_V/g
Vertical Stern Acceleration $(\bar{A}_V/g)$
MODEL
DATA

70

FIGURE 23

by the probability of occurrence of each sea state and arrive at a single curve that is at least one step closer to being a true long-term distribution curve.

The following sea state distribution from (14) for the North Atlantic (40-50° North Latitude) was used as an example:

$\hat{H}_{1/3}$ in feet	Probability of Occurrence
Calm	1.3%
less than 4.92	32.7
4.92 - 9.84	44.1
9.84 - 14.77	14.9
14.77 - 19.69	3.9
19.69 - 26.20	2.1
greater than 26.20	1.0
	100.0%

Plotting this information on probability paper gives one a continuous distribution of $\hat{H}_{1/3}$. By breaking this continuous distribution up into discrete increments centered on the $\tilde{H}_{1/3}$ values being used for prediction purposes (6,11,17,25 and 37 feet), it is reasonable, but not mathematically rigorous to state that:

$\tilde{H}_{1/3}$=6 ft	is representative of what occurs	70.0%	of the time
" 11	"	22.0	"
" 17	"	5.5	"
" 25	"	2.0	"
" 37	"	.5	"
		100.0%	

These statements are not mathematically precise because the ship response due to a discrete $\tilde{H}_{1/3}$ is said to be equivalent to the ship response resulting from a range of $\hat{H}_{1/3}$ values above and below that discrete value,

and this is obviously affected by the size of the $\tilde{H}_{1/3}$ increment between discrete values of $\tilde{H}_{1/3}$. The larger the increment, the larger would be the deviation in $\sqrt{E}$ values; larger than the deviations caused merely by variation in sea spectral shape.

However, in the analysis undertaken here, the degree of approximation seems reasonable with general regard to accuracy of the predictions.

The five curves in Figure 23 were weighted at various levels of acceleration by the above probabilities and the result was the curve shown in Figure 24 which I choose to call a quasi-long term distribution curve for a particular length ship under the assumed conditions of ship speed and heading. When statistical information is available regarding speed and heading distributions, inclusion of this information in the analysis will make a curve such as in Figure 24 completely general, and then it could honestly be called a long-term distribution curve.

Fortunately, however, a quasi-long term distribution curve such as that in Figure 24 is presently useful for systems analysis and design because the conditions of speed and heading used in this work are such as to yield conservative results. In other words, more work and increased knowledge will show us how much lower our predictions can safely be. Here again this is given more discussion in the next section.

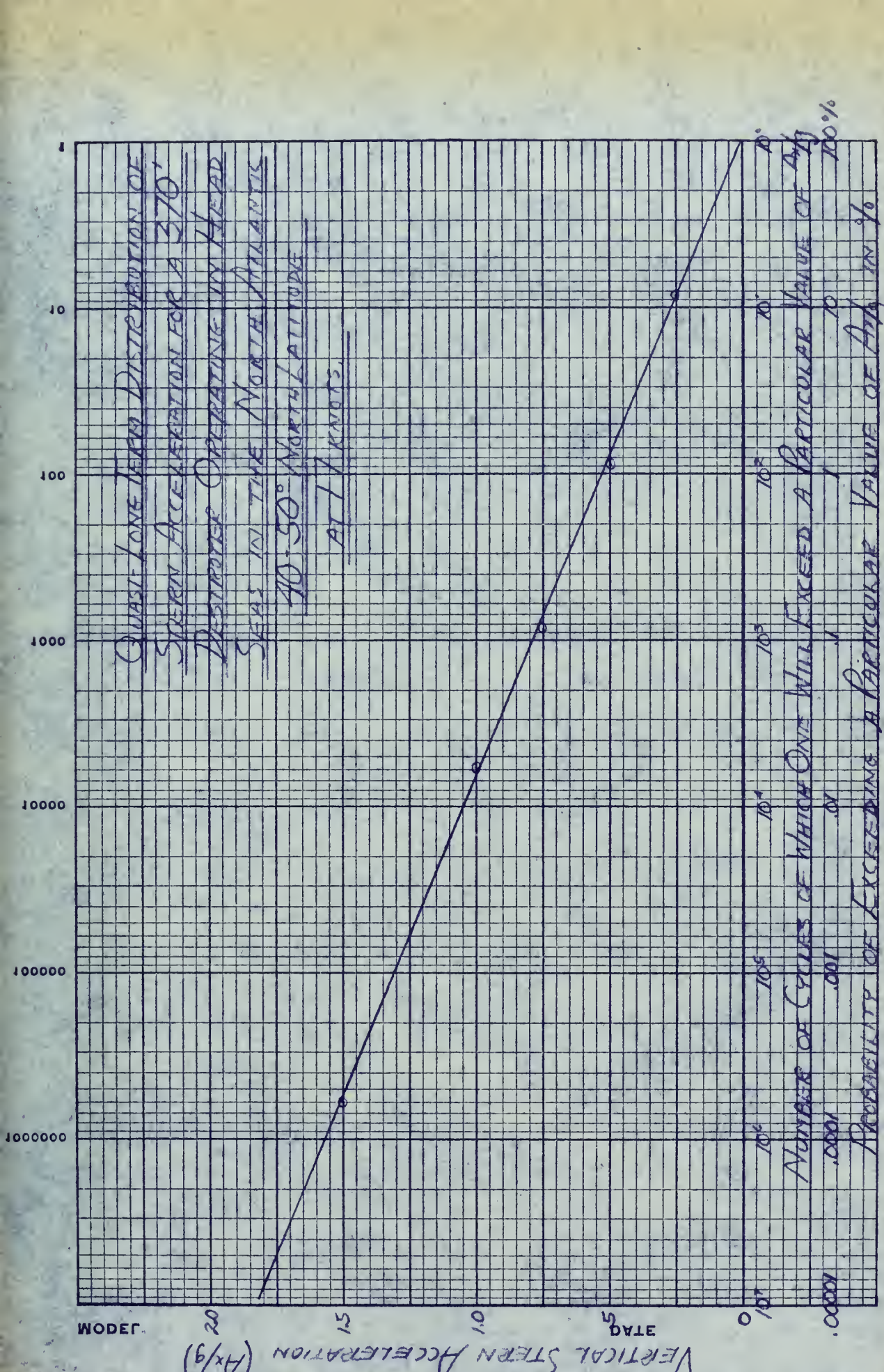
Quasi-Long Term Distribution of Steady Acceleration for a 270' Destroyer Operating in Heed Seas in the North Atlantic 40-50° North Latitude at 17 Knots.
Vertical Stern Acceleration $(\bar{A}_z/g)$
Number of Cycles of Which One Will Exceed a Particular Value of $\bar{A}_z/g$
Probability of Exceeding a Particular Value of $\bar{A}_z/g$ in %
JADOM
STAG
0
5
10
15
20
1
10
100
1000
10000
100000
1000000
10^7
10^6
10^5
10^4
10^3
10^2
10^1
1
.1
.01
.001
.0001
.00001
100%
10
1
.1
.01
.001
.0001

FIGURE 21

A DEMONSTRATION OF THE SYSTEMS VIEWPOINT

With predictions available such as those developed in the preceding section, it is possible to make an evaluation of system effectiveness, keeping in mind the assumptions as to ship speed and heading that were made. The significance of these assumptions will be discussed further later.

In the case under study, the system is the DD/VDS system. Destroyer vertical stern acceleration is no doubt the most important single parameter affecting operation of the DD/VDS system, given an otherwise operable system. The structural ability of the cable to remain intact in rough weather is a go/no-go situation dependent on vertical stern acceleration. Vertical stern acceleration also bears on understanding and solving the VDS control problem and on the design of the towing device.

A systems analysis has been done herein using vertical stern acceleration as the significant parameter- other parameters could be included in the same manner, if such were deemed necessary.

There are two basic areas of interest in this analysis of DD/VDS operational effectiveness based on vertical stern accelerations; they can best be posed as questions:

(a) in the case of an extant system, where a design assumption as to vertical stern acceleration has been made, what should the upper operational limit be, with respect to weather, in order to give reasonable assurance that the cable will not be snapped and that the VDS might be controllable, that is to say, in order that the design assumption of vertical stern acceleration will not be exceeded?

(b) in the case of a system under original feasibility or design study, what value of vertical stern acceleration should be used as a design requirement, so as to insure that the system will be operationally effective for an acceptable percentage of the time on a long-term basis?

For the extant system, the curves in Figure 23 are the most useful. Say, for example, that $\bar{A}x = 1.5$ g's was

used as a design assumption and therefore the design was based on this figure. Let us say, further, that it is desired that the probability of exceeding 1.5 g be .001% or less. Figure 23 tells us that in seas characterized by $\hat{H}_{1/3}$ = 25 feet, the probability of exceeding 1.5 g is slightly less than .001%, which is satisfactory. However, in the case of seas characterized by $\hat{H}_{1/3}$ = 37 feet, the probability of exceeding 1.5 g is about .095%, which is too great. Therefore, we would specify that this system avoid operating in seas having $\hat{H}_{1/3}$ greater than about 25 feet. Since seas of this severity might be expected to occur only two or three percent of the time, this system could be expected to be operationally useful 97-98 percent of the time, considering the restriction imposed and the probability of failure that was specified as being acceptable. The numbers used in this example are for illustration only - if a smaller probability of failure is desired, for example, a lower upper sea severity limit would have to be imposed, thus reducing the total percentage of the time that the system could be operated. This is obviously a situation involving various trade-offs and one must pick the combination best suited to his needs.

In the case of a new design, it can be seen that Figure 24 is the most useful, if it is desired, as it

certainly seems it would be, to avoid any sea severity upper limitation on the operation of the system. Once an assumption is made as regards likely areas of operation, a curve such as that shown in Figure 24 can be used to arrive at a reasonable value of stern acceleration for use as a basis for design.

For example, let us consider a DD/VDS system that is at sea for 40 percent of a ten-year life span (the ship will last longer, but most likely the weapons system will be changed), and assume that the VDS is streamed for half the time the ship is at sea. One could expect about 9 million cycles of stern acceleration during that period of time, based on an overall period of stern motion of about 7 seconds. Entering Figure 24 with N = 9 million, one reads off about 1.8 g's as the level of stern acceleration above which we can expect only one of the 9 million cycles to occur. The corresponding probability of failure if we use 1.8 g's as a basis for design is about .00002 percent.

It must be emphasized again at this point, as in the previous section, that curves similar to those being discussed are only as good as the assumptions made in deriving them. In the specific case under consideration in the present work, the curves in Figures 23 and 24 are based on a single ship speed of 17 knots and, of course,

the system will not spend its entire lifetime operating at 17 knots, although some weight may be given to the fact that 17 knots could be considered a typical speed for operation of the DD/VDS system. Another fact that must be kept in mind regarding these particular figures is that they are for head seas operation and, here again, the system will not spend its lifetime operating in head seas. As a matter of fact, as discussed previously, it would considerably lower the levels of stern acceleration if we were to design our destroyers with anti-rolling devices so as to be able to avoid head seas operation. Therefore, the curves given here will yield conservative results in any case.

My primary purpose in this section is to present a method for systems analysis that can be quite useful in evaluation of system effectiveness when the input to the analysis is reliable in magnitude and sufficient in scope. At present, I consider the available input information marginal in some respects, namely:

(a) probability distributions of ship heading to the sea are not presently available and should therefore be given some attention. It seems evident to me on the basis of four years at sea on board destroyers that as weather becomes more severe, the

tendency to steer so that seas are on the bow increases because of a desire for minimum motions and maximum maneuverability. It is due to the foregoing that I assumed head seas as being slightly more conservative than an assumption of bow seas. However, the more widespread use of such devices as anti-rolling fins will no doubt change the situation.

(b) it would be highly desirable to include the effect of speed in these predictions even though it probably has a second order effect compared with ship length and sea severity. At present there is no model test series available that covers all headings and speeds. Perhaps analytical derivation of the RAO's, such as is now being investigated at Webb, would solve this dilemma, by replacing the model testing process with an analytical procedure than can be done with a computer.

One further point that must be discussed is that of attempting a complete systems analysis. There are

many factors that affect a system as complex as a ship and its equipment, and I have examined only one subsystem of the larger overall system. The reliability of the machinery in its task of motivating the ship during VDS operations at the desired speed certainly affects the effectiveness of the DD/VDS system, but the inclusion of factors such as this is left to the operations analyst charged with maintaining the macroscopic view, more commonly referred to as the "big picture." It is my hope that the information developed in this thesis regarding destroyer stern acceleration might aid him in his task.

CORRELATION OF PREDICTIONS WITH FULL-SCALE MEASUREMENTS

As a result of interest in VDS systems, the U.S. Navy Underwater Sound Laboratory in New London, Connecticut, has recently embarked on a program of collecting a statistical sampling of vertical stern accelerations on destroyers at sea (17). For this purpose, Giannini Controls Corporation Model 2432 statistical accelerometers have been installed on various destroyers at the stern, as well as other locations.

Up to the present time, these accelerometers have been installed so as to detect instantaneous values of positive acceleration that exceed the following four thresholds: 1.20g, 1.35g, 1.50g and 1.65g, and record on the four counters, the number of exceedences above each of the thresholds.

It must be pointed out here that since these accelerometers are designed to be used horizontally as well as vertically, the zero reference for measuring vertical accelerations is one g rather than zero g, the latter being used throughout this thesis. As a consequence, the above thresholds become .20g, .35g, .50g and .65g in the zero g reference system for vertical

accelerations. No attempt will be made here to debate the pros and cons of the two systems - suffice it to say that there are arguments for both.

As of the present, there has been collected a small amount of this statistical data (and to my knowledge it is the only such data available) and it is of considerable interest to compare it with the predictions made in this thesis.

The data received from the Underwater Sound Laboratory is as follows:

USS MOALE (DD693)

Number of accelerations above .20g = 708
.35g = 239
.50g = 44
.65g = 4

Total time of test = 226 hours
Estimated number of cycles for 6 second period of motion = 135,600 cycles
Weather 1/6 - 6 foot wave heights observed
Headings and speeds - various

The probability of exceeding various levels of acceleration, therefore, would be as follows:

Probability of exceeding .20g = 708/135,600 = .530%
.35g = 239/135,600 = .176
.50g = 44/135,600 = .0325
.65g = 4/135,600 = .00294

USS PUTNAM (DD 757)

Number of accelerations over .18g = 6009
.38g = 1529
.46g = 149
.67g = 17

Total time of test 612 hours
Estimated number of cycles for 6 second
period of motion = 367,000 cycles
Weather 1-10 foot waveheights observed
Headings and speeds - various

Probability of exceeding .18g = 1.64%
.38g = .43
.46g = .041
.67g = .0046

USS H. J. ELLISON (DD 864)

Number of accelerations above .19g = 1229
.34g = 156
.48g = 18
.66g = 1

Total time of test 629 hours
Estimated number of cycles for 6 second
period of motion = 377,000 cycles
Weather 0-12 foot wave heights observed
Headings and speeds - various

Probability of exceeding .19g =.34%
.34g =.043
.48g =.0049
.66g =.0003

The Moale and Putnam are destroyers of the Sumner Class whose length on the waterline is 369 feet. The Ellison is a Gearing Class Destroyer whose length on the waterline is 383 feet.

The probabilities of exceeding the four levels of acceleration for each ship were plotted in Figure 23 (Pg.70) to compare them with predicted values.

Since the predicted curves are for head seas and 17 knots ship speed, one would expect them to be

high relative to the observed data which is for various headings and speeds. Therefore, since the observed data was taken in seas in the neighborhood of 0-11 feet in height, one would expect the observed data to plot somewhere below the $\breve{H}_{1/3}$ = 11 feet curve. As can be seen in Figure 23, this is exactly where the observed points plot. The dashed line shows the trend for the two 369 foot ships and the dot-dash line shows the trend for the 383 foot ship. The longer ship exhibits a tendency toward lower stern accelerations which agrees with the trends of stern acceleration with ship length previously discussed.

The fact that the lines drawn through the observed data have a larger slope than the individual $\breve{H}_{1/3}$ curves seems to reflect the fact that the observed data included the effect of a range of weather conditions. The curve of predicted values in Figure 24 has a larger slope and it likewise includes the effect of a range of weather conditions.

This section is intended in no way to be a comprehensive correlation of observed data with predicted data. Indeed, much more observed data is needed so one might cull it for information as to accelerations for a particular heading and speed. However, the information presented here tends to increase one's confidence in the

quantitative and qualitative aspects of the stern accelerations predicted by the method presented in this thesis.

CONCLUSIONS

1. The method presented in this thesis provides the system designer with a powerful technique — where ship response to the sea is a pertinent factor— for analyzing on paper the worth of a proposed system while still in the conceptual stage.

2. The available full-scale stern acceleration data tends to confirm the qualitative and quantitative aspects of the predictions made by the method presented herein.

3. From the standpoint of diminishing stern acceleration, ship heading to the seas is the most important single controllable factor and, therefore, destroyer-type vessels with installed equipment sensitive to stern accelerations should be designed so as to be able to tolerate rough seas operation in beam, quartering, and following seas. Installation of anti-rolling devices is a step in the right direction by enabling the ship to operate in beam seas and thereby paying a dividend of 50-60 percent diminution in stern acceleration.

4. Ship length has a greater percentage effect on stern acceleration in light seas than it does in

heavy seas. Consequently, increased ship length pays significant dividends during the majority of the time since the light seas are much more prevalent than are the heavy ones. The effect of ship length is not so marked when considering relative performance on a percentage basis in severe seas.

5. Sea spectrum shape has a significant effect on stern acceleration response and should therefore be accounted for in the method used to predict that response. The method used here seems to be effective in that regard.

6. As demonstrated in this thesis, the system approach seems particularly useful in certain aspects of ship design, since a ship-related system may most logically be considered in terms of its intended mission, for example, the location of enemy submarines.

7. In a problem such as the one studied here, the use of a high speed electronic computer virtually frees the designer from worries regarding time required for calculations and allows him to spend full time insuring the soundness of the analytical processes being used.

8. The generality of the analysis developed here insures that a similar method can be utilized to investigate other system characteristics related to seakeeping, such as shipping water over the bow, sonar degradation and slamming.

9. The analysis used in this thesis shows that the behavior and effectiveness of a ship-related system is ideally suited for expression in probabilistic terms. However, both ship designers and operators will need to develop a whole new framework of thought and reference as to acceptable probability levels of system failure and/or loss. Indeed it puts a designer face to face with his responsibilities when he has to express loss of resources, human and otherwise, in mathematical terms that are uncomfortably precise.

RECOMMENDATIONS FOR FUTURE WORK

1. Investigate means that would allow destroyer-type vessels to tolerate operation in rough quartering and following seas. The obstacles to be overcome include considerations of stability and maneuverability.

2. Continue work presently being done in the development of theory for analytical derivation of response amplitude operators, including experimental verification.

3. Investigate probability distributions of ship heading to the sea under various conditions.

4. When data becomes available, undertake a comprehensive correlation between full scale stern acceleration measurements and the predictions contained herein.

5. Give increased emphasis to collecting more seaway measurements useful for ship design, preferably directional data measured with a buoy rather than a shipborne recorder. In this regard, effective liaison between ship designers and oceanographers is of the utmost importance.

6. Investigate stern vertical velocities and displacements under various conditions of weather, ship

length and heading using a method similar to the one presented here. Also investigate the effect of ship speed on stern vertical acceleration, velocity and displacement.

7. Investigate the application, to the VDS cable stress situation, of an instrument similar to the flexing stress monitor described in (18). This instrument could be used to compute and present maximum probable cable stress during the ensuing 15 minutes or so of operation and thus give the ship's personnel an objective basis for making speed and/or heading changes when the probable cable stress becomes excessive.

REFERENCES

1. M. St. Denis and W. J. Pierson, Jr., "On the Motions of Ships in Confused Seas", Transactions of the Society of Naval Architects and Marine Engineers, Vol. 61, 1953.

2. G. Vossers, W. A. Swaan, H. Rijken, "Seakeeping Tests With Models of Three Destroyers", Publication No. 173 of the Netherlands Ship Model Basin, Wageningen, July 1959.

3. J. L. Reeves, "Comparative Seaworthiness Tests on DE-1040 and AGDE-1", David Taylor Model Basin Report 1718, March 1963.

4. Unpublished David Taylor Model Basin motion test data for models of various destroyer-type hulls.

5. E. V. Lewis and R. Bennet, "Lecture Notes on Ship Motions in Irregular Seas", Webb Institute of Naval Architecture, October 1963.

6. W. J. Pierson, Jr., G. Neumann and R.W. James, "Observing and Forecasting Ocean Waves", U. S. Hydrographic Office Publication No. 603, 1955.

7. L. Moskowitz, W. J. Pierson, Jr., and E. Mehr, "Wave Spectra Estimated from Wave Records Obtained by the O.W.S. WEATHER EXPLORER and the O.W.S. WEATHER REPORTER", New York University Research Division Report, Part I, November, 1962 and Part II, March 1963.

8. L. Moskowitz, "Estimates of the Power Spectra for Fully Developed Seas for Wind Speeds of 20 to 40 Knots", New York University Research Division Report, September, 1963.

9. A. M. Mood and F. A. Graybill, "Introduction to the Theory of Statistics", McGraw-Hill, 1963.

10. D. E. Cartwright and M. S. Longuet-Higgins, "Statistical Distribution of Maxima of a Random Function", Proceedings of Royal Society of London, 4 April 1956.

11. N. H. Jasper, "Statistical Distribution Patterns of Ocean Waves and of Wave-Induced Ship Stresses and Motions with Engineering Applications", Transactions of the Society of Naval Architects and Marine Engineers, Vol. 64, 1956.

12. N. Nordenström, "On Estimation of Long-Term Distribution of Wave-Induced Midship Bending Moments in Ships", Chalmers Institute of Technology, Göteborg, Sweden, 1963.

13. M. K. Ochi, "Extreme Behavior of a Ship in Rough Seas - Slamming and Shipping of Green Water", Transactions of the Society of Naval Architects and Marine Engineers, Vol. 72, 1964.

14. Proceedings, International Ship Structures Congress (ISSC), 20-24 July, 1964, Volume I, Issued by Ship Structures Laboratory, Delft-The Netherlands.

15. H. O. Pub. No. 606-e, "Sea and Swell Observations", U. S. Navy Hydrographic Office, 1952.

16. OPNAV INSTRUCTION P3140.37C, "Manual for Ship's Surface Weather Observations", Office of the Chief of Naval Operations, Navy Department, Washington, D. C. (For Official Use Only)

17. G. E. Christensen and D. A. Nichols, "Method for Obtaining Statistical Acceleration Data in a Destroyer at Sea", USL Technical Memorandum No. 933-355-64, 19 October 1964, U. S. Navy Underwater Sound Laboratory, New London, Connecticut (Unclassified).

18. N. H. Jasper and J. W. Church, "Structural Seaworthiness Studies", Transactions of the Society of Naval Architects and Marine Engineers, Vol. 71, 1963.

APPENDIX A

DISCUSSION OF THE $\sqrt{E}$ PARAMETER

A record of any wave-caused phenomenom in irregular seas such as stern acceleration would look something like

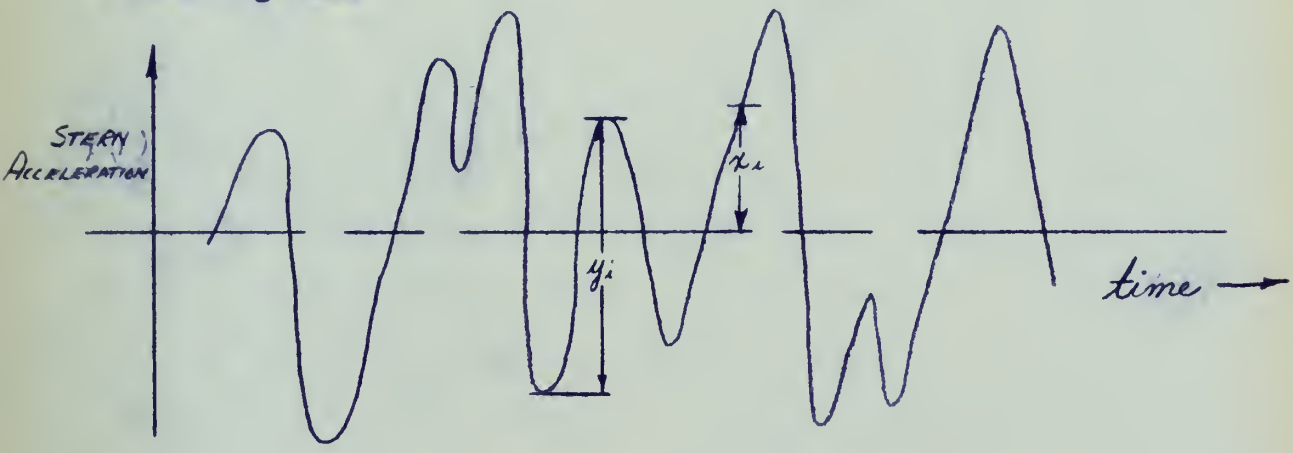

where x_i is stern acceleration measured from the mean value at equal or random time intervals and y_i is peak to peak stern acceleration measured wherever it occurs.

It is now widely accepted in the literature* that the x_i's are normally distributed and that the y_i's are Rayleigh distributed on a short-term basis. A short-term distribution is applicable so long as uniform conditions of sea, ship speed and course persist. This is to

*See for example, (11) and (13).

be distinguished from a long-term distribution which allows the sea, ship course and speed to vary over a range of conditions. Jasper introduced these definitions in (11) and they are used by many investigators, including Nordenstrom (12).

(Peak to peak) Rayleigh: $f(y) = \frac{2y}{R} e^{-y^2/R}$

(Sucessive Ordinates) Normal: $f(x) = \frac{1}{\sigma\sqrt{2\pi}} e^{\frac{-(x_i - \mu)^2}{2\sigma^2}}$ *

It is seen, then, that the parameters necessary to define the above distributions for a particular case are R and σ^2. Fortunately, it is possible to get these parameters from the Integrated Response Spectrum which, through the superposition concept, has certain mathematical properties in common with the irregular record shown.

* for brevity, the normal probability distribution function is often referred to as $N(\mu, \sigma^2)$.

It has been shown in the literature* and is now widely accepted that, for the type of spectrum being used in this work,

$$R = 8\sigma^2 = 4E \qquad (13)$$

Thus it is seen that R and σ^2 are known once E is known from the Integrated Response Spectrum.

It can also be demonstrated, using the concept of maximum likelihood estimation, that

$$R = \sum_{i=1}^{n} \frac{y_i^2}{n}$$

and since root mean square (of peak to peaks) is defined as

$$\text{RMS}\left(\begin{matrix}\text{peak to}\\ \text{peaks}\end{matrix}\right) \triangleq \sqrt{\frac{\sum_{i=1}^{n} y_i^2}{n}}$$

one may relate $\text{RMS}_{(ptp)}$ to R and thus E as follows

$$\text{RMS}_{(ptp)} \triangleq \sqrt{\frac{\sum_{i=1}^{n} y_i^2}{n}} = \sqrt{R} = 2\sqrt{E}$$

RMS of peak to peaks is commonly referred to as RMS of double amplitudes. Therefore RMS of single amplitudes

$$\text{RMS}\left(\begin{matrix}\text{single}\\ \text{amplitudes}\end{matrix}\right) = \text{RMS}_{ptp}/2 = \sqrt{E}$$

Thus it is seen that the $\sqrt{E}$ values plotted in the various figures can be thought of as being the root

*See (13)

mean square of single amplitudes of stern acceleration and such is the case throughout this thesis.

All of the above relationships were originally developed using an irregular record of wave height and the corresponding sea spectrum, but I have discussed the situation in terms of stern acceleration because ship characteristics dependent upon waves such as pitch and heave have been found to behave in the same fashion as the waves.

Since most often one is most interested in single or double amplitudes of motion, it is common practice to use the parameter E which defines the parameter R and thus the Rayleigh distribution of amplitudes to arrive at, for example, the average highest expected value of stern acceleration single amplitude in 20 cycles from

$$\left(\widetilde{Ax}/g\right)_{1/20} = 1.87\sqrt{E}$$

Multipliers for other numbers of cycles N (where N>50) may be computed to within 3% accuracy using the following formula from (10):

$$(\ln N)^{1/2} + \frac{\gamma}{2}(\ln N)^{-1/2} \quad \text{where } \gamma = \text{Eulers Constant} = .5772$$

Examples are as follows:

N=number of cycles	Average of highest expected values of single amplitude
50	$2.12\sqrt{E}$
100	$2.28\sqrt{E}$
200	$2.43\sqrt{E}$
500	$2.61\sqrt{E}$
1000	$2.74\sqrt{E}$

For the reader's convenience, the following are also quoted: (6)

Most frequent single amplitude	= 0.707 $\sqrt{E}$
Average of all single amplitudes	= 0.886 $\sqrt{E}$
Average of 1/3 highest single amplitudes	= 1.416 $\sqrt{E}$
Average of 1/10 highest single amplitudes	= 1.800 $\sqrt{E}$

APPENDIX B

A UNIFORM DEFINITION OF SEA STATES

For about fifteen years, a world-wide sea state scale (World Meteorological Organization Code 75) (15) has been in general maritime use by both naval and merchant ships for the collection of weather data at sea.

It seems logical, therefore, in the interest of meaningful full-scale correlation, that all our engineering predictions for ultimate application to the ships at sea should be in terms of WMO Code 75, which is quoted below for the reader's convenience:

STATE OF SEA-WIND WAVES (WMO CODE 75)

Code	Description	Height in Feet *
0	Calm-glassy	0
1	Calm-rippled	0-1/3
2	Smooth-wavelets	1/3-1 2/3
3	Slight	1 2/3-4
4	Moderate	4-8
5	Rough	8-13
6	Very Rough	13-20
7	High	20-30
8	Very High	30-45
9	Phenomenal	over 45

*It is proposed herein to consider this column as being $\hat{H}_{1/3}$.

In spite of the above, other sea state scales, such as the one reproduced in Figure 25, are in wide use by designers, presumably because of the mathematically convenient use of significant wave height ($\tilde{H}_{1/3}$) versus sea state designations. However, one simple and defensible assumption would remove the need to use anything but WMO Code 75. This is discussed in the two following paragraphs.

Both references (6) and (16) agree with what many oceanographers seem to feel in that at-sea wave height observers tend to overestimate wave height. Reference (16) even goes so far as to instruct the observer to record the average of the estimated heights of the larger, well-formed waves.

Consequently, it seems to make a great deal of sense to specify the assumption that <u>observed wave height equals significant wave height</u>, $\tilde{H}_{1/3}$, where $\tilde{H}_{1/3}$ is the average height of the 1/3 highest waves in a seaway. This would seem to bridge the gap between the designers who have been prone to use such scales as the one shown in Figure 25 because of its mathematically desirable use of $\tilde{H}_{1/3}$ and the ships at sea who have been making observations based on WMO Code 75.

It might be pointed out that the $\tilde{H}_{1/3}$ values of 6, 11, 17, 25 and 37 feet used in this thesis for predictions of stern acceleration were chosen as being representative of WMO Code 75 Sea States 4, 5, 6, 7 and 8 respectively.

WIND AND SEA SCALE FOR FULLY ARISEN SEA

SEA STATE[1]	SEA-GENERAL: DESCRIPTION[2]	WIND[3]: (BEAUFORT) WIND FORCE	WIND[3]: DESCRIPTION	WIND[3]: RANGE (KNOTS)	WIND[3]: WIND VELOCITY (KNOTS) AVERAGE	SEA[3]: WAVE HEIGHT FEET SIGNIFICANT	SEA[3]: WAVE HEIGHT FEET AVERAGE 1/10 HIGHEST	SEA[3]: SIGNIFICANT RANGE OF PERIODS (SECONDS)	SEA[3]: PERIOD OF MAXIMUM ENERGY OF SPECTRUM T_{max}	SEA[3]: $\bar{T}$ (AVERAGE PERIOD)	SEA[3]: T_L (AVERAGE WAVE LENGTH)	SEA[3]: MINIMUM FETCH (NAUTICAL MILES)	SEA[3]: MINIMUM DURATION (HOURS)
0	Sea like a mirror.	0	Calm	Less than 1	[a] 0	0	0	0	–	–	–	–	–
0	Ripples with the appearance of scales are formed, but without foam crests.	1	Light Airs	1 - 3	2	0.05	0.08	0.10	up to 1.2 sec	0.7	0.5	10 fn.	5	18 min
1	Small wavelets, still short but more pronounced; crests have a glassy appearance, but do not break.	2	Light Breeze	4 - 6	5	0.18	0.29	0.37	0.4-2.8	2.0	1.4	6.7 ft	8	39 min
2	Large wavelets, crests begin to break. Foam of glassy appearance. Perhaps scattered white horses.	3	Gentle Breeze	7 -10	8.5	0.6	1.0	1.2	0.8-5.0	3.4	2.4	20	9.8	1.7 hrs
2					10	0.88	1.4	1.8	1.0-6.0	4	2.9	27	10	2.4
2	Small waves, becoming longer; fairly frequent white horses.	4	Moderate Breeze	11-16	12	1.4	2.2	2.8	1.0-7.0	4.8	3.4	40	18	3.8
3					13.5	1.8	2.9	3.7	1.4-7.6	5.4	3.9	52	24	4.8
3					14	2.0	3.3	4.2	1.5-7.8	5.6	4.0	59	28	5.2
3					16	2.9	4.6	5.8	2.0-8.8	6.5	4.6	71	40	6.6
4	Moderate waves, taking a more pronounced long form; many white horses are formed. (Chance of some spray).	5	Fresh Breeze	17-21	18	3.8	6.1	7.8	2.5-10.0	7.2	5.1	90	55	8.3
4					19	4.3	6.9	8.7	2.8-10.6	7.7	5.4	99	65	9.2
4					20	5.0	8.0	10	3.0-11.1	8.1	5.7	111	75	10
5	Large waves begin to form; the white foam crests are more extensive everywhere. (Probably some spray).	6	Strong Breeze	22-27	22	6.4	10	13	3.4-12.2	8.9	6.3	134	100	12
5					24	7.9	12	16	3.7-13.5	9.7	6.8	160	130	14
6					24.5	8.2	13	17	3.8-13.6	9.9	7.0	164	140	15
6					26	9.6	15	20	4.0-14.5	10.5	7.4	188	180	17
7	Sea heaps up and white foam from breaking waves begins to be blown in streaks along the direction of the wind. (Spindrift begins to be seen).	7	Moderate Gale	28-33	28	11	18	23	4.5-15.5	11.3	7.9	212	230	20
7					30	14	22	28	4.7-16.7	12.1	8.6	250	280	23
7					30.5	14	23	29	4.8-17.0	12.4	8.7	258	290	24
7					32	16	26	33	5.0-17.5	12.9	9.1	285	340	27
8	Moderately high waves of greater length; edges of crests break into spindrift. The foam is blown in well marked streaks along the direction of the wind. Spray affects visibility.	8	Fresh Gale	34-40	34	19	30	38	5.5-18.5	13.6	9.7	322	420	30
8					36	21	35	44	5.8-19.7	14.5	10.3	363	500	34
8					37	23	37	46.7	6-20.5	14.9	10.5	376	530	37
8					38	25	40	50	6.2-20.8	15.4	10.7	392	600	38
8					40	28	45	58	6.5-21.7	16.1	11.4	444	710	42
9	High waves. Dense streaks of foam along the direction of the wind. Sea begins to roll. Visibility affected.	9	Strong Gale	41-47	42	31	50	64	7-23	17.0	12.0	492	830	47
9					44	36	58	73	7-24.2	17.7	12.5	534	960	52
9					46	40	64	81	7-25	18.6	13.1	590	1110	57
9	Very high waves with long overhanging crests. The resulting foam is in great patches and is blown in dense white streaks along the direction of the wind. On the whole the surface of the sea takes a white appearance. The rolling of the sea becomes heavy and shocklike. Visibility is affected.	10	Whole Gale*	48-55	48	44	71	90	7.5-26	19.4	13.8	650	1250	63
9					50	49	78	99	7.5-27	20.2	14.3	700	1420	69
9					51.5	52	83	106	8-28.2	20.8	14.7	736	1560	73
9					52	54	87	110	8-28.5	21.0	14.8	750	1610	75
9					54	59	95	121	8-29.5	21.8	15.4	810	1800	81
9	Exceptionally high waves (Small and medium-sized ships might for a long time be lost to view behind the waves.) The sea is completely covered with long white patches of foam lying along the direction of the wind. Everywhere the edges of the wave crests are blown into froth. Visibility affected.	11	Storm*	56-63	56	64	103	130	8.5-31	22.6	16.3	910	2100	88
9					59.5	73	116	148	10-32	24	17.0	985	2500	101
9	Air filled with foam and spray. Sea completely white with driving spray; visibility very seriously affected.	12	Hurricane*	64-71	> 64	> 80[b]	> 128[b]	> 164[b]	10-(35)	(26)	(18)	~	~	~

*For hurricane winds (and often whole gale and storm winds) required durations and fetches are rarely attained. Seas are therefore not fully arisen.

a) A heavy box around this value means that the values tabulated are at the center of the Beaufort range.

b) For such high winds, the seas are confused. The wave crests blow off, and the water and the air mix.

1) Encyclopedia of Nautical Knowledge, W.A. McEwen and A.H. Lewis, Cornell Maritime Press, Cambridge, Maryland, 1953, p. 483

2) Manual of Seamanship, Volume II, Admiralty, London, H.M. Stationery Office, 1952, pp. 717-718

3) Practical Methods for observing and forecasting Ocean Waves, Pierson, Neumann, James, N.Y. Univ, College of Engin, 1953.

This table compiled by Wilbur Marks, David Taylor Model Basin

SEE REF (6)

FIGURE 25